QATAR UNIVERSITY

COLLEGE OF ENGINEERING

STUDY OF REACTION KINETICS OF CO2 WITH AQUEOUS SOLUTIONS GLYCINE , L-ARGININE AND THEIR MDEA BLENDS USING STOPPED-FLOW TECHNIQUE

BY

NAFIS MAHMUD

A Project Submitted to

the Faculty of the College of

Engineering

in Partial Fulfillment

of the Requirements

for the Degree of

Master of Science in Environmental Engineering

June 2018

COMMITTEE PAGE

The members of the Committee approve the Project of Nafis Mahmud

defended on 23/05/2018.

_____

Dr. Abdelbaki Benamor
Thesis/Dissertation Supervisor

_____

Prof. Shaheen A. Al-Muhtaseb
Committee Member

_____

Dr. Riyadh Ibrahim Al-Raoush
Committee Member

ABSTRACT

MAHMUD, NAFIS, Masters : June : 2018,

Masters of Science in Environmental Engineering

Title: STUDY OF REACTION KINETICS OF CO2 WITH AQUEOUS SOLUTIONS GLYCINE , L-ARGININE AND THEIR MDEA BLENDS USING STOPPED-FLOW TECHNIQUE

Supervisor of Project: Dr. Abdelbaki Benamor.

Global warming and its harmful implications is a major concern for the government and scientific community worldwide. CO_2 being a greenhouse gas is considered to be a major contributor to the global warming. To reduce the anthropogenic emissions of CO_2, capture of CO_2 from the industrial processes is a must. The solvent based CO_2 capture process is considered to be the most mature and promising technology to capture CO_2 from the exhaust streams. Alkanolamines are the most widely used solvents in the CO_2 capture processes. However, they are energy intensive and there are still needs for development of novel solvents that can make the CO_2 capture technology more energy efficient. Amino acids have recently emerged as potential candidate to be used as an alternative in the CO_2 capture technology.

Since it is crucial to know the reaction kinetics of a particular amine solvent, before it can be suggested for chemical absorption of CO_2, the main focus of this project is to investigate the reaction kinetics of two amino acids, namely; Glycine and L-Arginine with CO_2 and their kinetic behavior when they are used in combination of an alkanolamine, such as MDEA, using the stopped flow technique. The experiments were carried out at a

temperature range of 293-313 K and different amine/amino acid proportions for a total concentration ranging from 0.5 to 2 mole/L. The obtained kinetic results showed that amino acids and their blends of MDEA have great potential to be used as an alternative solvent for CO_2.

Key words: Amino acids, Kinetics, Glycine, L-Arginine, MDEA-Glycine, MDEA-L-Arginine, Stopped-Flow Kinetics, Zwitterion mechanism, Termolecular Mechanism.

DEDICATION

This project is dedicated to my parents for their constant support and to my supervisor

Dr. Abdelbaki Benamor

For his unending motivation and guidance throughout this project

ACKNOWLEDGMENTS

First and foremost, I would like to express my gratitude and appreciation to my project supervisor Dr. Abdelbaki Benamor for letting me join his group to complete this research work. I would also like to thank him for his invaluable support and encouragement throughout the course of my study and his constant push that motivates and encourages me to become a better researcher.

I would also like to thank Prof. Hazim Ali Mohd Qiblawey for his constant advice and guidance during the course of the Environmental Engineering Master program.

I would like to acknowledge the GPC lab technicians Mr Ahmed Soliman and Mr Dan Jerry Cortez for providing me with all the necessary chemicals and helping me solving equipment troubleshoot and experiments related problems.

I would also like acknowledge all the faculty and staff at the GPC, whose daily influence had helped me grow and become more professionally adept in the past few years.

Last but not least, I would like to thank my parents, for the love and support they have been giving me for my entire life.

TABLE OF CONTENTS

LIST OF TABLES

LIST OF FIGURES

ABBREVIATIONS

MDEA		: N-methyldiethanolamine
Arg		: Arginine
Gly		: Glycine
MEA		: Monoethanolamine
DEA		: Diethanolamine
AMP		: 2-Amino-2-Methyl-1-Propanol
$r_{CO2\text{-}MDEA}$	$[l.mol^{-1}.s^{-1}]$	: Reaction rate of CO_2 with MDEA
$r_{CO2\text{-}OH}$	$[l.mol^{-1}.s^{-1}]$	: Reaction rate of CO_2 with hydroxyl ions.
$r_{CO2\text{-}Arg}$	$[l.mol^{-1}.s^{-1}]$	: Reaction rate of CO_2 with arginine
$r_{CO2\text{-}Gly}$	$[l.mol^{-1}.s^{-1}]$	: Reaction rate of CO_2 with glycine
r_{CO2}	$[l.mol^{-1}.s^{-1}]$	: Reaction rate of CO_2 with MDEA-arginine
k_{MDEA}	$[s^{-1}]$	: Overall reaction rate of CO_2 and MDEA
k_{OH}	$[s^{-1}]$	: Overall reaction rate of CO_2 and hydroxyl ion.
k_{Arg}	$[s^{-1}]$	: Overall reaction rate of CO_2 and arginine.
k_{ov}	$[s^{-1}]$	: Overall reaction rate with CO_2 with MDEA and arginine or glycine
k_{app}	$[s^{-1}]$	: Apparent reaction rate of CO_2 and Arginine or Glycine within the blend.
k_2	$[m^3.kmol^{-2}.s^{-1}]$	: Reaction rate constant of the formation of the

		intermediate Zwitterion
k_{MDEA}	$[m^3.\ kmol^{-2}.s^{-1}]$	: Reaction rate constant of CO_2 and MDEA reaction.
k_{OH}	$[m^3.\ kmol^{-2}.s^{-1}]$	: Reaction rate constant of CO_2 and hydroxyl ion reaction.
k_{-1}	$[s^{-1}]$	: Reaction rate constant of the consumption of the intermediate zwitterion
$k_{b,I}$	$[s^{-1}]$	: Individual reaction rate constants according to zwitterion mechanism
T	[K]	: Temperature
t	[s]	: Time
K_w	$[mol.l^{-1}]$	: Water dissociation constant
k_{Pi}	$[mol.l^{-1}]$	: Protonation constant for MDEA and arginine
$K_{Arg\text{-}pred}$	$[s^{-1}]$	: Predicted apparent rate constant
E_a	$[kJ.mol^{-1}]$	: Activation energy
E_a^Z	$[kJ.mol^{-1}]$	: Activation energy obtained in zwitterion mechanism
E_a^T	$[kJ.mol^{-1}]$	: Activation energy obtained in termolecular mechanism
k_{Arg}	$[m^6.kmol^{-2}.s^{-1}]$	: Catalytic contribution of arginine in the reaction rate according to zwitterion mechanism
k_{Gly}	$[m^6.kmol^{-2}.s^{-1}]$	: Catalytic contribution of glycine in the reaction

		rate according to zwitterion mechanism
k_{hyd}	$[m^6.kmol^{-2}.s^{-1}]$	: Catalytic contribution of hydroxyl ion in the reaction rate according to zwitterion mechanism
k_{α}	$[m^6.kmol^{-2}.s^{-1}]$	: Catalytic contribution of MDEA in the reaction rate according to zwitterion mechanism

Chapter 1: Introduction

In this modern age of industrial economy, the socio and technological growth of a country is highly dependent on the inputs of natural sources, particularly energy. Energy plays a pivotal role in the current world and it is considered to be main driver of economic growth [1]. Consequently, the demand for energy has been ascending over the past few decades. In the year 2014 alone, primary energy consumed by the world was equivalent to around 13 billion tons oil [2]. This accounts for an overall increase of around 22% when compared to the energy consumed in the year 2004 and about 54% when compared to the year 1994 [3, 4]. The overall growth in energy demand is expected continue over the next few decades.

The world's ever-growing demand for energy is primarily met through the usage of fossil fuels like coal, natural gas and oil. Despite of the continuous efforts of the scientific and research community to base the energy supply on the renewables, several forecast expects that fossil fuel will still dominate as the primary supply for the worlds energy for the next few decades [5]. The predominance of the fossil fuel for future energy demands was further affirmed in the 'World Energy Outlook 2010' report by the International Energy Agency (IEA), where it was anticipated that even by the year 2030, 75-80% of the world energy requirement will be achieved by using the fossil fuels [6]. However, this accelerated use of fossil fuels has some major environmental implications.

Energy is obtained through the burning of the fossil fuels which results in the emission of harmful greenhouse gases (GHGs). GHGs once released to the atmosphere

forms a heat trap that blocks all forms of outward radiations which can eventually increase the earth's surface temperature [7]. This increase in temperature will cause a polar ice caps to melt eventually leading to a rise in sea levels and coastal flooding. Also, the rise in temperature will have negative impacts on several aspects of the environment including wildlife, forests, agricultural productivity and human health [8, 9]. Therefore, it is essential to reduce the emissions of GHGs to diminish the severity of these impacts.

Among all identified GHGs, emission of carbon dioxide (CO_2) is considered to have major impact on the environment due to it abundance [10]. In the year 2012, 82% the CO_2 emissions accounted for the most significant GHG being emitted from human activities [11]. Majority of the anthropogenic CO_2 emissions is generated from industrial sources like coal-fired power generation plants, refinery processes, natural gas plants and other processes involved in energy related industries. Unsurprisingly, the amount of CO_2 emission has been growing proportionately with the rapid growth of world's energy demand. Concerted effort must be taken to reduce CO_2 emissions from large point sources to eliminate or reduce severity of its impacts. Being one of the major contributor of global carbon dioxide emissions, the energy industry is now faced with challenge of meeting the global energy demand while managing CO_2 emissions. Therefore, it is now essential for the energy industries to develop and implement technologies for carbon dioxide capture.

Currently, there are three options available for removal of carbon dioxide from industrial processes, they are; pre-combustion, post-combustion and oxyfuel combustion. Different technologies can be used to remove CO_2 from the industrial

processes that are primarily based on physical and chemical processes like absorption, adsorption, membrane or a combination of the three, cryogenics and so on [12]. However, amine-based post combustion technology is considered to be the most cost friendly and feasible option for CO_2 capture as they have no interference with the combustion process and are relatively easier to retrofit into existing power plants [13].

The amine-based post combustion technologies are based on chemical absorption of CO_2. In these process, the amine solvent undergoes a reversible reaction with the carbon dioxide. Amine solvent can chemically bind the CO_2 present in the flue gas and release a cleaner gas to the atmosphere. The CO_2 rich amine solutions are then heated to release the CO_2 from the amine solvent ensuring the regeneration of the amine solvent, which can be reused for further absorption. The CO_2 released can then be compressed and transported for storage or further utilization. Alkanolamines like monoethanolamine (MEA), diethanolamine (DEA), methyldiethanolamine (MDEA) and 2-amino-2-methyl-1-propanol (AMP) are frequently used in the commercial CO_2 absorption processes [14]. Primary amines like MEA exhibits high reaction rate with CO_2 and similar case also observed for secondary amines like DEA as they both form carbamates. However, they are known to have a relatively high heat for CO_2 absorption which adds to the cost of regeneration. Furthermore, their absorption capability is quite low at around 0.5 mol CO_2 per mol of amine. On the other hand, tertiary amines like MDEA have higher loading capability (1 mol CO_2 / mol MDEA) but their reaction with CO_2 is much slower compared to primary and secondary amines. AMP are well known sterically hindered primary amine that also exhibits high reactivity with CO_2, however, they are known to form unstable

carbamates when reacted CO_2 [15, 16]. It is evident that each of the conventional amines have some sort economic drawbacks associated with their use causing difficulty for large scale implementation [17, 18]. Therefore, it is important to develop new cost effective and environmentally safe solvents that can absorb CO_2 while overcoming the limitations of the conventional ones.

Amino acids can be used as promising alternatives to conventional alkanolamines for CO_2 capture processes. Structurally they are similar to primary amines, but they are less volatile and environmentally benign. They have the possibilities of being used as promoter to tertiary amines. There has already been suggestion to use salts of amino acids for capturing CO_2 because of their high performance for CO_2 capture such high loading and faster reactivity towards CO_2. However, the use amino acids alone as a single amine or in blended system has not yet been explored.

1.1 Aim and Scope of this project

The objective of this master project is to investigate the reaction kinetic of amino acids in CO_2-amino acid systems and also as a promoter in CO_2-MDEA-amino acid systems under relevant conditions for CO_2 capture. Adequate knowledge of reaction kinetics is CO_2-amine systems is paramount for proper design and simulation of the absorber column. The experimental data on the reaction kinetics of two amino acids, namely; Glycine and L-arginine with CO_2 were obtained using stopped flow conductivity method. Stopped-flow conductivity method is a direct method that has the capability of covering

a wide range of reaction rates with reproducible results [19]. Moreover, the experimental procedure is relatively easier and it requires the use of very small amount of solvent making the stopped-flow technique more suitable for screening novel solvents [20]. For CO_2-amino acid systems, to obtain the kinetics data, the experiments were carried out at 0.05 to 0.20 mol.l^{-1} within the temperature range of 293 to 313 K with 5 k increments.. For the blended systems, the experiments CO_2-MDEA-Glycine and CO_2-MDEA-L-Arginine were carried out at total concentration range of 0.25 to 1 mol.l^{-1} within the temperature range of 293 to 313 K and 298 to 313 K, respectively. The concentration range for CO_2-amino acid and the blended amine systems was chosen according to the detection limit of the stopped-flow apparatus while temperature range was chosen based on the standard operating condition of an industrial CO_2 absorption unit. The obtained experimental kinetic data were modelled using the zwitterion and termolecular mechanisms to evaluate the rate constants and their associated activation energies. All in all, this project targets to provide valuable insights into the fundamental kinetics and mechanism for the reactions of Glycine and L-arginine with CO_2, paving the way for the development of new solvent systems for carbon capture and storage.

1.2 Research Outcome (Publications)

1. N. Mahmud, A. Benamor, M. S. Nasser, M. J. Al-Marri, H. Qiblawey, and P. Tontiwachwuthikul, "*Reaction kinetics of carbon dioxide with aqueous solutions of l-Arginine, Glycine & Sarcosine using the stopped flow technique*," *International Journal of Greenhouse Gas Control,* vol. 63, no. Supplement C, pp. 47-58, 2017.
2. .N Mahmud, A. Benamor, M. J. Al-Marri, M. Khraisheh, M. S. Nasser, and P. Tontiwachwuthikul, "*Reaction kinetics of carbon dioxide in aqueous blends of N-methyldiethanolamine and glycine using the stopped flow technique*," *Journal of Natural Gas Science and Engineering,* vol. 33, pp. 186-195, 2016.
3. N. Mahmud, A. Benamor, M. S. Nasser, M. J. Al-Marri, H. Qiblawey, and P. Tontiwachwuthikul, "*Reaction kinetics of carbon dioxide in aqueous blends of N-Methyldiethanolamine and L-Arginine using stopped flow technique". (In Progress)*

Chapter 2. CO_2 Capture Technologies

The impact of global warming from GHGs emission, especially due to CO_2 emissions has now become a major concern for both the political and scientific communities around the world. It is estimated that if the current rate of CO_2 emissions is not reduced then by the year 2100, the atmospheric CO_2 content may reach to 570 ppmv which may subsequently result in an increase in sea levels by as high as 3.8 m and also increase the mean temperature of the world by 2 ^oC [21, 22]. Although, there are several natural phenomena like plant and animal respiration, wildfire, volcanoes, decomposition of organic matter and ocean release can cause carbon emissions but it is anthropogenic emission of CO_2 that has increased rapidly over the past few decades and it has now become a matter of great concern [23]. Majority of the anthropogenic emissions are the result of continuous burning of the fossil fuel to meet the growing energy demands of the world. This demand will continue to increase with the increase in world population. As a consequence of which, CO_2 emissions can also be expected to be on the rise. Therefore, carbon capture technology has been identified as one of the most probable solution to cope with this major issue [24]. Majority of scientists and researchers around the world have been trying to remedy the emissions from the industries by developing different technologies. These technologies can be classified generally into precombustion, postcombustion and oxycombustion processes [25]. All these methods have been in around for a quite a while and continuous research is being done to further improve the already available carbon capture technologies that would not only satisfy the industrial needs but also solve the

problem of Carbon Dioxide emissions. These technologies can be majorly divided into three main categories on the basis of their pathways. They are;

1. Post Combustion CO_2 Capture: involves removal CO_2 from flue gases after combustion.
2. Pre-combustion CO_2 Capture: involves removal CO_2 from the feed before combustion
3. Oxy-Combustion: Involves mixing of pure O_2 with flue gases to produce CO_2 and water, from which CO_2 is removed.

Each of these technological pathways has advantages and disadvantages of its own which has been shown in Table 1 below:

Table 1: *Advantages and Disadvantages of CO_2 Capture Technologies [25-27]*

Technologies	Advantages	Disadvantages
Post-Combustion Technology	• Can be retrofitted to an existing power plant • Capable of handling huge amount of exhausted stream.	• Might require solvent makeup because of degradation • Requires high energy during the regeneration • Solvent might corrode the columns and process equipment adding to cost.

Pre-Combustion Technology	• High partial pressure of CO_2 favors separation. • Can reduce the cost for compression.	• Can't be retrofitted to an existing plant • Requires extensive supporting systems that add to the cost.
Oxy-combustion	• Can be retrofitted. • Can be used for streams with high CO_2 concentration	• Requires cryogenic oxygen production which is costly. • Requires higher energy for cooling recycled CO_2

Each of the above-mentioned technologies are further discussed in the coming sections.

2.1 Post Combustion Capture

After the combustion of the fuel, a large amount of CO_2 is produced along with other gases which are discharged to the atmosphere in the form of flue gas. Post-Combustion CO_2 capture mainly targets the removal of CO_2 discharged through the flue gases. Generally, in the industry air is used for combustion and flue gas is produced at the end of this combustion process. The total concentration CO_2 contained in this flue gas is as low as 15%. Therefore, due to the low partial pressure of CO_2, it is quite challenging to

develop capture process that are both cost-effective and efficient. However, since these capturing processes can easily be retrofitted to any plants, it has got the best potentials to reduce the CO_2 emissions [25]. A typical post combustion carbon capture process connected to a power plant has been shown in figure 1.

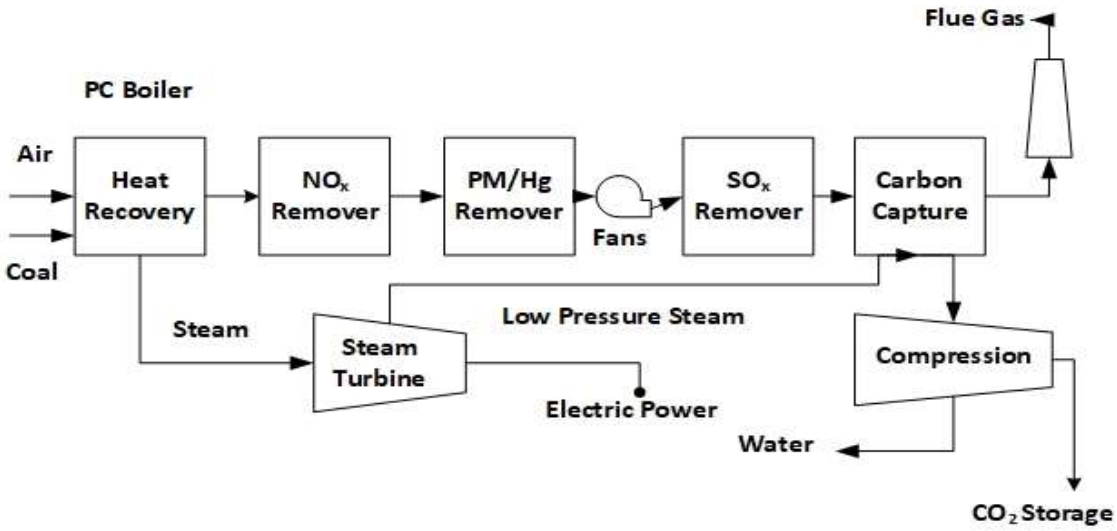

Figure 1: Post-Combustion CO_2 capture

Already many different technologies have been developed that can accomplish post - combustion CO_2 capture, which will be discussed in the following sections.

2.1.1 Amine Based CO_2 Capture Process:

One of the most conventional and widely used technological pathways for removal of CO_2 is the amine-based post combustion CO_2 capture. It is most commonly used for acid gas removal from natural gases. Amines capture CO_2 at low partial pressure by reacting with CO_2 forming water soluble compounds. Based on the structure, amines are available can be of many different forms; namely primary, secondary, tertiary and sterically. Methyl ethanol amine (MEA), Diethyl Ethanol amine (DEA) and N,N –Methyl Diethanol amine (MDEA) are the most common amines used in the conventional CO_2 capture processes[14]. The amine molecules chemically bind the CO_2 molecules present in the flue gas, resulting in a release of cleaner gas from the column. Using this process most of the CO_2 can be removed with typically recovery ranging from 80 to 95% [28]. Different amine solvents have different loading capabilities and sometimes different additives are added to the amine itself to improve the loading capability and capture efficiency. Blended amines can also be used instead of using a single amine, that way the undesirable properties of one amine in the blend is compensated by the presence of the other [29]. The amine-based CO_2 capture processes are fairly simple and it is also possible to make these processes more cost friendly with improved energy integration by making different design modifications. A typical flow diagram (Figure 2) of amine-based carbon capture process has been given in the following page;

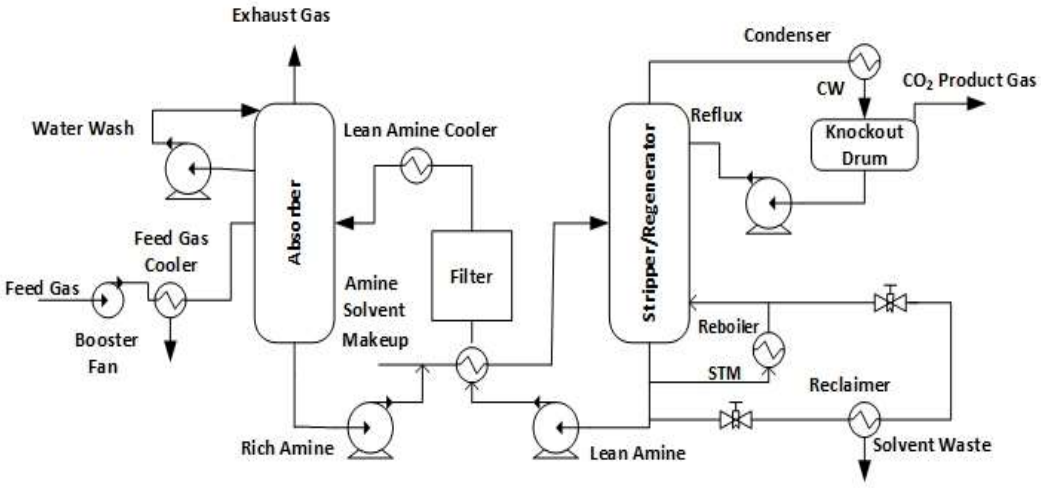

Figure 2: Amine based Carbon Capture

However, there some drawbacks like low loading, solvent degradation, low regeneration energy and slow rate of reaction with CO_2 associated with this technology [30]. In order to overcome the drawbacks associated with the amine-based CO_2 capture processes, scientist and researchers worldwide has been experimenting with different solvents other than the conventional amines. A few of the solvents other than amines that are now being suggested instead of the conventional amines are discussed in the following sections;

2.1.2 Carbonate Systems:

Use of carbonated systems instead of the conventional amines has been widely suggested because of their low energy requirements during the regeneration. In these systems, carbonate reacts with the carbon dioxide forming bicarbonates. When heat is applied to these systems it reverts to the initial carbonate form with the release of carbon dioxide.

Sometimes amine-based promoters are added to these carbonate systems to improve their equilibrium characteristics. The carbonate systems reportedly requires 5% low energy compared to the MEA based CO_2 Capture with 10% higher loading capability [31]. However, cost of the promoted carbonate solvents is little expensive. K_2CO_3 is one the most highly studied carbonate solvent which has been widely studied [25].

2.1.3 Ammonia:

Another solvent that is being suggested is aqueous ammonia as it contains of the similar functional group as of the amines. Therefore, it shows similar functionalities like that of the amines. Ammonium carbonate reacts with water and carbon dioxide which then form ammonium bicarbonate. Ammonia is relatively low cost and has lower regeneration energy with moderate CO2 loading capability. In addition to that ammonia can react with SO_X and NO_X of the flue gas to produce ammonium sulfate and ammonium nitrate, respectively. Thus, adding additional marketable products for the industry [32]. However, like other solvents, ammonia have a few drawbacks too. There are possibilities of solvent loss under high temperature as they are highly volatile. Researches are being conducted on determining the optimum conditions to eliminate the solvent loss and to ensure safe operation [33].

2.1.4 Membranes:

Another suggestion to improve the CO_2 capture process is through Membranes. Different concepts have been put forward so far, one of which is the using the membranes as the tube and the amine solvent as the shell. When the flue gas passes through the membrane tubes, the CO_2 of the flue gas will get absorbed by the amine. The membrane will block the passage of the impurities to the amine thus ensuring lower solvent loss. This amine then can be regenerated for further usage. Several researches are being carried out in order to improve the quality of the membranes to ensure better selectivity, pore size and in developing newer better quality of the membranes [34]. One of the ways of producing membranes for carbon capture purposes is the sol-gel dip processing. The major drawback associated with the use of the membranes is the longevity of the membranes as it might need to replace from time to time [30].

2.1.5 Metal organic frameworks:

Another widely suggested solvent that has been suggested is the metal organic framework or MOF's. MOF's comprises of metal ion and ligands. These metal ions have a very nicely organized geometry and are bound organically with the ligands to form this hybrid material. In the last few years, as many 600 MOF's of different chemical and structural characteristics have in developed [35]. One of the major advantages associated with the use of MOF's is its high storage capability because of the presence large enough cavities. A wide variety of MOF'S can be developed. However, there are still a lot of study need to be conducted to as their behavior under the presence of typical flue gas

impurities and capability of sustaining within multiple cycles are still unknown.

2.1.6 Ionic liquids:

Another class of solvents that have been of great interest to applied for the purpose of CO_2 capture are the ionic liquids. The ionic liquids are salts consisting of an organic cation with an inorganic or organic anion. They are thermally stable with the good capability to dissolving carbon dioxide. Furthermore, they require low heat for regeneration. The first ionic liquid functionalized with an amine group in cation by Davis [36] and it reportedly had a loading capability of 0.5 mol of CO_2 per mol of ionic liquid. Later, it was reported by Gurkan et al.[37] that the loading can be improved to a unity when the amine group is present in anion. Therefore, it has garnered high interest among the scientific community for development of this particular field. However, studies have revealed that the amine based ionic liquids becomes dramatically viscous during the absorption process, which is limiting it to be applied for full-scale CO_2 capture process [38-40]. Furthermore, there aren't many commercially available ionic liquids as they still in the development phase. Ones that can be used are being synthesized in the laboratories. Raising further questions for their large-scale application.

2.2 Pre-Combustion CO_2 capture

The pre-combustion carbon capture involves the removal of the CO_2 from the feed or fuel itself before burning. One of the major advantages of this process is that it allows the reduction of the capture units as the concentration of carbon dioxide and its pressure can be increased. However, since the process in question has to be attached to the feed itself, it cannot be integrated to an existing process [41]. But if this process is attached with the initial design it can be proved to be highly cost-effective in the long run. A schematic of the pre-combustion carbon capture process has been given in figure 3;

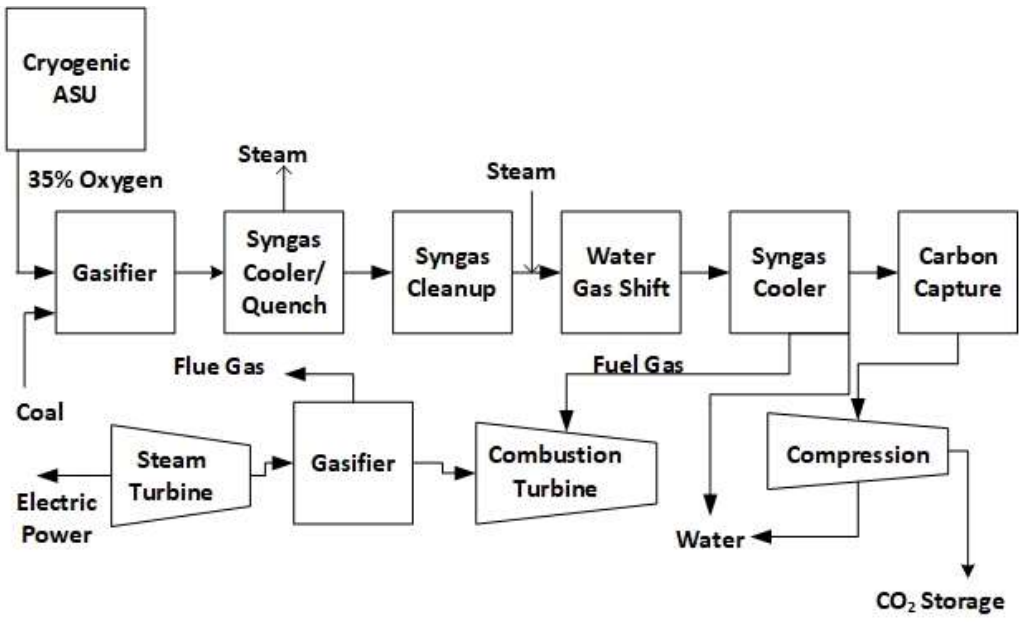

Figure 3: Pre-Combustion CO2 capture

There are different ways to achieve the purpose of pre-combustion carbon capture and a few of them are discussed in the following sections.

2.2.1 Integrated gasification combined cycle (IGCC)

In this process, syngas (CO + H_2) is produced by the gasification of coal in presence of oxygen. This then undergoes water gas shift reaction in a shift converter unit. At the end of which CO_2 is produced along with H_2. From this the carbon dioxide is separated. Several processes namely, Selexol and Rectisol have been developed to serve the purpose of capturing carbon dioxide. However, it has not been applied in plant scale which rise several questions regarding its technical and economical reliability.

2.2.2 Physical Solvent Processes

Physical solvents can also be used for the purpose of capturing carbon dioxide. They require less energy for regeneration. One of the biggest advantages of using the physical solvents is the possibility of achieving high loading corresponding to the partial pressure of the carbon dioxide. But this can only be achieved at lower temperatures. One of the common physical solvent is propylene carbonate [25]. Research is being conducted to discover or to improve the available physical solvents that can achieve high carbon dioxide loading at higher temperature.

2.2.3 Chemical looping

Another way to achieve concentrated CO_2 stream for the purpose of pre-combustion carbon capture is through looping. The combustion process is this method is divided into two reactors. In the first reactor oxygen is taken from the air. This is then transferred to the other reactor. Combustion takes place in the reactor along with the formation of carbon dioxide. Usually a metal is used for transferring oxygen from the first to the second reactor. The metal gets oxidized to metal oxides in the first reactor then it subsequently gets reduced in the second reactor by reacting with the fuel. The reactions involved in this process are as follows;

1st Reactor:

$$2Me + O_2 \longrightarrow 2MeO \tag{2.1}$$

2nd Reactor:

$$(2n+m)\,MeO + C_nH_{2m} \longrightarrow (2n+m)\,MeO + m\,H_2O + n\,CO_2 \tag{2.2}$$

A schematic of the chemical looping process has been shown in figure 4.

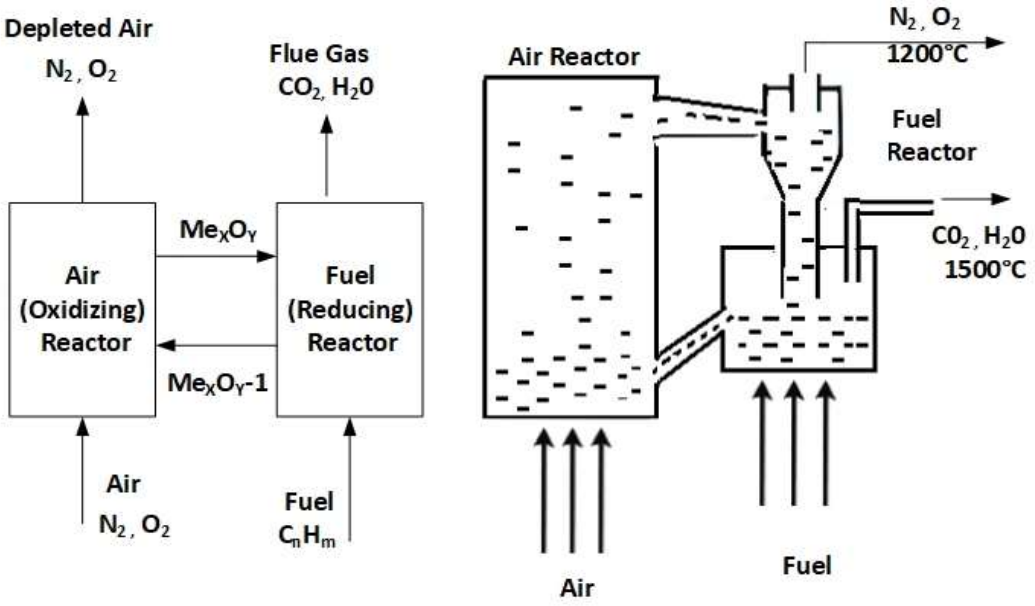

Figure 4: Chemical looping process

2.3 Oxy-combustion

Oxy-combustion process helps improve the concentration of CO_2 in the flue gas ensuring better carbon capture. This process involves the burning of the fuel with highly pure oxygen along with a recycle stream coming out of the flue gas. This process sometimes involves a cryogenic air separation unit. Nearly pure oxygen is produced from this cryogenic air separator unit which is then mixed flue gas prior to combustion. This process produces flue gas which consists of CO_2 and water. From which carbon dioxide can be easily separated. The overall operational cost of the oxy-combustion process is expected

to be lower than that of the pre-combustion processes. However, cryogenic air separators are known to be expensive which might result in a higher capital cost [25]. The schematic of the oxy-combustion process has been shown in figure 5.

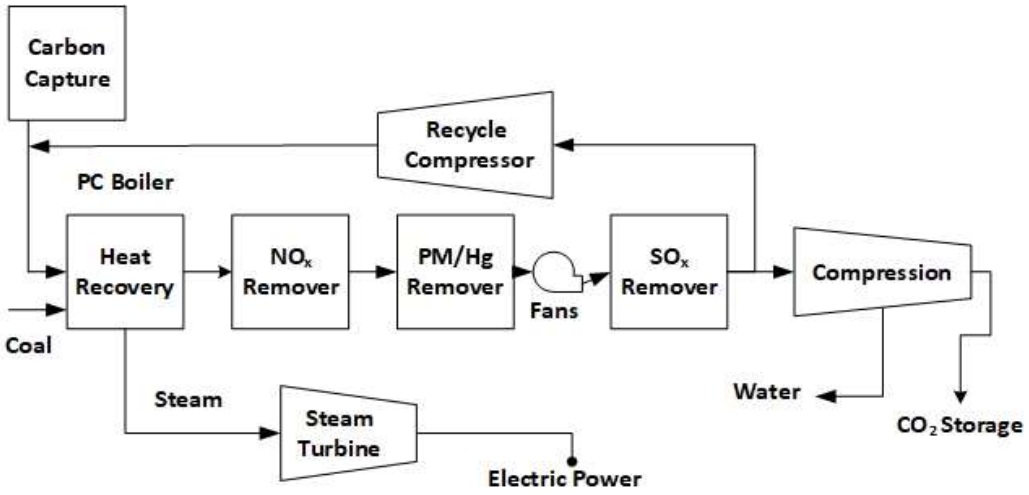

Figure 5: Oxy-combustion process

In order to tackle the overall issue of CO_2, knowledge regarding the different technologies that helps in its reduction is highly compulsory. Different possible technologies can be used in accordance of the industrial and governmental needs. Continuous research is being done to further improve the already available technologies. However, to ensure these technologies are used in the industry will require sincerity to take necessary steps to abate the carbon emissions to ensure better environment for the future generations. Since the Amine based post-combustion technology is accepted as the most cost-effective

technology, this project discovers the kinetics of amino acids and its MDEA blends to be used as an alternative to the amines in this technology. The following chapter discusses the solvents that are currently being used in post-combustion carbon capture along with their drawbacks and introduces amino acids as promising solvent for CO_2 capture.

Chapter 3. Solvents for CO_2 Capture

The solvent-based CO_2 capture processes have been in use in the industries in the last few decades. The process involves chemical absorption of CO_2 and is considered to be most mature technology for capturing CO_2 [13, 42]. Although, the growing concern to address the issues related to global warming has driven the need for solvent based absorption to reduce the carbon dioxide emissions from industry, quite surprisingly, this technology was first introduced to recover CO_2 to applied in the enhanced oil recovery (EOR). Between the late 1970's to early 1980's, the solvent based CO_2 capture plants were being operated in the US for the purpose of EOR. However, the plants were closed in the mid 1980's as 4the oil prices dropped and capturing CO_2 became economically unreasonable [42]. However, now that the importance of capturing CO_2 from the power plant cannot be undermined, the solvent based CO_2 capture plants has re-emerged as the most promising technology and continuous research is being conducted to develop new solvents in order to make the technology both economically and environmentally feasible.

3.1 Amine-based Post Combustion CO_2 Capture

Since the present work focuses on amino acids to be used as solvent for PCCC, it is quintessential to understand the process of an ideal solvent-based CO_2 capture plant. In this process, CO_2 undergoes a reversible reaction with the amine solvent. This reversible reaction is temperature dependent, this temperature dependency of CO_2 capture plants

can be manipulated to remove the carbon dioxide from the flue gas. At first, the NO_x and SO_X present in the flue gas are removed before it is introduced in the absorber column. This step is required to prevent the formation of any unnecessary by-products. Afterwards, the flue gas is cooled and fed to the bottom of the absorber column. The temperature of the absorber column varies between 313 K to 333 K, the solvent is introduced from the top of absorber and it gets saturated with CO_2 from the feed gas as it leaves the absorber bottom [43]. This CO_2 saturated solvent is known as the rich amine solvent. The treated gas leaves from the top of the absorber and it is either further processed or simply released to the atmosphere. The rich amine solvent is then heated by the lean amine solvent coming from the desorber column and introduced at the top of the column. While the pressure in the desorber or stripping column is little above the atmospheric pressure, the temperature varies between 373 K to 413 K, this increase in temperature triggers a reversible reaction, causing the CO_2 to be removed from rich amine solvent within the column [42, 43]. The heat required for regeneration is supplied through reboilers. Thus, the amine solvent is regenerated which can be pumped back into the absorber for further CO_2 absorption. The stripped gas coming from the top of the desorber consists of CO_2 and steam. The steam is recovered in the condenser while the CO_2 is compressed. Thus, CO_2 is removed in this process through continuous recycling of the amine solvents between the absorber and the desorber column. A typical amine-based CO_2 capture process has been shown in figure 6.

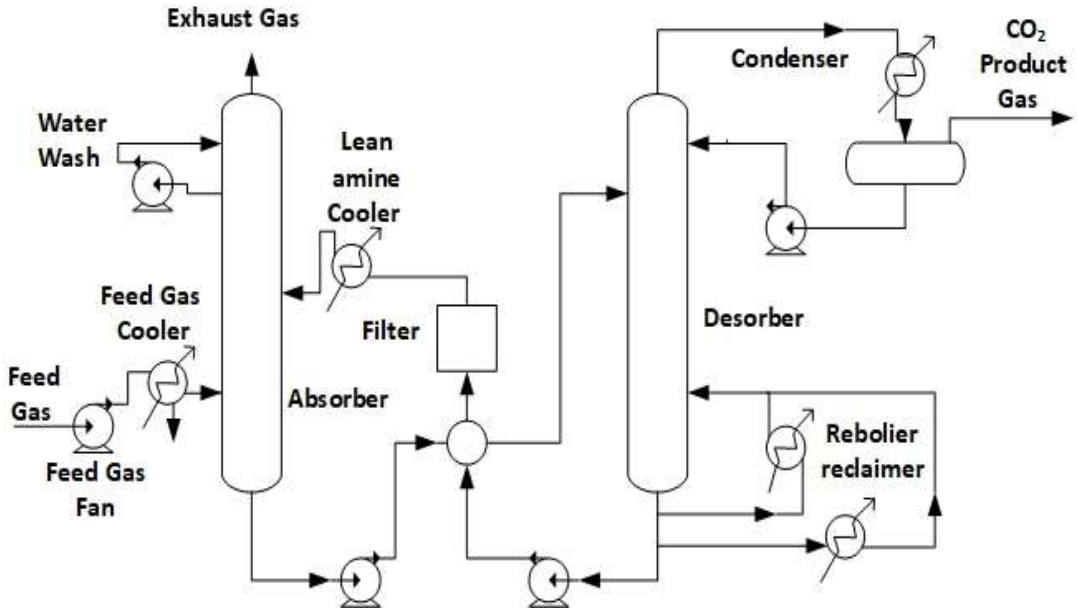

Figure 6: A typical amine-based CO2 capture process [43]

Since the success of this CO_2 capture process depends on the reaction of CO_2 with the amine solvent, different types of amine solvents have been used for this process. The common alkanolamine solvents used in CO_2 capture process are further discussed in the following section.

3.2 Alkanolamines

Alkanolamines are the most common types of amine solvents used for a typical CO_2 capture plant. The alkanolamines have hydroxyl (-OH) and an amine ($-NH_2$) functional group present within their structure which favor the absorption of CO_2 [17, 44].

Alkanolamines can mainly categorized into different types on the basis of their structure; they are primary, secondary, tertiary and sterically hindered amines [17]. Their reaction mechanism and kinetics with CO_2 varies depending on their structure [45]. Monoethanolamine (MEA), Diethanolamine (DEA), Methyldiethanolamine (MDEA) and 2-Amine-2-Methyl-1-Propanol (AMP) are the most common types f amine used for carbon dioxide absorption [14, 15]. On the basis of their structure, MEA is primary amine, DEA is secondary amine, MDEA is tertiary amine and AMP is sterically hindered amine.

MEA is the most extensively studied amine for CO_2 capture. The cost of MEA is comparatively lower than the other amines yet Its reaction of CO_2 is very fast, which helps in limiting the height of the absorber column [42, 46]. MEA being a primary amine, reacts with CO_2 to form carbamates. Because of which it has a relatively high heat of CO_2 absorption. This also adds to the requirement of more heat for solvent regeneration. Furthermore, formation of carbamates also limits the loading capability of the MEA solvents. Moreover, it can undergo oxidative degradation depending on the flue gas condition and it also undergoes thermal degradation at high temperatures. Because of which MEA based CO_2 capture plants might require regular solvent makeup. Similar disadvantages are also observed in the case of secondary amines like DEA, as it also forms a carbamate when reacted with CO_2 [42].

MDEA, is a tertiary amine, unlike the primary and secondary amines, their reaction does not involve the formation of carbamates. It does not react with carbon dioxide directly, it rather acts as base to hydrolyze CO_2 into forming protonated amine along with bicarbonates. They require less heat for regeneration as heat formation of bicarbonates

is fairly lower than the heat for carbamate formation. Moreover, MDEA have higher loading capability compared to that of the primary and secondary amines. However, their rate of reaction with CO_2 is very slow [47].

Sterically hindered amines like AMP, also forms carbamates like the primary and secondary amines when reacted with CO_2. However, the carbamate formed is very unstable. This formation of unstable carbamates is directly related to their molecular structure [46, 48]. They have molecular substituent groups attached to their α-carbon which causes a steric effect resulting in the formation of unstable carbamates. As a result of this effect, sterically hindered amines reportedly have higher loading capability with lower heat of absorption compared to the primary and secondary amines. Also, their reaction rate with CO_2 is relatively faster than MDEA [48]. The structures of alkanolamines are shown in figure 7 below;

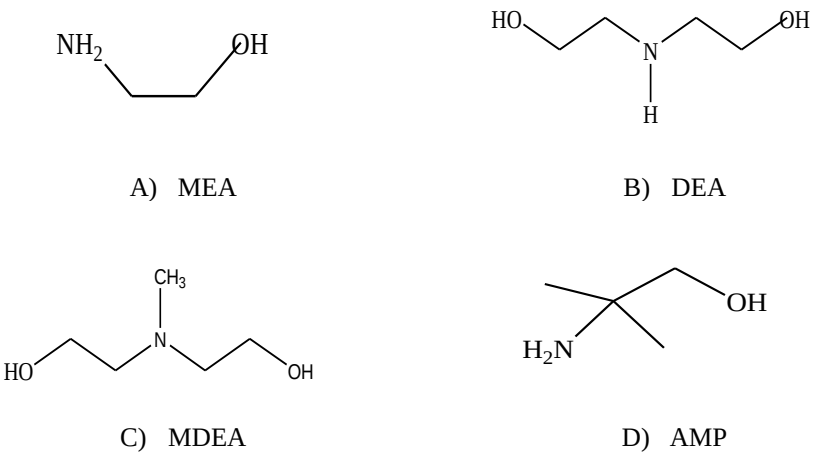

A) MEA B) DEA

C) MDEA D) AMP

Figure 7: Structures of Conventional alkanolamines

Blended alkanolamine systems have also garnered a lot interest to be used in the CO_2 capture process. These systems involve the combination of two or more amines in such a way that the undesirable property of one particular amine is compensated by the presence of the other amine with the blend. The development of such solvents was first coined by Chakraverty et al.[49] when they proposed to mix the tertiary amine with either a primary or secondary amine. Since then a number research has been carried out on development on blended systems. Most of the blended systems, make use of MDEA as a key component to make use of their high loading capability while adding a small amount primary or secondary amine to act as a promoter to enhance the rate of their reactions [18]. The benefits of blended amine systems are many and common blended amine systems that have been widely studied includes MDEA-MEA, MDEA-DEA and MDEA-AMP [4, 14, 29, 50].

Clearly, there are several advantages of using alkanolamines as solvent for CO_2 capture, However, they have some undesirable characteristics such as;

- Regular Solvent Make-up: Significant loss in solvent can caused by oxidative and thermal degradation, which needs to compensated through regular solvent make up.
- High energy requirement for regeneration: Depending on the reaction of the amine solvent with CO_2, the regeneration energy varies. The energy required for regeneration is adds to the cost of the whole CO_2 capture process.
- Low loading capability: The low loading capability of makes the whole CO_2 process less efficient.

- Corrosion: Degradation of amine solvent forms several by-products presence of which can corrode the absorber and stripper units.
- Environmental Concerns: Some of the degradation products of alkanolamines are non-biodegradable and toxic in nature. They may come out with the exhaust streams and cause harm to surrounding environment.

Therefore, it is necessary to develop new cost effective and environmentally safe solvents that can be used as alternative to the conventional ones. The following section discusses the potential of Amino acids to be used as a replacement for the conventional amine solvents.

3.3 Amino Acids

Amino acids are quite similar in structure to the conventional alkanolamines. They generally have one amino group ($-NH_2$) along with an additional carboxyl acid group (-COOH) or a sulfonic acid group ($-SO_3H$). The amino acids are amphoteric in nature which means they exist as zwitterion in aqueous solutions with a net neutral charge. Addition of an acid, triggers the basic part of the amino acid to accept a proton while addition of an base, triggers the removal of proton from its ammonium group [43, 51]. CO_2 reacts with amino acids and acts as acid resulting in the deprotonation of the zwitterion formed from amino acids. Thus the reaction of amino acids with CO_2 will form carbamates and zwitterions. The amino acids are referred to as α-amino acids [52]. Primarily because of the presence of an α-carbon that has both the amino and carboxylic acid attached to its

either sides. The structure of an α-amino acid is shown in figure 8 Below;

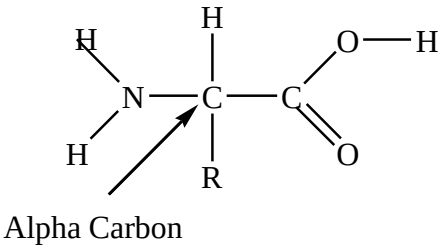

Figure 8: α-amino acid structure

Since the α-carbon present in the structure of amino acids is asymmetrical in nature, the amino acids can exist in the form of two different stereoisomers [52]. This characteristic is prevalent among most of the amino acids except for glycine. It is to be noted this characteristic of presence of an α-carbon is similar to the characteristics observed in the case of the sterically hinder amine, AMP. Based on this it can be concluded, that all the amino acids are sterically hindered except for glycine. The molecular structure of different amino acids is shown in the figure 9 in the following page.

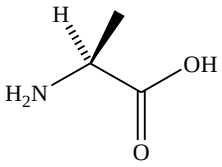

1. L-alanine

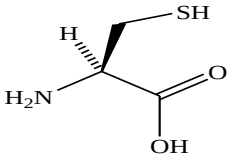

2. L-cysteine

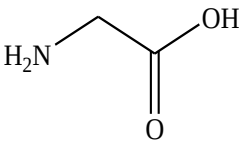

3. Glycine

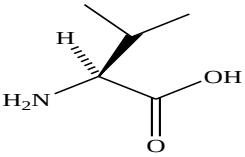

4. L-valine

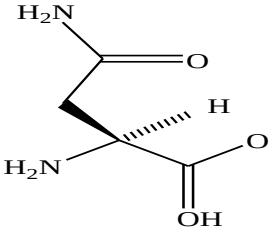

5. L-asparagine

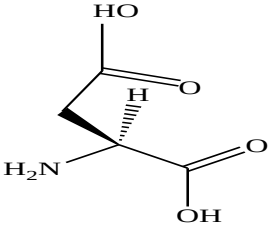

6. L-aspartic Acid

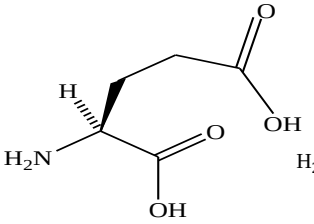

7. L-glutamic acid

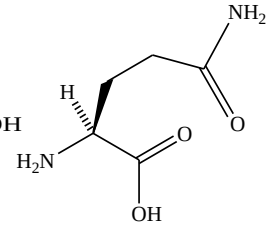

8. L-glutamine

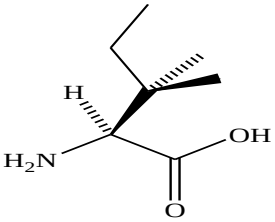

9. L-isoleucine

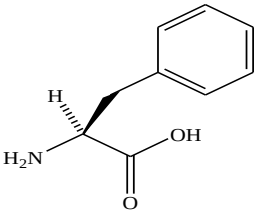

10. L-phenylalanine

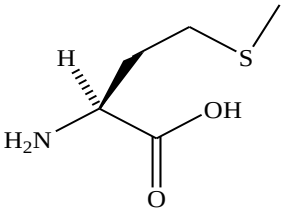

11. L-methionine

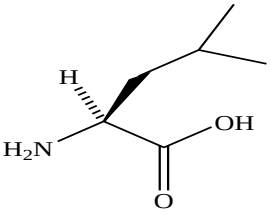

12. L-leucine

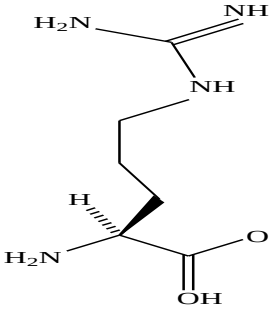

13. L-arginine

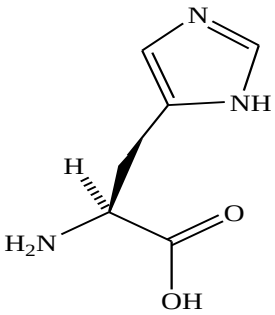

14. L-histidine

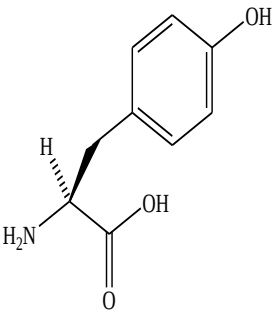

15. L-tyrosine

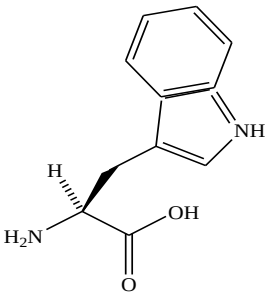

16. L-tryptophan

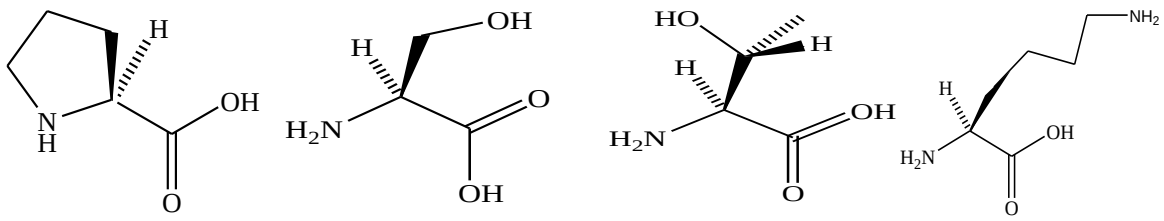

17. L-proline 18. L-serine 19. L-threonine 20. L-lysine

Figure 9: Structures of amino acids [51]

As it can be observed from figure 9, the amino acids are chemically diverse. The amino acids are crystalline in nature. They are non-toxic with no environmental drawbacks [43]. The zwitterion formed by the amino acids acts as a salt with properties of inorganic salts [53]. The amino acid glycine has been used in the Giammarco-Vetrocoke process for activation of alkali carbonate solutions. The use of glycine was alternated with the use of secondary amine, DEA for the same purpose in this process. Of the two solutions, It was observed that the glycine activated solution showed higher absorption rates with better overall efficiency compared to the DEA-activated solutions. Furthermore, they were found to be more stable and less corrosive to the conventional alkanolamines [14, 49]. Because of these favorable properties, a wide range of amino acids are now being studied for purpose of CO_2 capture.

In the recent years, the aqueous alkaline salts of amino acids (AAS) have also emerged as another most promising alternative to be used for CO_2 capture both as an individual solvent or a rate promoter [54]. Their structure comprises of an amino group (-

NH_2) which is synonymous to alkanolamines, along with an additional carboxylic acid group(-COOH) and a counter ion (Na^+ or K^+). The aqueous salts of amino acids (AAS) are environmentally benign, less volatile and resistive to oxidative degradation [17, 54-57]. Since the knowledge of the reaction kinetics and mechanism between the AAS and CO_2 is essential for proper design of absorption processes and several studies have presented data on the reactions kinetics of CO_2 with different AAS [55-71]. Van Holst et al. [72] investigated the overall rate constants of glycinate, prolinate, sarcosinate and taurate and came to a conclusion that they were comparable to that of alkanolamines. Portugal et al. [73] studied the reaction rate of potassium salts of glycine over a concentration and temperature range of 0.1–3 mol/l and 293-313 K, respectively and concluded that at same temperature and same concentration, the reaction rate of potassium salt of glycine was higher than MEA. Majchrowicz et al. [62] studied the absorption rate of CO_2 in the potassium salts of proline (ProK) within the concentration range of 0.5-3 mol/l over 290-323 K using stirred cell reactor. Upon comparing, they observed that their (ProK) reactivity towards CO_2 was also higher than MEA and comparable with glycinate. Majchrowiz et al. further noted that the presence of Potassium (K) instead sodium (Na) as a counter ion in the amino acids can enhance the reactivity towards CO_2. This statement can be further affirmed by noticing the higher rate constant obtained for CO_2-KGly reaction from the work of the thee et al. compared to that of CO_2-NaGly reaction obtained in the work of Lee et al.[59, 71].

Paul and Thompson investigated the potassium salts of proline and concluded the same [61]. Simons et al. and Van Holst et al. studied the kinetics of salts of sarcosine using

stirred cell reactor [57, 74]. Aronu et al. studied the same using string-of-disks contactor [69]. All three of the works observed higher reaction rate for salts of sarcosine (SarK) compared to alkanolamines. However, there were significant difference between their reported absorption rates of CO_2 in potassium salts of sarcosine. The kinetics of CO_2 in potassium salts of Threonate (ThrK) were studied within the concentration range of 0.1 to 3.0 mol/l at different temperatures by Hwang et al. and Portugal et al., which the latter concluded that it showed slower kinetics than primary amines due to formation of unstable carbamates [60, 70]. Lim et al. and kim et al. studied potassium salt L-alanine and observed higher CO_2 loading capacity than the MEA but lower CO_2 absorption rate [64, 65]. Kinetics of CO_2 into aqueous potassium Lysinate (KLys) and aqueous potassium salt of Histidine (KHis) was recently investigated at a temperature range of 298-333 K within concentration range of 0.25 to 2.0 mol/l and 0.26 to 2.07 mol/l, respectively by Shen et al. using a wetted wall column. Upon comparing reactivity towards CO_2 with MEA, they observed that reactivity of KLys was more than that of MEA, while the reactivity of KHis was comparable to the same [67, 68]. Potassium salts of taurine (KTau) is also another promising aqueous amino acid salt. Their structure is almost similar to the structure of AAS, except they contain one sulfonic group instead of a carboxylic acid, which makes them more resistive to degradation and less corrosive compared to other amino acid salts [56]. Sodiq et al. investigated the Ktau reaction kinetics at very low concentrations and observed that CO_2-KTau reactions were slower than the CO_2-MEA [63]. Contrary to their work, Kumar et al. studied their reaction kinetics at a concentration range of 0.1-4 mol/l at temperature of 285-305 K using stirred cell reactor. Their

investigation revealed that CO_2-KTau reactions were faster than the CO_2-MEA reactions. They also added that the reaction order increases from 1 to 1.5 with the increase in concentrations [55]. From all these works, It is evident the use of highly reactive amino acid salts can significantly improve the CO_2 absorption processes. But there are some drawbacks associated with their use as well. It has been reported that the amino acid salts precipitates when used at high concentrations or high CO_2 loading. Formation of precipitate will reduce the mass transfer rate, eventually increasing the possibility of damaging process equipment [17]. These drawbacks may prevent them from being used as individual solvents. However, owing to their reactive properties, they can be utilized as promoters to enhance the reaction rate of CO_2 with tertiary amines.

The amino acids have undeniable potentials to be used as an individual solvent or a promoter for CO_2. However, before suggesting a particular amino acid to be used for CO_2 capture process, a number of questions needs to be addressed regarding their reaction mechanism and kinetics with CO_2, loading capability, degradability, heat of absorption CO_2 and so on. This project focusses to present kinetic data on the CO_2-Glycine and CO_2-L-Arginine reactions and study their reaction mechanisms using the stopped-flow technique. It also aims to present their kinetic effect when blended with MDEA. Since the kinetics of alkanolamines with CO_2 have been extensively studied over the past few years, a number of theories regarding the reaction pathways are available in the literature. In the following chapter discusses the different reaction pathways of CO_2-amine systems and suggests the possible pathways for the four targeted amine systems.

Chapter 4. Kinetics of Amino Acids and their Blends

4.1 Reaction Mechanisms

Since the alkanolamines are frequently used for the purpose of acid gas removal (CO_2 and H_2S) from several industrial processes, correct understanding of their reaction mechanism with CO_2 is of paramount importance. Over the years, various reaction mechanisms have been proposed to interpret the reaction kinetics of CO_2 with alkanolamines. However, it is widely accepted that their reaction is commonly based on three mechanisms i.e. the zwitterion mechanism, termolecular mechanism and base catalyzed hydration mechanism. The zwitterion and termolecular mechanism is mainly used to describe the reaction of primary, secondary and sterically hindered amines with CO_2, while the base catalyzed hydration mechanism is used to describe the reaction of tertiary amines with CO_2 [75]. The molecular structure of amino acids is quite similar to the primary amines; therefore, it can be expected that the reaction pathway of CO_2-Amino Acids will be similar to that of the reaction pathway of CO_2-Amine [55]. Hence, in order to describe their reaction with amino acids and their blends, the zwitterion and termolecular mechanisms will be used in this work.

4.1.1 Zwitterion Mechanism

One of the most common mechanism used to explain the reaction of CO_2 with amines is the zwitterionic mechanism. It is a two-step mechanism that was suggested by Caplow et al. [76] and later it was reintroduced by Danckwerts [77]. In the first step, the CO_2 is

bounded with amino group of the primary or secondary amine which results in the formation of a zwitterion. In the second step, the zwitterion formed, undergoes rapid deprotonation via H^+ ions exchange of with water and the other bases eventually leading to the formation of a Carbamate.

$$CO_2 + NHRR'COO^- \underset{k_{-1}}{\overset{k_2}{\rightleftharpoons}} {}^-OOCNH^+RR'COO^- \tag{4.1}$$

$${}^-OOCNH^+RR'COO^- + B \underset{k_{-b}}{\overset{k_b}{\rightleftharpoons}} {}^-OOCNRR'COO^- + BH^+ \tag{4.2}$$

Upon applying the steady-state principle to the intermediate zwitterion, the rate of reaction of CO_2 in aqueous solutions of amines can be described as:

$$r_{CO_2} = -k_{ov}[CO_2] = -\frac{k_2[CO_2][AA]}{1+(k_{-1}/(\sum k_{b_i}[B_i])} \tag{4.3}$$

where the terms in brackets represents the concentrations in mol.L^{-1}, the term 'B' represents all the bases, while k_{bi} denotes the rate of the deprotonation of the zwitterion by any bases. The equation can be further simplified by assuming some asymptotic cases [55]. When the term $\frac{k_{-1}}{\sum k_{b_i}[B_i]}$ << 1, the equation (3) simplifies to;

$$r_{CO_2} = k_2[AA][CO_2] \tag{4.4}$$

This usually occurs for amines that exhibit second order kinetics and it indicates that the deprotonation of zwitterion is faster than the reversion reaction of CO_2 and amine. When the term $\frac{k_{-1}}{\sum k_{b_i}[B_i]}$) >> 1, the equation (3) can be rewritten to the following form;

$$r_{CO_2} = k_2[AA][CO_2](\frac{\sum k_{b_i}[B_i]}{k_{-1}}) \tag{4.5}$$

This equation enables the interpretation of reaction of any order depending on the contribution of the available bases for the deprotonation of the zwitterion. In case of the

secondary amines, change in the concentration can result in the shift in the reaction order as observed in case of diethanolamines [78]. The equation 5 enables the interpretation of this shift observed in the case of secondary amines. Furthermore, it can also be used to interpret the third order reactions.

However, when the deprotonation zwitterion is solely caused by the amine, then the equation (3) is enough to describe the reaction. In case of amino acids, deprotonated amino acid, water molecules and hydroxyl ions will act as the bases. Therefore, the overall reaction rate becomes:

$$k_{ov} = \frac{k_2[AA]}{1+\frac{k_{-1}}{k_{AA}[AA]+k_{OH^-}[OH^-]+k_{H_2O}[H_2O]}} \tag{4.6}$$

Now by defining new constants as $k_\beta = \frac{k_2 k_{AA}}{k_{-1}}$, $k_{hyd} = \frac{k_2 k_{OH^-}}{k_{-1}}$ and $k_w = \frac{k_2 k_{H_2O}}{k_{-1}}$, equation 6 then can be rewritten as:

$$k_{ov} = \frac{[AA]}{\frac{1}{k_2}+\frac{1}{k_\beta[AA]+k_{hyd}[OH^-]+k_w[H_2O]}} \tag{4.7}$$

4.1.2 Termolecular Mechanism

Crooks and Donnellan [79] questioned the validity of the two-step zwitterion mechanism and proposed a single step mechanism known otherwise as the termolecular mechanism. In this mechanism, the amine molecule simultaneously reacts with a molecule of base and a molecule of CO_2 forming a loosely bound complex intermediate.

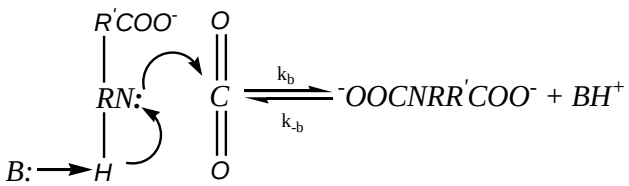

(4.8)

Da Silva and Svendson [80] further investigated the termolcular mechanism and suggested that the loosely bound complex intermediate is formed via the bonding of the CO_2 molecule with the amine which is stabilized by solvent molecules with hydrogen bonds. They also noted that the carbamate only forms when the amine molecule is in the vicinity of zwitterion. When carbamates are not formed it means the zwitterion has reverted back to free CO_2 and amine. The rate expression analysis of the termolecular mechanism shows that the reaction of CO_2 with amine is second order with respect to amine. Therefore, in this case, equation (3) becomes,

$$r_{CO_2} = k_{ov}[CO_2] = [CO_2][AA]\{\sum k_{b_i}[B_i]\} \quad (4.9)$$

In case of the amino acids, using the previously defined constants, the overall reaction rate based on the termolecular mechanism can be written as:

$$k_{ov} = [AA]\{k_{\beta}[AA] + k_{hyd}[OH^-] + k_w[H_2O]\} \quad (4.10)$$

Regardless of the mechanism is employed, a carbamate and a protonated base are the generally accepted products of the CO_2 reaction with amine.

4.1.3 Base-Catalyzed Hydration Mechanism

Donaldson and Nguyen [81] proposed the base-catalyzed hydration mechanism to account for the reaction of tertiary amines based on the suggestion that tertiary alkanolamines cannot react with CO_2 directly. These amines are expected to have base catalyzed effect on CO_2 hydration. The credibility of this mechanism was further investigated by Versteeg and Van Swaaij [75] via absorption of CO_2 into water-free MDEA and ethanol. They concluded that the CO_2 is only physically absorbed, proving the

correctness of the proposed mechanism. Base catalyzed hydration can be represented by following reaction;

$$R_3N + H_2O + CO_2 \xrightarrow{k'} R_3N^+H + HCO_3^- \quad (4.11)$$

Amine dissociation in aqueous solution may occur in the following manner:

$$R_3N + H_2O \rightleftharpoons R_3N^+H + OH^- \quad (4.12)$$

In general, the direct reaction of between tertiary amines and CO_2 may only occur at high pH values with formation of monoalkyl carbonate as reported by Jorgensen and Faurholt [82]. However, when the pH value is less than 12, the rate of this reaction can be neglected [83]. Hence, rate of reaction of CO_2 based on base catalysis mechanism can be given by;

$$r_{CO_2} = [CO_2]\{k'^{[R_3N]} + k_{hyd}[OH^-] + k_w[H_2O]\} \quad (4.13)$$

Based overall reaction rate of this reaction can be given by;

$$k_{ov} = k'[R_3N] + k_{hyd}[OH^-] + k_w[H_2O] \quad (4.14)$$

The apparent reaction rate of the tertiary amine can be eventually defined as:

$$k_{app} = k'[R_3N] \quad (4.15)$$

4.2 Reaction Scheme and Kinetics of amino acid systems

On the basis of the reaction mechanisms discussed, a suitable reaction kinetics model capable of predicting the kinetics data can be developed by taking into account all the possible reactions taking place in a particular amine system.

4.2.1 Kinetics of Glycine-CO_2 reaction

If the reaction of Glycine with CO_2 proceeds via the zwitterion mechanism, then the chemical reactions taking place in the aqueous system of CO_2-Glycine are primarily governed by the following equations:

$$CO_2 + OH^- \xrightarrow{k_{OH}} HCO_3^- \quad (4.16)$$

$$H_2O \overset{K_W}{\longleftrightarrow} H^+ + OH^- \quad (4.17)$$

$$CO_2 + NHRCOO^- \underset{k_{-1}}{\overset{k_2}{\rightleftharpoons}} {}^-OOCNH^+RCOO^- \quad (4.18)$$

$${}^-OOCNH^+RCOO^- + B \underset{k_{-b}}{\overset{k_b}{\rightleftharpoons}} {}^-OOCNRCOO^- + BH^+ \quad (4.19)$$

In the equation above, the term 'R' represents the methyl (-CH_4) group and the term 'B' represents all the bases that are present within this system. In case of CO_2-Glycine system, deprotonated Glycine, the hydroxyl ion and the water molecules act as the bases. Based on which the rate of reaction of CO_2 with Glycine can be given by the following equation;

$$r_{CO_2} = -k_{ov}[CO_2] = -\frac{k_2[CO_2][Gly]}{1+(k_{-1}/(\sum k_{b_i}[B_i]} \quad (4.20)$$

Now by defining new constants as $k_{Gly} = \frac{k_2 k_G}{k_{-1}}$, $k_{hyd} = \frac{k_2 k_{OH^-}}{k_{-1}}$ and $k_w = \frac{k_2 k_{H_2O}}{k_{-1}}$, the overall reaction rate can be defined as:

$$k_{ov} = \frac{[Gly]}{\frac{1}{k_2}+\frac{1}{k_{Gly}[Gly]+k_{hyd}[OH^-]+k_w[H_2O]}} \quad (4.21)$$

Due to the slow kinetics exhibited by the reaction of the hydroxide ions with CO_2 in aqueous solution to form bicarbonate ion was has been neglected in the analysis of CO_2-Amino acid systems as was already demonstrated in the work of Guo et al.[84]. On the

other hand, if the reaction Glycine with CO_2 proceeds via the termolecular mechanism, then their reaction can be represented by the following equation;

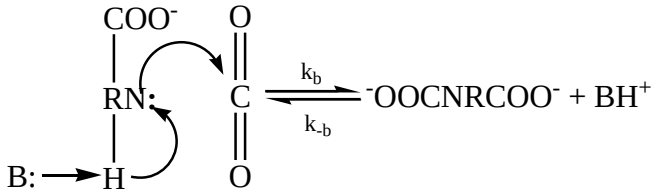

(4.22)

Similar to the zwitterion mechanism, here, the term 'B' also represents all the bases that are present within the system and the overall reaction rate for the CO_2-Glycine system based on the termolecular mechanism can be given by;

$$k_{ov} = [Gly]\{k_{Gly}[Gly] + k_{hyd}[OH^-] + k_w[H_2O]\} \quad (4.23)$$

4.2.2 Kinetics of L-Arginine-CO_2 reaction

Similar to that of CO_2-Glycine system, when the reaction of L-Arginine with CO_2 proceeds via the zwitterion mechanism, then the chemical reactions for CO_2-L-Arginine are primarily governed by the following equations:

$$CO_2 + OH^- \xrightarrow{k_{OH}} HCO_3^- \quad (4.24)$$

$$H_2O \xleftrightarrow{K_W} H^+ + OH^- \quad (4.25)$$

$$CO_2 + H_2NR'COO^- \underset{k_{-1}}{\overset{k_2}{\rightleftharpoons}} {}^-OOCNH^+R'COOH \quad (4.26)$$

$$^-OOCNH^+R'COOH + B \underset{k_{-b}}{\overset{k_b}{\rightleftharpoons}} {}^-OOCNH^+R'COOH + BH^+ \quad (4.27)$$

In the equation above, R'=$C_5H_{12}N_3$ and the term 'B' represents deprotonated l-Arginine, the hydroxyl ion and the water molecules that act as the bases. Based on which the rate

of reaction of CO_2 with L-Arginine can be given by the following equation;

$$r_{CO_2} = -k_{ov}[CO_2] = -\frac{k_2[CO_2][Arg]}{1+(k_{-1}/(\sum k_{b_i}[B_i]} \quad (4.28)$$

Now by defining new constants as $k_{Arg} = \frac{k_2 k_A}{k_{-1}}$, $k_{hyd} = \frac{k_2 k_{OH^-}}{k_{-1}}$ and $k_w = \frac{k_2 k_{H_2O}}{k_{-1}}$, the overall reaction rate can be defined as:

$$k_{ov} = \frac{[Arg]}{\frac{1}{k_2}+\frac{1}{k_{Arg}[Arg]+k_{hyd}[OH^-]+k_w[H_2O]}} \quad (4.29)$$

On the contrary, when the reaction L-Arginine with CO_2 proceeds via the termolecular mechanism, then their reaction can be represented by the following equation;

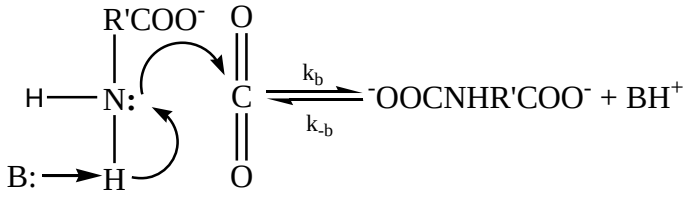

(4.30)

Considering the term 'B' as a representation of all bases present within in the system, the overall reaction rate for the CO_2-L-Arginine system on the basis of the termolecular mechanism can be given by;

$$k_{ov} = [Arg]\{k_{Arg}[Arg] + k_{hyd}[OH^-] + k_w[H_2O]\} \quad (4.31)$$

4.2.3 Kinetics of MDEA-Glycine-CO_2 reaction

The reaction of CO_2 with MDEA-Glycine blend is expected to be governed by the same set of reactions of CO_2-Glycine system but with an additional reaction accounting for CO_2-MDEA reaction given below;

$$CO_2 + H_3CN(C_2H_4OH)_2 + H_2O \underset{}{\overset{k_{MDEA}}{\rightleftharpoons}} H_3CNH^+(C_2H_4OH)_2 + HCO_3^- \quad (4.32)$$

Since, MDEA is a tertiary amine, the rate of reaction of CO_2 with MDEA can be given by the following equation;

$$r_{CO_2-MDEA} = -k_{MDEA}[CO_2][MDEA] \quad (4.33)$$

When the reaction is expected proceed via the zwitterion mechanism then the following are the reactions in the CO_2-MDEA-Glycine system.

$$CO_2 + OH^- \xrightarrow{k_{OH}} HCO_3^- \quad (4.34)$$

$$H_2O \overset{K_W}{\longleftrightarrow} H^+ + OH^- \quad (4.35)$$

$$CO_2 + H_3CN(C_2H_4OH)_2 + H_2O \overset{k_{MDEA}}{\rightleftharpoons} H_3CNH^+(C_2H_4OH)_2 + HCO_3^- \quad (4.36)$$

$$CO_2 + NHRCOO^- \underset{k_{-1}}{\overset{k_2}{\rightleftharpoons}} {}^-OOCNH^+RCOO^- \quad (4.37)$$

$${}^-OOCNH^+RCOO^- + B \underset{k_{-b}}{\overset{k_b}{\rightleftharpoons}} {}^-OOCNRCOO^- + BH^+ \quad (4.38)$$

The rate of reaction CO_2 with hydroxide to form carbonate can be given by the following equation;

$$r_{CO_2-OH^-} = -k_{OH}[CO_2][OH^-] \quad (4.39)$$

Overall, the rate of reaction of CO_2 with the blend of MDEA-Glycine can be considered to be the sum of the CO_2-MDEA, CO_2-OH^- and CO_2-Glycine reactions.

$$r_{CO_2} = r_{CO_2-MDEA} + r_{CO_2-Gly} + r_{CO_2-OH^-} \quad (4.40)$$

Which can be written as:

$$r_{CO_2} = k_{ov}[CO_2] = \left(\frac{k_2[Gly]}{1+\frac{k_{-1}}{\Sigma k_{b_i}[B_i]}} + k_{MDEA}[MDEA] + k_{OH}[OH^-]\right)[CO_2] \quad (4.41)$$

The overall reaction rate can be given by;

$$k_{ov} = k_{app} + k_{MDEA}[MDEA] + k_{OH}[OH^-] \quad (4.42)$$

It is to be noted that the similar approach will be followed to determine the apparent rate constant, when the reaction of CO_2-MDEA-Glycine system is expected to proceed via the termolecular mechanism. Based on which the overall reaction rate for CO_2-MDEA-Gly system can be given as;

$$k_{ov} = [Gly]\{k_{Gly}[Gly] + k_{hyd}[OH^-] + k_w[H_2O]\} + k_{MDEA}[MDEA] + k_{OH}[OH^-] \quad (4.43)$$

4.2.4 Kinetics of MDEA-Arginine-CO_2 reaction

The reaction of CO_2 with MDEA-L-Arginine blend can also be depicted using the same approach used for CO_2-MDEA-Glycine system. The set of reactions that govern the MDEA-L-Arginine system are as follows;

$$CO_2 + OH^- \xrightarrow{k_{OH}} HCO_3^- \quad (4.44)$$

$$CO_2 + H_3CN(C_2H_4OH)_2 + H_2O \underset{}{\overset{k_{MDEA}}{\rightleftharpoons}} H_3CNH^+(C_2H_4OH)_2 + HCO_3^- \quad (4.45)$$

$$CO_2 + H_2NR'COO^- \underset{k_{-1}}{\overset{k_2}{\rightleftharpoons}} {}^-OOCNH^+R'COOH \quad (4.46)$$

$${}^-OOCNH^+R'COOH + B \underset{k_{-b}}{\overset{k_b}{\rightleftharpoons}} {}^-OOCNH^+R'COOH + BH^+ \quad (4.47)$$

Overall, the rate of reaction of CO_2 with the blend of MDEA-L-Arginine can be given by;

$$r_{CO_2} = r_{CO_2-MDEA} + r_{CO_2-Arg} + r_{CO_2-OH^-} \quad (4.48)$$

Which can be written as:

$$r_{CO_2} = k_{ov}[CO_2] = \left(\frac{k_2[Arg]}{1+\frac{k_{-1}}{\Sigma k_{b_i}[B_i]}} + k_{MDEA}[MDEA] + k_{OH}[OH^-]\right)[CO_2] \quad (4.49)$$

The overall reaction rate can be given by;

$$k_{ov} = k_{app} + k_{MDEA}[MDEA] + k_{OH}[OH^-] \quad (4.50)$$

Based on the termolecular mechanism, the overall reaction rate for CO_2-MDEA-Gly system can be given as;

$$k_{ov} = [Arg]\{k_{Arg}[Arg] + k_{hyd}[OH^-] + k_w[H_2O]\} + k_{MDEA}[MDEA] + k_{OH}[OH^-] \quad (4.51)$$

It can be observed for all four of the amine systems, there are several kinetic parameters that needs to be determined to correctly predict the overall reaction rate regardless of the mechanism employed. Therefore, in order to calculate these kinetic parameters Non-linear regression method has been used throughout this work. The following chapter discusses the materials used and the experimental procedures used to obtain the kinetic data for the four amine systems.

Chapter 5. Materials and Experimental Procedures

In this chapter, a detailed description of the experimental procedure used for obtaining the kinetic data along including the materials used for the experiments and the description of the stopped-flow apparatus used during this investigation is presented.

5.1 Materials

The amino acids Glycine and L-Arginine both of purity 99%, used in this work were obtained from Riedel de Haen and Fluka, respectively. Analytical grade N-methyldiethanolamine (MDEA) with a mass purity of 99% were obtained from Sigma-Aldrich. All chemicals were used as received without further purification. Analytical grade CO_2 (99.99 %) and Helium (99.99 %) were obtained from NIGP, while N_2 (99.99%) was obtained from Buzwair Industries. Standard 1.0 M HCl was obtained from Sigma-Aldrich and the Ortho Phosphoric Acid of purity 85% was obtained from BDH laboratory supplies. Deionised water was used as solvent throughout the experiments.

5.2 Solvent Preparation

The solvent for Glycine and L-Arginine were prepared using the standard method. Depending concentration required the mass of the amino acid required was determined and weighed on ADAM PW 214 balance with an accuracy of 0.0001 grams (Figure 10). The weighed amino acids are then transferred into a volumetric flask. After which deionized water was added to the volumetric flask to obtain the solutions of desired concentrations.

To prepare the blended solution of MDEA with Glycine and MDEA with L-Arginine, the same approach was followed with only an additional step of adding MDEA to volumetric flask to meet the concentration requirements. The concentrations of the solution was checked via titration using standard HCl.

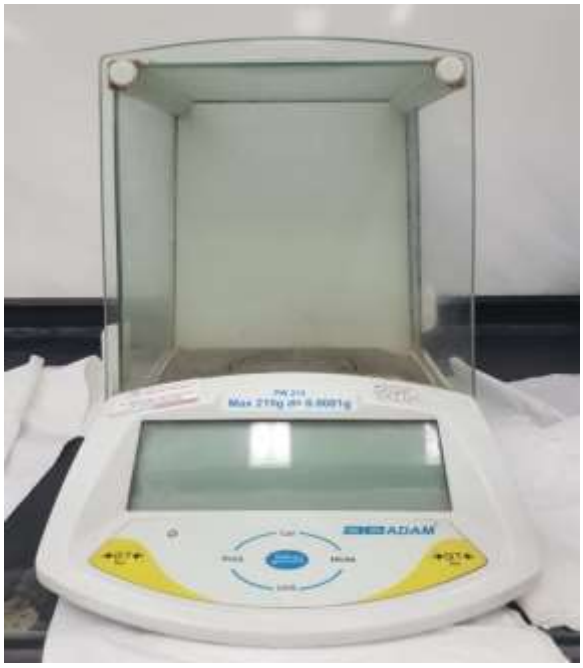

Figure 10: ADAM PW 214 Balance.

5.3 Gas Chromatography

As the mentioned earlier in this chapter, the CO_2 solutions were prepared by bubbling analytical grade CO_2 for at least half an hour in deionised water. To measure the concentration of CO_2 Shell method®-SMS 2239-04 was used that required an Agilent 6890

model Gas chromatographer with PORAK QS ss column. The scheme of the CO_2 concentration measurement is shown in the figure 11 below.

A) Sampling injection Unit

B) Agilent GC 6890

C) Sample injecting vessel and Dry ice Trap

Figure 11:: CO2 concentration measurement using GC

The CO_2 solution is injected in a small vessel in the sample injection unit. The small vessel is filled with Ortho Phosphoric Acid and heated to 90 ^oC by means of a Julaba ME3 external water bath. The ortho-phosphoric acid reacts with the bases present in the CO_2 solution, while the heat from water bath helps stripping the CO_2 present with the solution. The GC is equipped with helium cylinder that acts as the carrier gas. This carrier gas will flow through the sample injection unit and then help carry the CO_2 out of the vessel through a glass tube. The tube with carrier gas and CO_2 is then introduced to another dry ice trap. This trap will remove the water vapor or ortho phosphoric acid saturations from the CO_2 solutions. As a result of this process, pure CO_2 is injected into the Agilent GC which then calculates and reports the amount CO_2 in that particular solution. The oven temperature of GC was also maintained at 90 ^oC.

5.4 Stopped-Flow Apparatus

The determination of the kinetic data of the amine systems with CO_2 were accomplished by using a Model SF-61DX2 stopped-flow apparatus manufactured by Hi-Tech Scientific Ltd. (UK). The dead time of this stopped-flow apparatus is 1 ms. The working principal of the stopped flow apparatus has been previously described in works of Liu et al and li et al.[85, 86] The major parts of a typical stopped flow unit along their functionalities are briefly described below;

1. Sample Handling Unit: This unit consists of the drive syringes where the amino acid and CO_2 solutions are loaded. This unit is mostly made of stainless steel. The front side of the

unit is equipped with pneumatic plates that drives the solutions in the mixing chamber attached to the unit and the mode selector that can manually control the pneumatic plates to empty and clean the waste from the mixing chamber. The sample handle unit has inlet where pressure is supplied using N_2 or Air to facilitate the motion of the pneumatic plates. The unit also consists of temperature and pressure display. The unit also contains a valve that switch between the stop and waste positions during the experimental runs. The temperature within the sample handling unit is usually controlled via an external water bath. To accomplish that a Lauda RA8 model water bath was attached to the sample handling unit. The figure 12 shows the sample handling unit of the stopped-flow apparatus.

Figure 12: The Sample Handling Unit

2. Conductivity Detection Unit: During the experimental runs, the intrinsic rate of the reactions taking place within the mixing chamber is measured within the conductivity detection unit. The conductivity detection unit measures the formation of ions as a function of time, which also triggers a change in voltage within the unit. The change in conductivity with respect to time within the unit produces an output voltage which is then sent to the processor in the computer.

3. Computer: The computer attached with the stopped flow unit is responsible for processing the output voltage coming out of the conductivity detection unit. This voltage is generally directly proportional to the conductivity of the reacting solutions and the computer converts this voltage to generate the pseudo-first-order constant using the 'KinetAsyst' software.

The figure 13 below shows the stopped-flow apparatus used to conduct the experiments for this work.

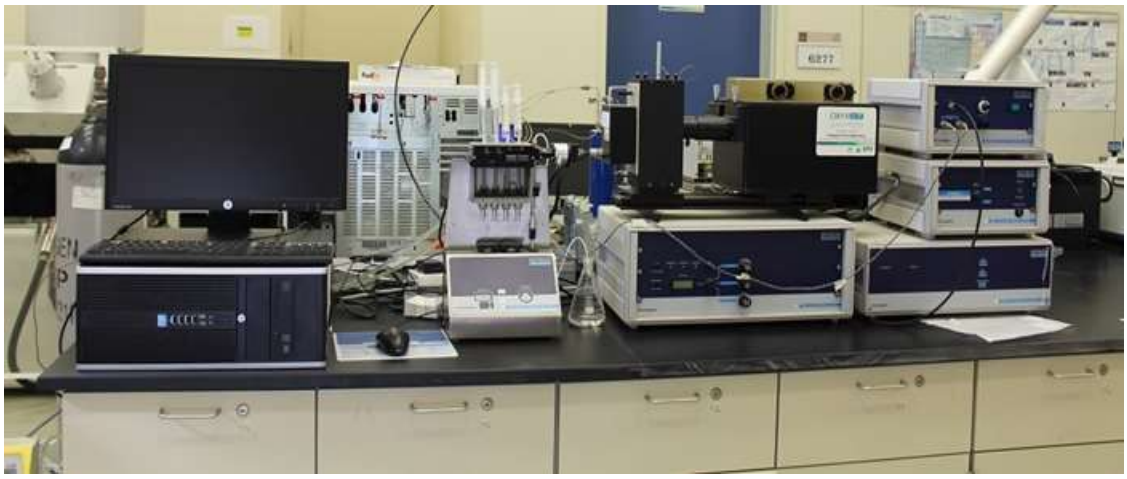

Figure 13: Stopped-Flow Apparatus

5.5 Experimental Procedure:

The following were steps involved to obtain the kinetic data for the reaction of CO_2 with different amine systems.

1. The amine solutions of desired concentrations were prepared in a volumetric flask.

2. The concentrations of the amine solutions were verified via titration with HCl.

3. The CO_2 solutions were prepared by bubbling CO_2 into deionized water for at least half an hour.

4. The concentration of CO_2 was measured using Agilent 6890 model Gas Chromatogram.

5. The CO_2 solutions were then diluted to maintain the concentrations of the amine systems 15-20 times higher than the CO_2. This step was mainly done to ensure the reaction conditions with respect to [CO_2] fall within the pseudo first order regime [87].

6. The CO_2 solution and the amino acid solutions were then loaded into two different syringes on to the sample handling unit of the stopped flow unit.

7. Using a Lauda RA8 model water bath the temperature of the sample handling unit was controlled and maintained within ±0.10 K of the required temperature.

8. To supply the pressure required to move the pneumatic plates N_2 was used was used and the pressure was set at 6 bars.

9. The conductivity detection unit was then switched on along with the computer.

10. The 'Kinetasyst' software was then opened to set the experimental run time depending on the sample used and the temperature.

11. Once the desired temperature was reached within the sample handling unit, the 'KinetAsyst' software was used to charge equal volumes amino acid solutions and the CO_2 solutions into the mixing chamber.

12. The conductivity-detection unit then measures the conductivity change as a function of time and sends an output voltage back to the computer. The 'KinetAsyst' software, then reports change in the conductivity, Y, with respect to time as described by Knipe et al [88] was fits to an exponential equation resembling a first-order kinetics equation:

$$Y = -A.\exp(-k_{ov}.t) + Y_{\infty} \qquad 5.1$$

Where the term 'k_{ov}' is the pseudo first-order reaction rate constant.

13. To ensure the reproducibility of the obtained k_{ov}, the experiment were repeated three times and the average value of three k_{ov} was considered. The error in reproducibility was found to be less than 3% in all experiments.The typical conductivity profile generated in the 'kinetAsyst' software of the stopped-flow apparatus has been presented in the figure 14 in the following page, where the term R stands for 'k_{ov}'.

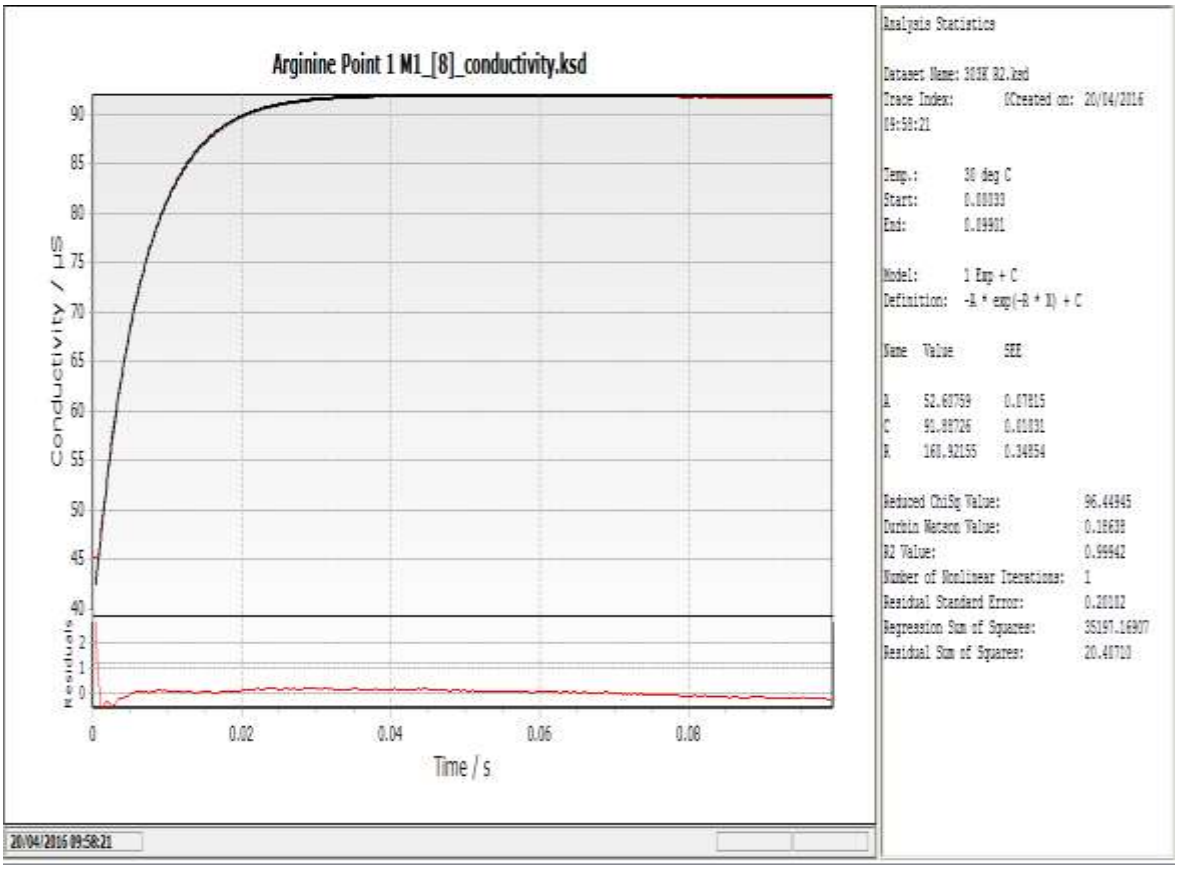

Figure 14: Typical Stopped-flow Conductivity Profile

Chapter 6. Calculation Technique and Data Analysis Method

This chapter describes the calculation techniques applied to determine different parameters required to accurately interpret the kinetic data obtained from the stopped-flow technique. It also briefly describes the approach used for data analysis.

6.1 Determination of Concentrations via titration

The amino acid and amine/amino acid concentrations were expected to remain constant throughout the experiments and were prepared according to the method mentioned in section 5.2. To reconfirm the concentration, a predetermined volume (V_A) of the amino acid solutions was titrated using standard 1.0 M HCl. To neutralize the basic species, certain volume HCl (V_{HCl}) was required to be added to this solution, this 'V_{HCl}' can be determined from the end points of the titration. Afterwards, the concentration, 'C_A', was then calculated from the following;

$$C_A = \frac{C_{HCl} \cdot V_{HCl}}{V_A} \qquad (6.1)$$

The discrepancy between the concentrations were found to be less than 3% in all cases, justifying our assumption of constant concentration.

6.2 Determination of Hydroxyl ion concentrations

To approximate the concentration of the hydroxyl ion in the amino acid and amino acid/amine solution, the relation given by Astarita et al.[89] deduced the following equations;

$$[\mathrm{OH}^-] = \sqrt{\frac{k_w}{k_p}[C_A]} \quad \text{for } \alpha \leq 10^{-3} \tag{6.2}$$

Here, the terms 'k_w' and 'k_p' represents the dissociation constants of water and the amino acid respectively. Both terms k_w and k_p are expressed as a function of temperature according to the following equation:

$$\mathrm{LnK_i} = \frac{a_i}{T} + b_i \ln T + c_i T + d_i \tag{6.3}$$

Values of the constants a_i–d_i are given in Table 2.

Table 2: Values *of different equilibrium constant used to estimate [OH^-]*

Parameter	a_i	b_i	c_i	d_i	validity range	source
K_{p1} (MDEA)	−8483.95	−13.83	0	87.38	293–333 K	[90]
K_{p2} (Arginine)	−3268.30	0	0	−9.97	293–323 K	[91]
K_{p3} (Glycine)	-9059.94	-16.51	0.012946	98.094	278–398 K	[92]
Kw	−13445.90	−22.48	0	140.93	273–498 K	[93]

In case of the amino acid/MDEA blends, the total [OH^-] was taken to be the sum of [OH^-] ions produced by MDEA and those produced by Amino acid.

6.3 Determination of H_2O concentration

The concentrations of the water in the amine systems were determined based on the parameters like concentration of the amino acid, 'C_A', molecular weight of amino acid, 'M_A' , the purity of amino acid and the molecular weight of water, 'M_W' using the following equation;

$$[H_2O] = \frac{1000 - \frac{C_A * M_A}{Purity}}{M_W} \quad (6.4)$$

In case of the amino acid/MDEA blends, the total [H_2O] was taken to be the sum of [H_2O] obtained using both MDEA and the Amino acid parameters.

6.4 Steps for Data Analysis

After obtaining the pseudo first order rate constants, '$k_{ov\text{-}exp}$' from the stopped-flow experiments and determining the concentration of different species of the amine systems at different temperatures using the equations 6.2-4, they were fitted in accordance to equations 4.21 and 4.23 for zwitterion and termolecular mechanisms, respectively. This was done to determine the rate expressions for CO_2-Glycine system by performing nonlinear regression using Excel solver. The effect of the different species were then evaluated based on their rate expressions and the species with no effects on the CO_2-Glycine reaction were discarded from their respective zwitterion or termolecular equation and the non-linear regression was then repeated using the new equation. Once the rate expressions were obtained, they were then used to predict the pseudo first order rate constant based on that particular mechanisms. The validity of the newly predicted

pseudo first order rate constant for each mechanism were then verified by comparing it with the obtained experimental data using the following equation;

Absolute average deviation = 100 * $ABS(\frac{k_{ov-exp}-k_{ov-pre}}{k_{ov-pre}})$ (6.5)

Based on AAD%, it was determined whether a particular mechanism suited to describe the reaction scheme or not. The same was done for the CO_2-L-Arginine systems as well.

In case of the blended systems of MDEA-Glycine and MDEA-L-Arginine, first the rate expressions for CO_2-MDEA were obtained. Using the rate expression for CO_2-MDEA reactions and the concentration MDEA within the blends, its kinetics effect was determined and subtracted from the pseudo first order constant for CO_2- MDEA-Glycine and CO_2- MDEA-L-Arginine systems. The effect of the hydroxyl ion concentrations was also subtracted from the same. This leaves only the kinetic data associated with the amino acid termed as 'k_{app}' in equation 4.42 and 4.50, which is fitted into their zwitterion and termolecular equations. The equation contains all rate expressions common for the individual CO_2-Amino acid reactions with an additional term to account for the catalytic effect of MDEA, 'k_{α}'. Therefore, regression was carried out on the k_{app} to determine the rate expression for this catalytic effect. The following chapter discusses the results obtained for the four amine systems.

Chapter 7. Results and Discussions

Using the experimental methods mentioned in the chapter 5 combined with reaction mechanism and kinetics discussed in chapter 4 and calculation and data analysis technique mentioned in chapter 6, the kinetic data for the CO_2-Glycine, CO_2-L-Arginine, CO_2-MDEA-Glycine and CO_2-MDEA-L-Arginine were analyzed. The results achieved from these analyses is presented, discussed and compared in this chapter.

7.1 Reaction of CO_2 with Glycine

The pseudo first order rate constant (k_{ov}) for the reaction of CO_2 with Glycine at different temperatures and concentrations was obtained through the stopped-flow experiments are shown in table 3 below;

Table 3: *Kinetic Data of CO2-Glycine reaction*

Solution Concentration, M	Temperature, K				
	293	298	303	308	313
0.1000	1.4	2.4	3.5	5.2	8.0
0.0875	1.1	1.8	2.9	4.4	7.1
0.0750	1.0	1.7	2.7	4.1	6.3
0.0625	0.9	1.4	2.2	3.5	5.2
0.0500	0.7	1.1	1.9	2.6	4.3

Upon plotting the obtained kinetic data as the function of amine concentrations (Figure 15), it was observed that the data increased progressively with the increasing amine concentration and temperature.

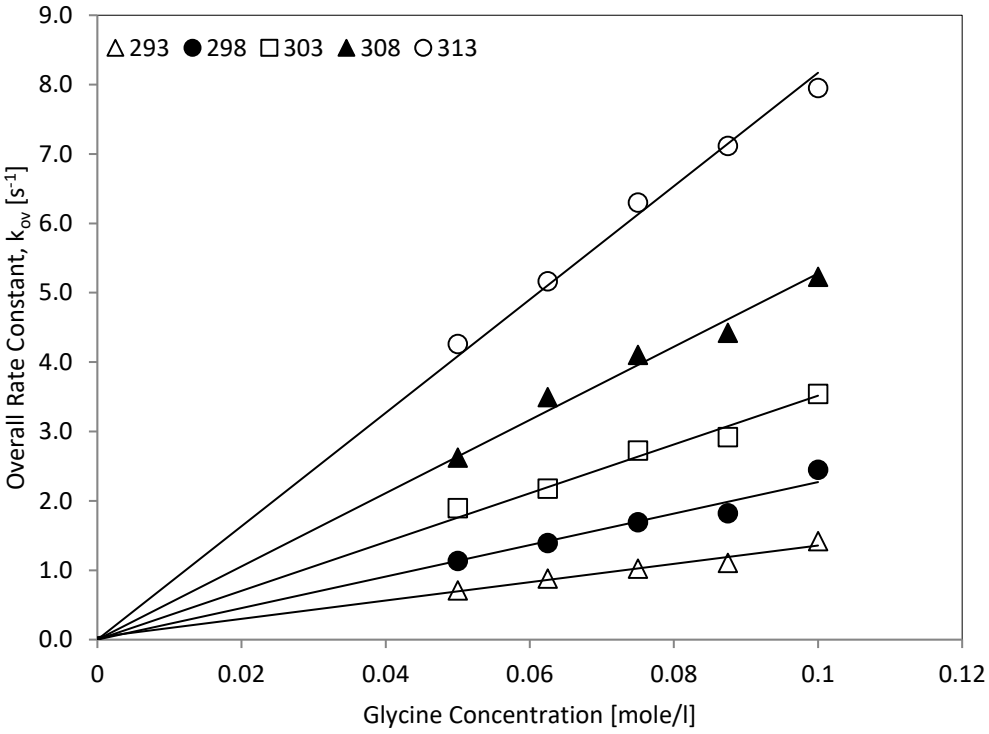

Figure 15: Plot of overall rate constant (k_{ov}) as a function of Glycine

Applying the power law kinetics to model the overall rate constants against the concentration of glycine, an average exponent of 0.95 was achieved as shown in figure 16 for the reaction of CO_2 with Glycine. This affirms that within the experimental concentration and temperature range, pseudo first order regime prevails and the reaction

of CO_2-Glycine reaction can be analyzed using the zwitterion mechanism [94].

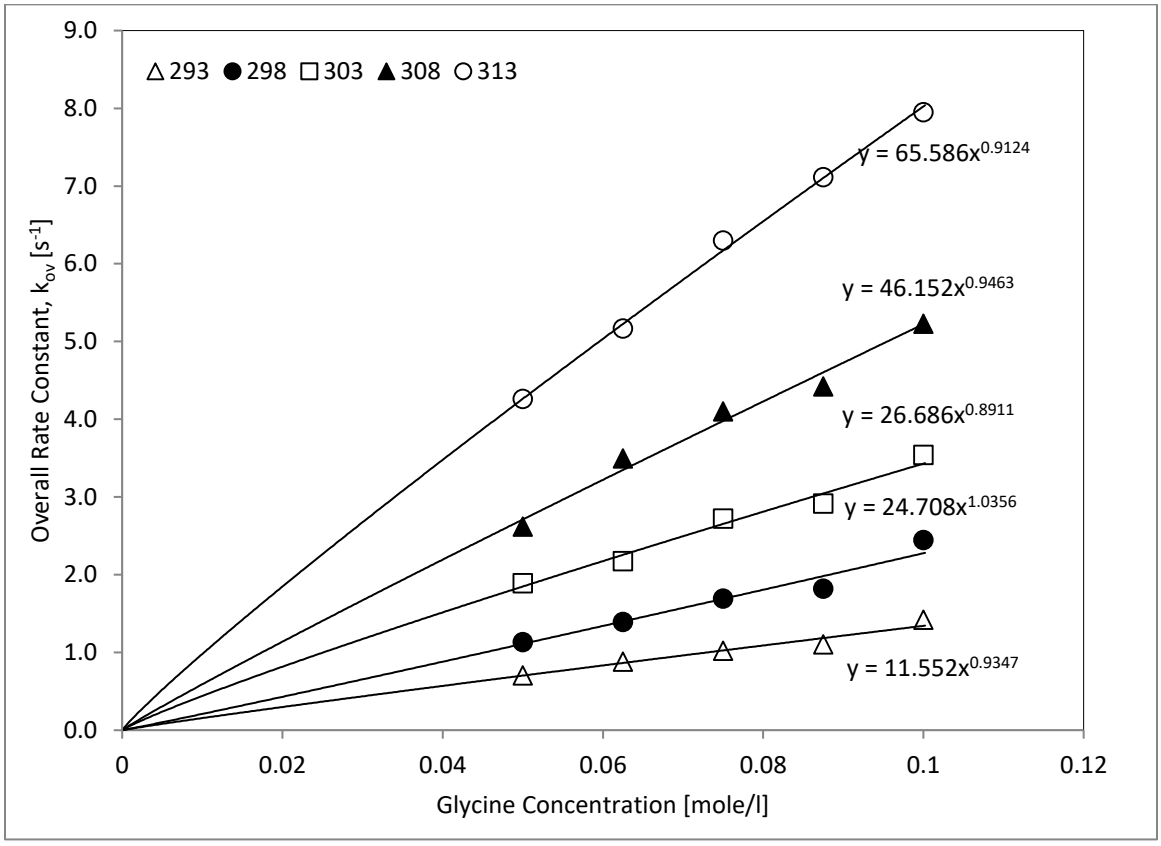

Figure 16: Overall rate constant (k_{ov}) as a function of Glycine based on power law

7.1.1 Zwitterion Analysis of the CO_2-Glycine reaction

Before analyzing the kinetic data of the CO_2-Glycine reaction using the zwitterion ion mechanism. The concentrations of different species were determined using the equations 6.2-4. The obtained data were then fitted into the equation 4.21 to individual rate constants were obtained by nonlinear regression using excel solver. By applying the

zwitterion mechanism for CO_2-Glycine reaction, it was noticed that the effects of hydroxyl ion (k_{hyd}) and the catalytic contribution of Glycine in the formation of carbamate (k_{Gly}) were negligible. In other words, only the effects of k_2 and k_w were found to be important. The natural logarithm of individual blocks of rate constants k_2 and k_w were plotted against the T^{-1} for Glycine in order to obtain the Arrhenius plots and they are shown in Figure 17.

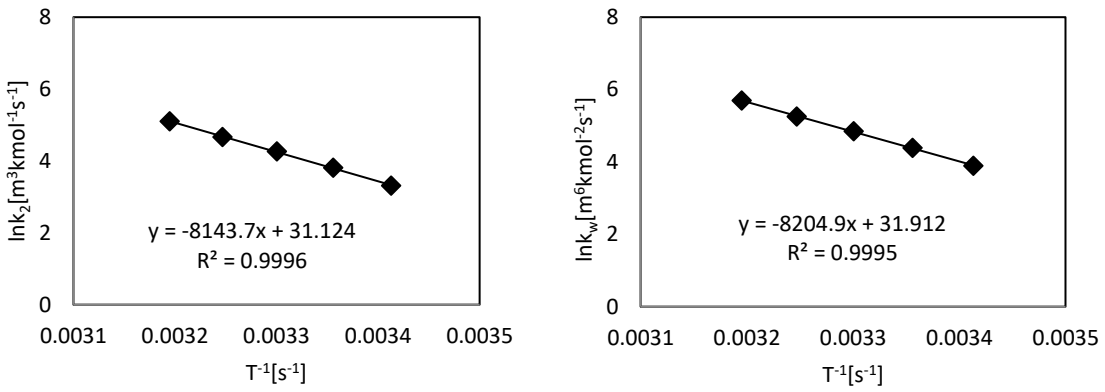

A) Ln k_2 against T^{-1} B) Ln k_w against T^{-1}

Figure 17: Arrhenius plots of CO_2-Glycine reaction

From Arrhenius plots of CO2-Glycine reaction, the rate expressions for k_2 and k_w were obtained along with their corresponding activation energies and are given in the Table 4 in the following page.

Table 4: *Summarized kinetic rate constants for CO_2-Glycine over 293-313 K based on Zwitterion mechanism*

Rate	$\ln k_0$	E_a/R	E_a (kJ/mol)	*Equation*
k_2 (m^3/kmole.s)	31.12	8143.7	67.71	$k_2 = 3.29x10^{13}e^{-\frac{8143.70}{T}}$
k_w (m^6.$kmole^{-2}$.s^{-1})	31.92	8204.9	68.22	$k_w = 3.52x10^{13}e^{-\frac{8204.90}{T}}$

A table with the summary of the concentrations of different species, generated individual reaction rate constant at different temperatures and predicted overall rate constant based on the generated individual reaction rate for CO_2-Glycine reactions using the zwitterion mechanism are provided in the appendix (Table A1). Furthermore, the validity of the zwitterion rate model to represent the experimental data was verified by plotting the predicted overall rate constant i.e. $k_{ov\text{-}pre}$ values against the experimental one for CO_2-Glycine reaction (Figure 18). It was evident that the adopted rate model along with the extracted blocks of individual rate constants perfectly represent the experimental results with AAD of 3.2 %.

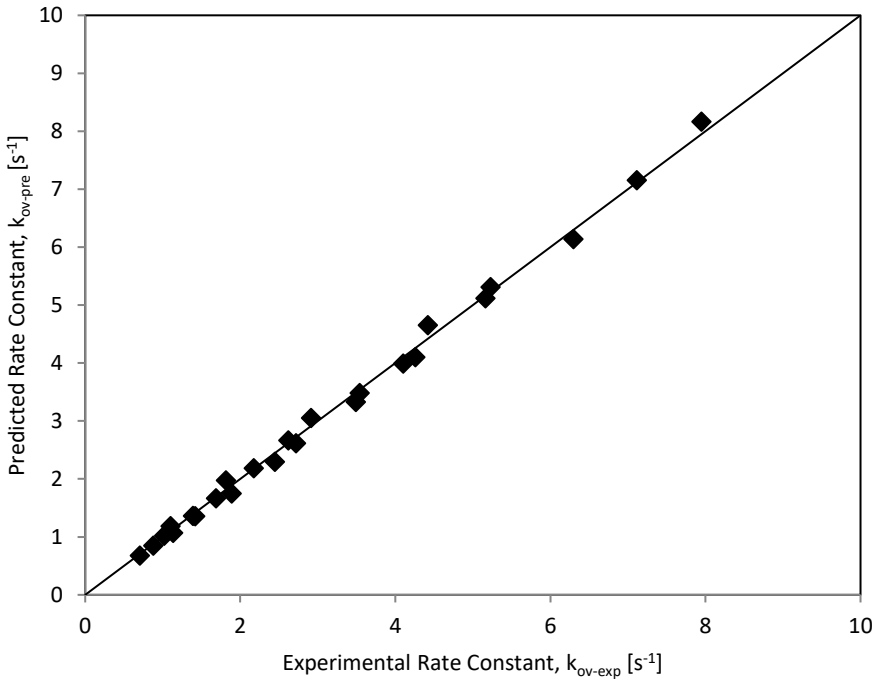

Figure 18: Parity plot of predicted vs experimental rate constants for CO_2-Glycine

7.1.2 Termolecular Analysis of the CO_2-Glycine reaction

The kinetics of CO2 with the Glycine was set to be further investigated using the termolecular mechanism. However, prior to any regression work, the applicability of the termolecular mechanism was verified. To do this, knowing that Glycine concentration is low enough to assume that the concentration of water is constant, Equation 4.23 was reduced to the following [95]:

$$\frac{k_{ov}}{[Gly]} = k_{Gly}[Gly] + k_w[H_2O] \qquad (7.1)$$

Since the plot kov/[Gly] against [Gly] did not show any satisfactory trend for as shown in the Figure 19, the analysis of the CO_2-Glycine reaction using termolecular mechanism was discarded.

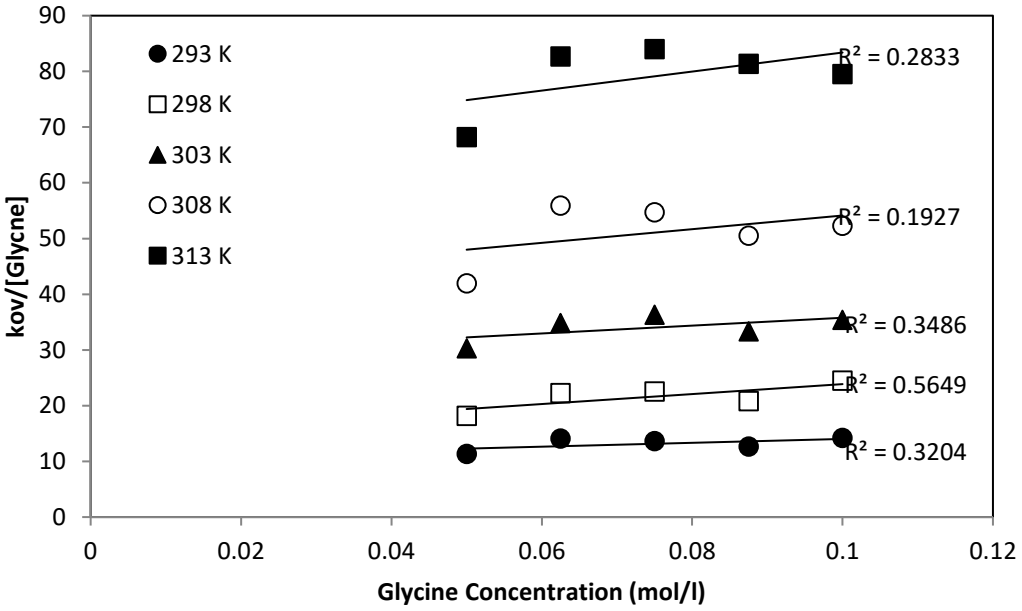

Figure 19: Plot of k_{ov}/[Glycine] vs [Glycine]

7.2 Reaction of CO_2 with L-Arginine

The pseudo first order rate constant (k_{ov}) for the reaction of CO_2 with L-Arginine at different temperatures and concentrations was obtained through the stopped-flow experiments are shown in table 5 below;

Table 5: *Kinetic Data of CO2-L-Arginine reaction*

Solution Concentration, M	Temperature, K				
	293	298	303	308	313
0.20	522.6	680.7	920.7	1140.2	1475.8
0.15	374.2	482.2	634.1	792.3	961.9
0.10	226.5	290.1	374.2	465.5	545.0
0.05	96.1	126.9	161.9	209.6	259.4

Upon plotting the obtained kinetic data as the function of L-Arginine concentrations (Figure 20), it was observed that the data increased progressively with the increasing amine concentration and temperature.

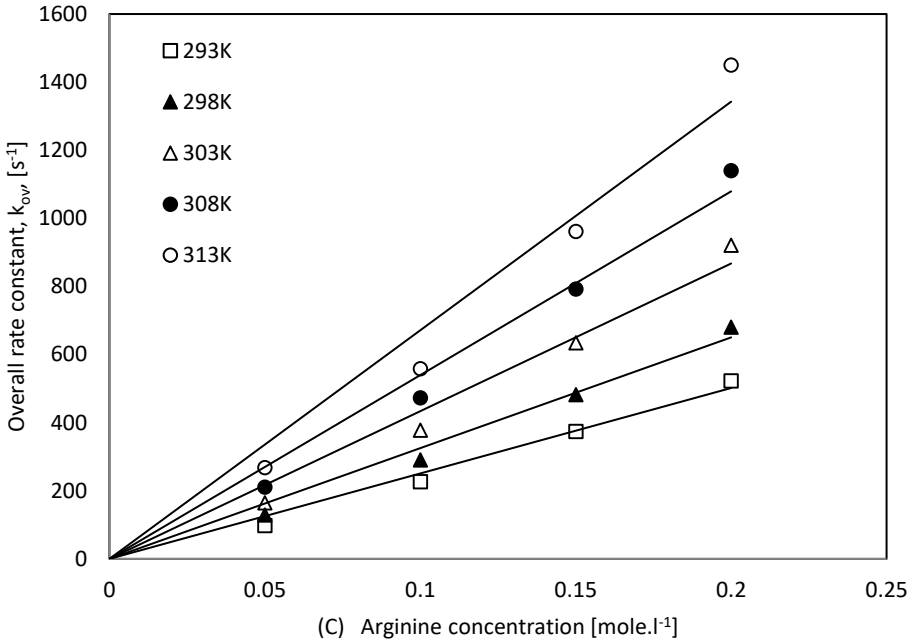

Figure 20: Plot of overall rate constant (k_{ov}) as a function of L-Arginine

Applying the power law kinetics to model the overall rate constants against the concentration of L-Arginine, an average exponent of 1.22 was achieved as shown in figure 21 for the reaction of CO_2 with L-Arginine. This affirms that within the experimental concentration and temperature range, the reaction of CO_2-L-Arginine reaction can be analyzed using both the zwitterion and termolecular mechanism [94].

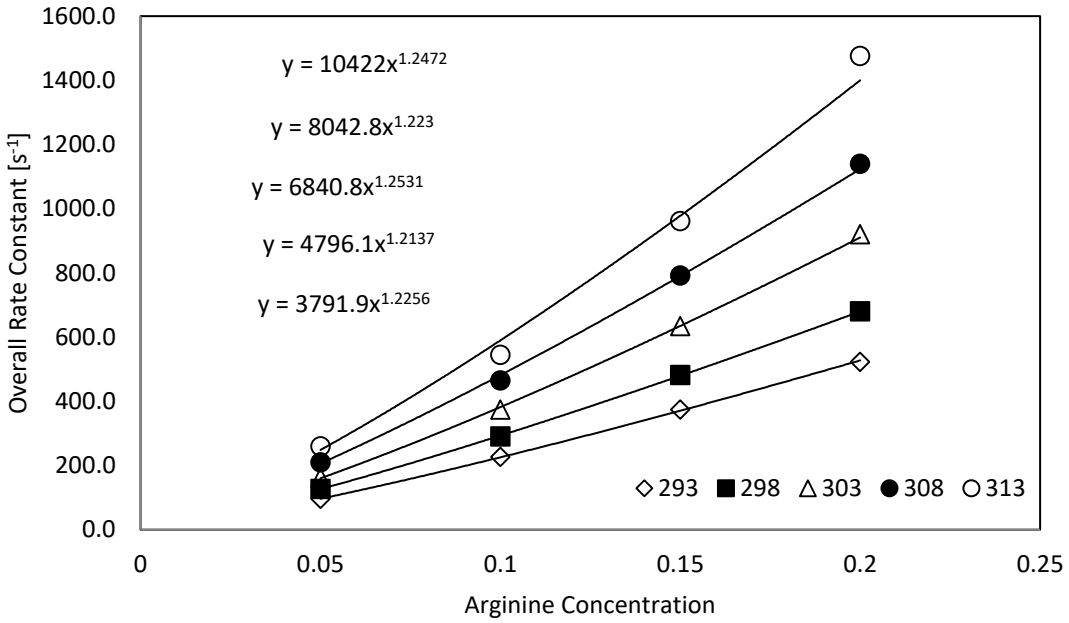

Figure 21: Overall rate constant (k_{ov}) as a function of L-Arginine based on power law

7.2.1 Zwitterion Analysis of the CO_2-L-Arginine reaction

Similar to the CO_2-Glycine reactions, the concentrations of different species were determined using the equations 6.2-4 to analyze the kinetic data of the CO_2-L-Arginine reaction using the zwitterion ion mechanism, the obtained data were then fitted into the equation 4.29 to individual rate constants were obtained by nonlinear regression using excel solver. By applying the zwitterion mechanism for CO_2-L-Arginine reaction, it was noticed that It was noticed that the k_2 showed more variations with the increase in temperature compared to k_{Arg}, which in turn was more sensible to temperature than k_w. It is to be noted that the effect of hydroxide ion on the overall reaction rate was initially considered in the regression; however, sensitivity analysis as in the case CO_2-L-Arginine

showed that OH^- ion has negligible effect on k_{ov}. The natural logarithm of individual blocks of rate constants k_2, k_{Arg} and k_w were plotted against the T^{-1} for L-Arginine in order to obtain the Arrhenius plots and they are shown in Figure 22.

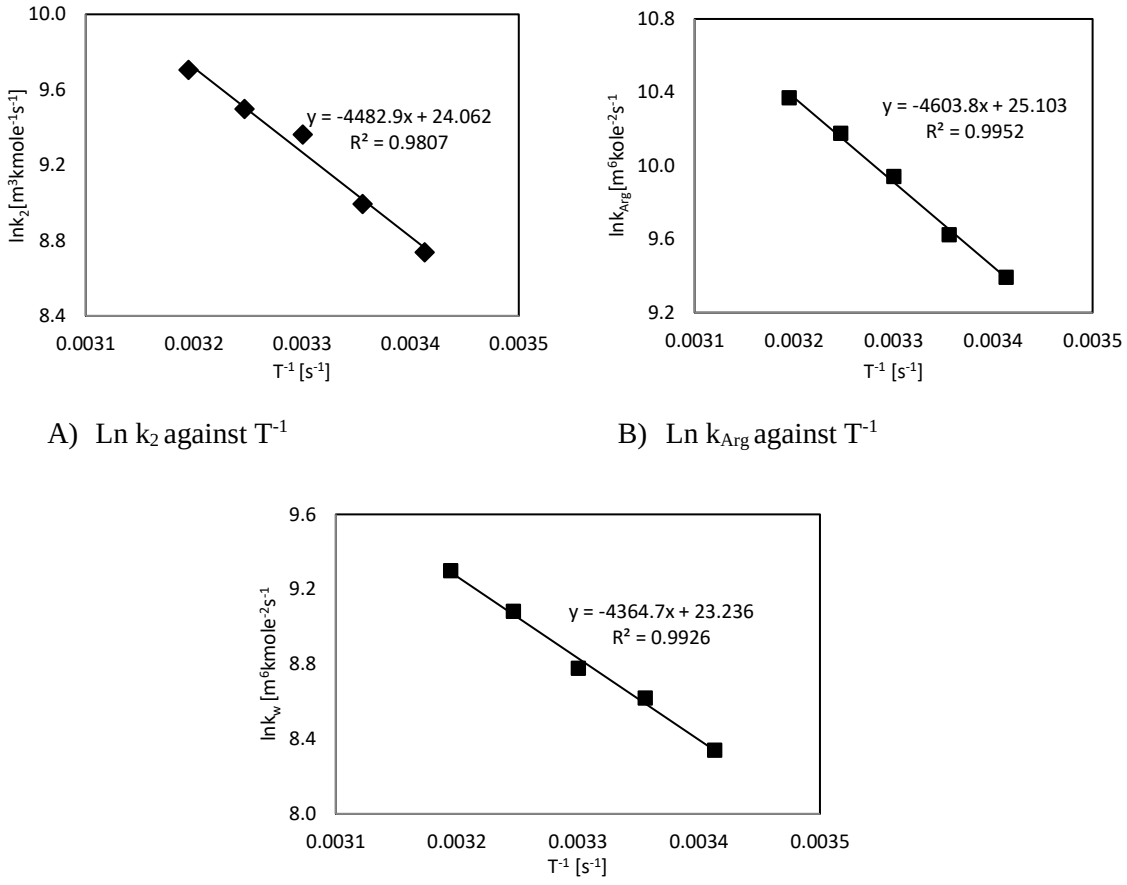

A) Ln k_2 against T^{-1}

B) Ln k_{Arg} against T^{-1}

C) Ln k_W against T^{-1}

Figure 22: Arrhenius plots of CO_2-L-Arginine reaction based on Zwitterion Mechanism

From Arrhenius plots of CO2-L-Arginine reaction, the rate expressions for k_2, k_{Arg} and k_w were obtained along with their corresponding activation energies and are summarized in Table 6.

Table 6: *Summarized kinetic rate constants for CO_2-Arginine over 293-313 K based on Zwitterion mechanism*

Rate	$\ln k_0$	E_a/R	E_a (kJ/mol)	Equation
k_2 (m^3/kmole.s)	24.06	4482.9	37.28	$k_2 = 2.81x10^{10} e^{-\frac{4482.9}{T}}$
K_{Arg} ($m^6.kmole^{-2}.s^{-1}$)	25.10	4603.8	38.28	$k_{Arg} = 7.96x10^{10} e^{-\frac{4603.8}{T}}$
k_w ($m^6.kmole^{-2}.s^{-1}$)	27.84	4364.7	36.29	$k_w = 1.23x10^{09} e^{-\frac{4364.7}{T}}$

A table with the summary of the concentrations of different species, generated individual reaction rate constant at different temperatures and predicted overall rate constant based on the generated individual reaction rate based on zwitterion mechanism for CO_2-L-Arginine reactions are provided in the appendix (Table B1). Furthermore, the validity of the zwitterion rate model to represent the experimental data was verified by plotting the predicted overall rate constant i.e. kov-pre values against the experimental one for CO_2-L-Arginine (Figure 23). It was evident that the adopted rate model along with the extracted blocks of individual rate constants perfectly represent the experimental results

with AAD of 1.1 %.

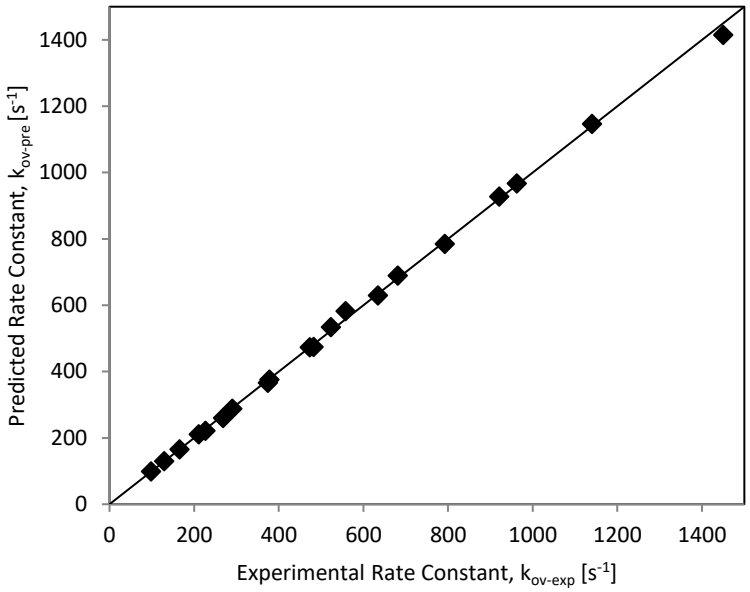

Figure 23: Parity plot of predicted vs experimental rate constants for CO_2-L-Arginine via zwitterion mechanism

7.2.2 Termolecular Analysis of the CO_2-L-Arginine reaction

The kinetics of CO2 with the L-Arginine was further investigated using the Termolecular mechanism. kov values were regressed using Excel solver to generate the individual rate constants according to Equation 4.31. However, prior to any regression work, the applicability of the termolecular mechanism was verified. To do this, knowing that L-Arginine concentration is low enough to assume that the concentration of water is

constant, Equation 4.31 was reduced to the following [95]:

$$\frac{k_{ov}}{[Arg]} = k_{Arg}[Arg] + k_w[H_2O] \quad (7.2)$$

By plotting kov/[Arg] against [Arg] as shown in the Figure 24, straight lines were obtained which indicates that the termolecular mechanism might be used to interpret the data. Therefore the data was fitted to equation 4.31 by performing non-linear regression using excel solver. A table with the species concentration and summary of individual reaction rate based on termolecular mechanism for CO_2-L-Arginine reactions are provided in the appendix (Table C1).

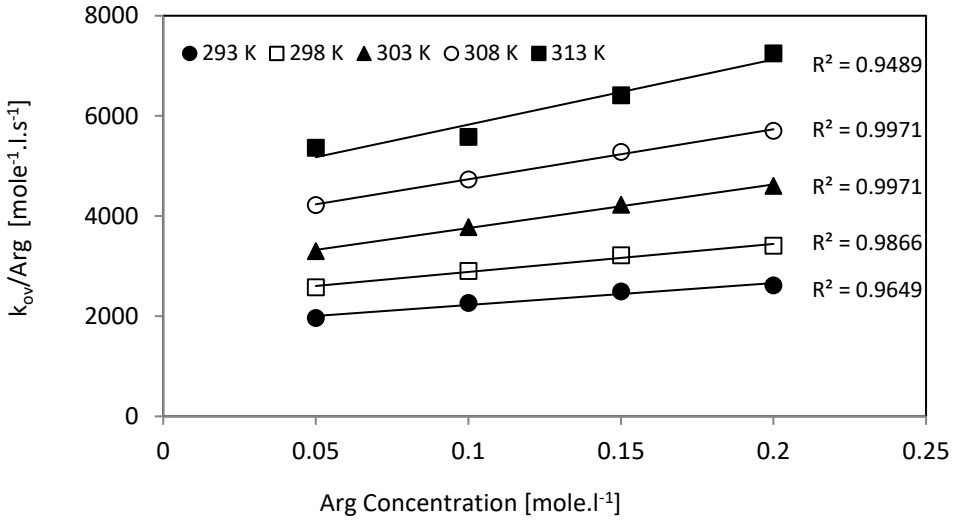

Figure 24: Plot of k_{ov}/[Arginine] vs [Arginine]

The obtained fitting results for CO_2-Arginine reaction using termolecular mechanism showed that hydroxyl ion (k_{hyd}) had a negligible effect similar to the results obtained using the zwitterion mechanism. only amino acid and water concentrations effects (k_{Arg} and k_w) were found to be significant. Plotting the natural logarithm of the individual rate constants k_{Arg} and k_w against T^{-1} according to Arrhenius equation as shown in Figure 25 in the following page, the activation energy of each reaction was determined and the obtained rate expressions for k_α and k_w are summarized in Table 7 in the following page.

.

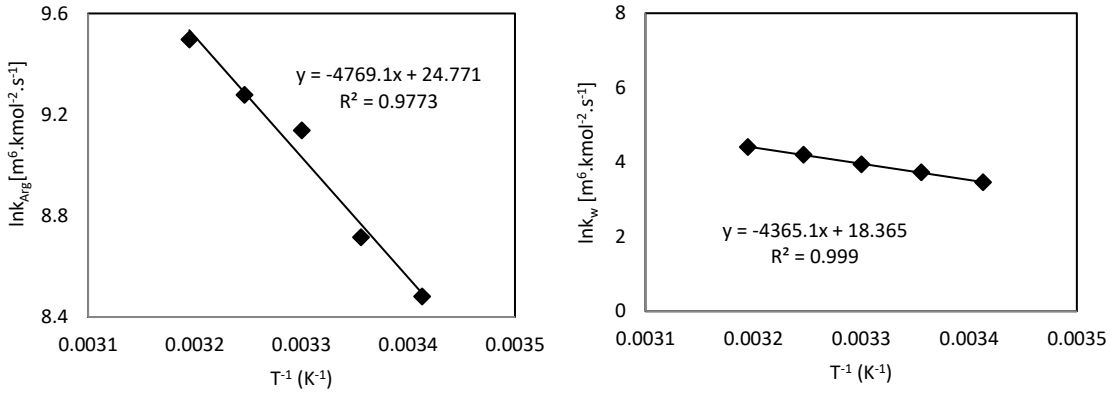

A) Ln k_{Arg} against T^{-1} B) Ln k_w against T^{-1}

Figure 25: Arrhenius plots of CO_2-L-Arginine reaction based on Termolecular Mechanism

Table 7: *Summarized kinetics of CO2-L-Arginine over 293-313 K based on termolecular mechanism*

Rate	$\ln k_0$	E_a/R	E_a (KJ/mol)	*Equation*
k_α ($m^6.kmole^{-2}.s^{-1}$)	24.77	4769.0	39.65	$k_a = 5.72x10^{10}e^{-\frac{4769.00}{T}}$
k_w ($m^6.kmole^{-2}.s^{-1}$)	18.36	4365.0	36.29	$k_w = 9.41x10^{7}e^{-\frac{4365.00}{T}}$

Using the generated individual rate constants, the predicted overall rate constant values were again compared to the experimental ones as shown in Figure 26, an excellent agreement exists between both of them with an AAD of 1.35 % which is very close the AAD obtained in case of zwitterion mechanism (1.12 %), which indicates that the proposed termolecular mechanism can be also used to interpret the experimental data. Furthermore, an analysis of the activation energies of kw based on the two models, we found that E_a was identical for both models (36.29 kJ/mole). Based on this, we conclude that both reaction mechanisms can be used to explain the CO_2-Arginine reaction. However, it is well known that, there is one basic Guanidinium group in their side chain within the structure of L-Arginine [96] which can add up a step towards the formation of carbamates. Therefore, it can be suggested that the CO_2-Arginine reaction can be better explained by the two-step zwitterion mechanism rather to that of the single step termolecular mechanism.

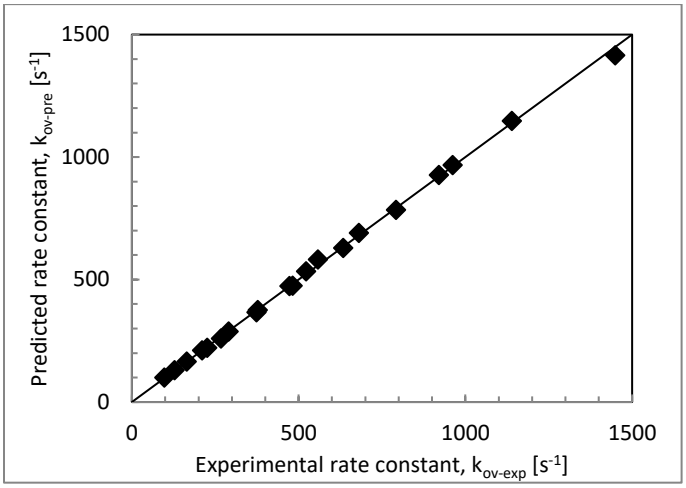

Figure 26: Parity plot of predicted vs experimental rate constants for CO_2-L-Arginine via termolecular mechanism

On the basis of the results obtained previously, it can be proposed that Glycine and L-arginine reactions with CO_2 can be explained by the zwitterion mechanism. The obtained experimental kov data for both Glycine reaction with CO_2 could be successfully fitted in the zwitterion model with an AAD% of 3.2. While, the kov data for the reaction of L-Arginine with CO_2 could be fitted to both termolecular and the zwitterion models. However, due to the presence of the gaunidinium group it can be suggested that CO_2-Arginine reaction is more inclined to undergo a two-step zwitterion mechanism.

7.3 Comparsion between Glycine and L-Arginine

The rate constants of the two amino acids were compared at 0.2 mole/l concentration and different temperatures and are shown in Figure 27. The rate constant of L-Arginine had the higher than rate constant of glycine. This could be attributed to the presence of an additional basic Guanidinium group that makes the reaction between arginine and CO_2 much faster.

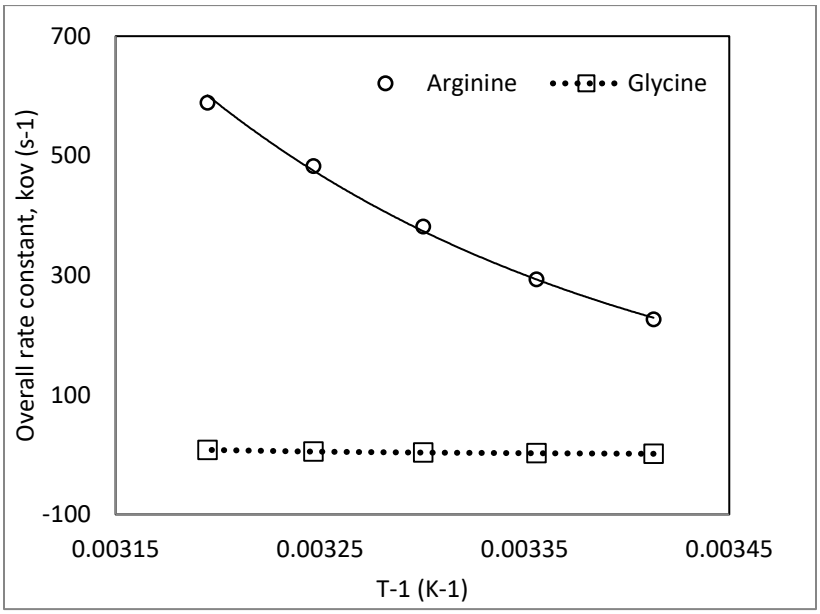

Figure 27: Comparison between reaction rate constants of the three amino acids

7.3.1 Comparsion with available literature data

The obtained kinetics data were compared to the ones available in literatures. Gou et al.[84] studied the reactions of neutral Glycine with CO_2 and obtained the rate expression of $k(M^{-1}s^{-1})=8.18\times10^{12}\exp(-\frac{8624}{T(K)})$ compared to $k(M^{-1}s^{-1}) =3.29\times10^{13}\exp(-\frac{8143.7}{T(K)})$ as obtained in this work . Moreover, the activation energy of neutral Glycine with CO_2 in that study was found to be 71.7±9.6 $kJmol^{-1}$ which is comparable to 67.71 $kJmol^{-1}$ determined in this work (Table.8). Since, there are no available data on the pure L-arginine, hence it was not compared.

Table 8: *Comparison of the obtained data with the literature data*

Amino Acid	Rate Expressions ($M^{-1}s^{-1}$)	Activation Energy, E_a (kJ/mol)	Source
Glycine	$k = 3.29x10^{13}e^{-\frac{8143.70}{T}}$	67.71	This work
	$k = 8.18x10^{12}e^{-\frac{8624}{T}}$	71.7±9.6	Guo et al.[84]

7.4 Reaction of CO_2 with blends of MDEA-Glycine

The pseudo first order rate constant (k_{ov}) for the reaction of CO_2 with blends of MDEA-Glycine at different temperatures and concentrations was obtained through the stopped-flow experiments are shown in table 9 below;

Table 9: *Kinetic Data of CO2-MDEA-Glycine reaction*

Concentration, M		Temperature, K				
MDEA	GLY	293	298	303	308	313
1.95	0.05	97	116	147	191	257
1.9	0.1	243	283	360	444	584
1.8	0.2	512	660	856	998	1290
0.95	0.05	67	111.8	140	171	215
0.9	0.1	157	210	266	329	373
0.8	0.2	368	459	572	687	789
0.45	0.05	39	55	73	93	110
0.4	0.1	89	126	169	221	262

The obtained pseudo first order rate constants,'k_{ov}', were plotted against temperature for a one molar total concentration (Figures 28). The overall rate constants (k_{ov})

increased with increasing solution temperature as well as with increased glycine proportion in the total mixture. The effect of solution total concentrations under different temperatures and fixed Gly/MDEA ratio of 0.11 on the overall rate constants is shown in Figure 29. The overall rate constants also seemed to increase with the increase in total concentrations at different temperatures at fixed Glycine to MDEA ratio of 0.11.

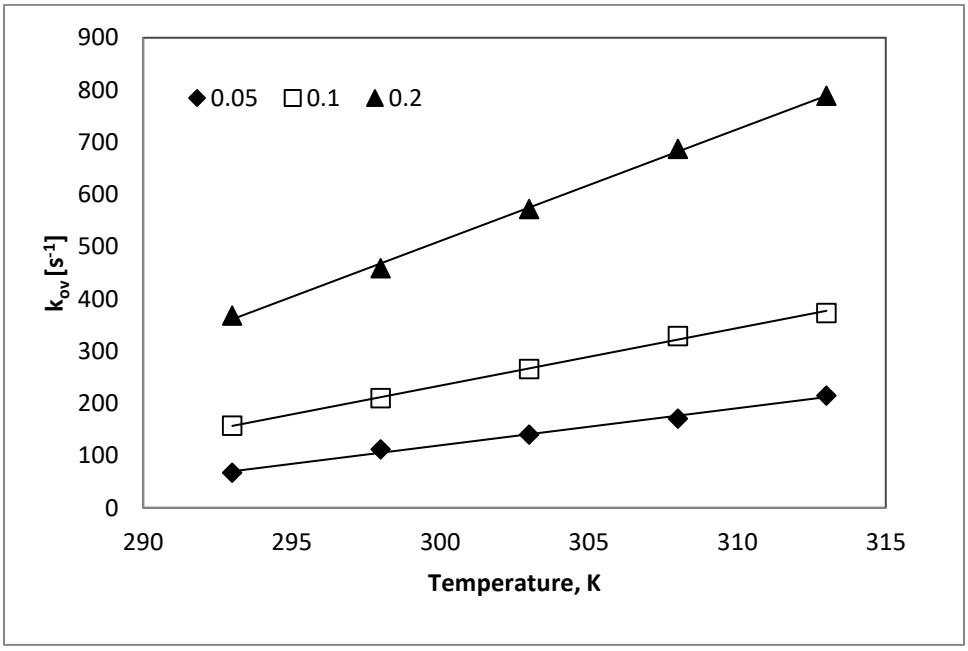

Figure 28: Rate constant, 'k_{ov}' , versus temperature for total 1 M solution

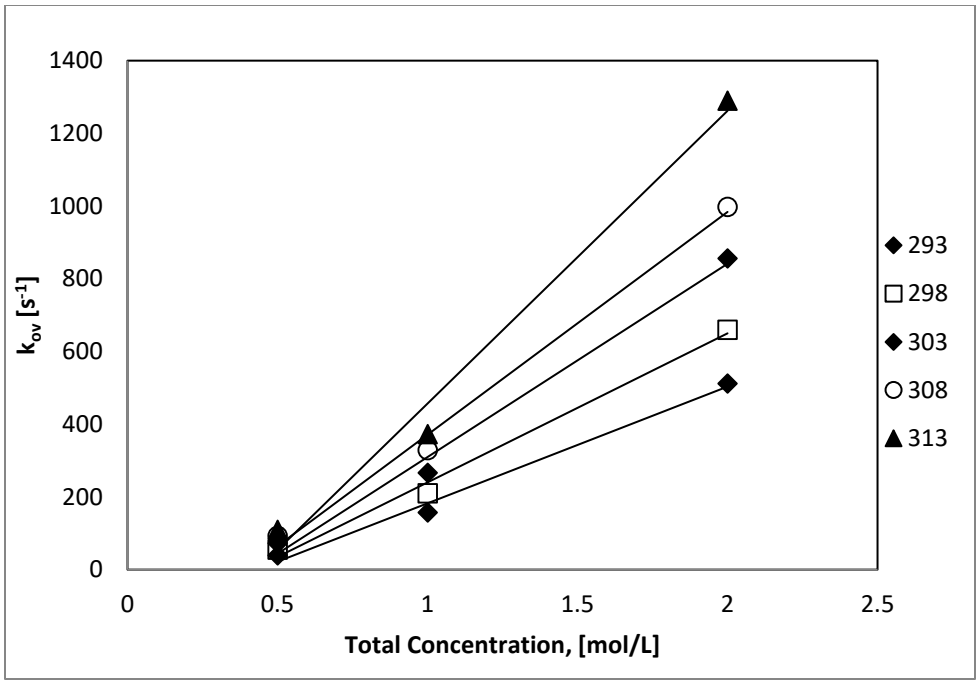

Figure 29: Rate constant, 'k_{ov}' , at different total concentrations for 0.11 Arg/MDEA ratio

7.4.1 Zwitterion Mechanism for CO_2-MDEA-Glycine system

To determine the individual rate expressions for the CO_2-MDEA-Glycine system, the method mentioned in the section 6.4, was followed in the beginning. However, it was observed that the rate expressions obtained for CO_2-Glycine system could not be used to the kinetic data. It was reported in the work Guo et al.[84], that glycine at higher pH behaves different in comparison to the neutral pH. At elevated pH the glycine reacts much fast, thus the rate expressions obtained for the individual CO_2-Glycine system cannot be used for the CO_2-MDEA-Glycine system. Therefore, these kinetic data reanalyzed using the equation 4.41. Rate expression for the MDEA and OH^- taken from the work of Benamor et al. [97] and Pinsent et al. [98]. And they are listed in the table 10.

Table 10: *Rate expression for MDEA and OH^-*

Rate	Equation	Sources
k_{MDEA} ($m^3.kmol^{-2}.s^{-1}$)	$k_2 = 2.56x10^9 e^{-\frac{5922.0}{T}}$	[97]
k_{OH} ($m^3.kmol^{-2}.s^{-1}$)	$k_{OH} = 4.33x10^{10} e^{-\frac{66666.0}{T}}$	[98]

Using the known concentration of the MDEA and OH^- in the CO_2-MDEA-Glycine. These terms were then subtracted from the k_{ov} of the equation 4.41, leaving only the k_{app} term associated with the effect of glycine. By performing non-linear regression using excel solver, on this k_{app} term, individual rate expressions for system were obtained. A Table showing the summary of the obtained constant for this system has been provided in the appendices (A4). The Arrhenius plot of the individual rate constants are shown in the figure 30 and rate expressions extracted from those Arrhenius plots along with all the other required expression to describe the kinetic data are summarized in the table 11.

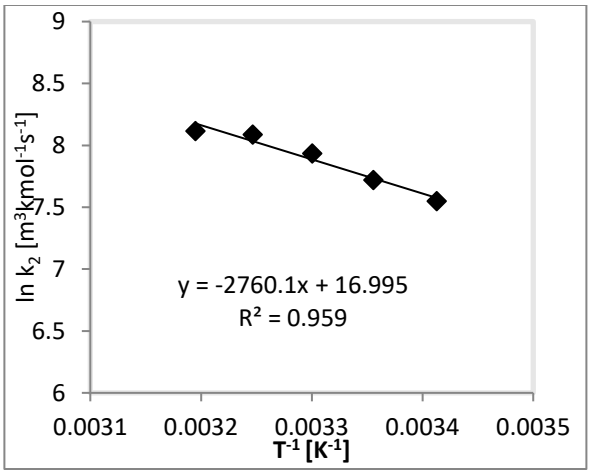

A) Lnk_2 vs T^{-1}

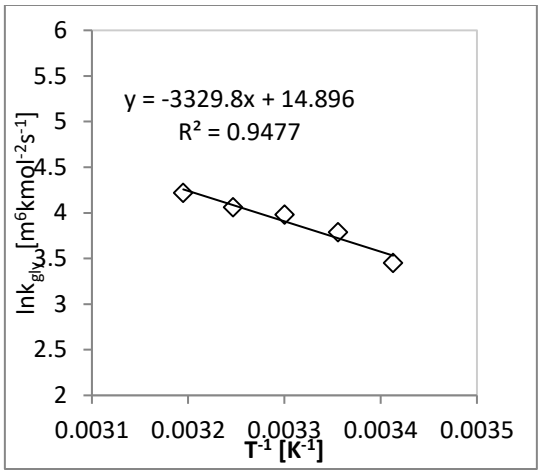

B) Lnk_{gly} vs T^{-1}

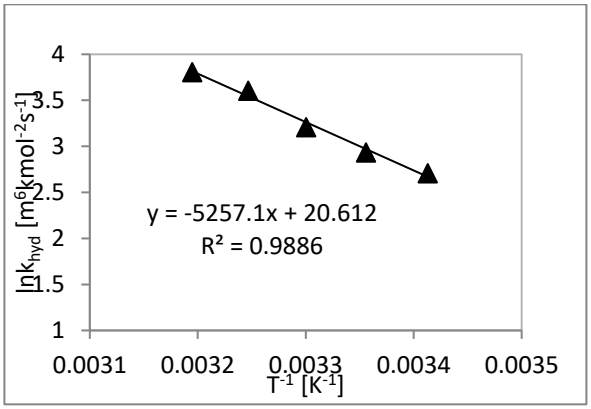

C) Lnk_{hyd} vs T^{-1}

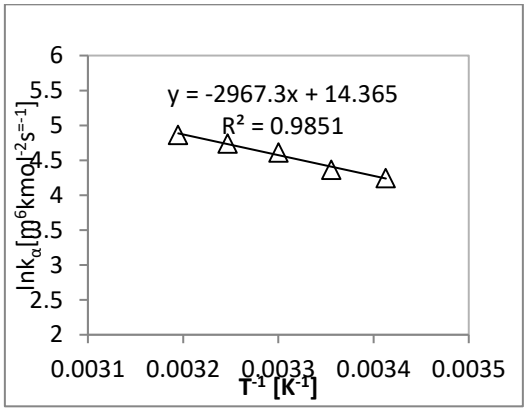

D) Lnk_{α} vs T^{-1}

Figure 30: Arhenius plots of CO_2-MDEA-Glycine system

Table 11: *Summary of rate expression for CO2-MDEA-Glycine systems*

Rate	$k_{ov} = k_{MDEA}[MDEA] + k_{OH^-}[OH^-] + \frac{[Gly]}{\frac{1}{k_2} + \frac{1}{k_{Gly}[Gly] + k_{\alpha}[MDEA] + k_{hyd}[OH]}}$		
	Lnk_0	E_a (kJ.mol^{-1})	Expression
k_{MDEA} ($m^3\,kmol^{-2}\,s^{-1}$)	21.66	49.24	$k_{MDEA} = 2.56x10^9 e^{-\frac{5922.0}{T}}$
k_{OH} ($m^3\,kmol^{-2}\,s^{-1}$)	24.49	554.26	$k_{OH} = 4.33x10^{10} e^{-\frac{66666.0}{T}}$
k_2 ($m^3\,kmol^{-2}\,s^{-1}$)	17.00	22.95	$k_2 = 2.40x10^7 e^{-\frac{3887.0}{T}}$
k_{gly} ($m^6\,kmol^{-2}\,s^{-1}$)	12.59	27.68	$k_{gly} = 2.94x10^5 e^{-\frac{42986}{T}}$
k_{α} ($m^6\,kmol^{-2}\,s^{-1}$)	14.37	24.67	$k_{\alpha} = 1.73x10^{06} e^{-\frac{4133}{T}}$
k_{hyd} ($m^6\,kmol^{-2}\,s^{-1}$)	13.70	43.71	$k_w = 8.95\,x10^5 e^{-\frac{45646}{T}}$

From the table 11, it is evident that activation energy for the formation of intermediate zwitterion, 'k_2'is for the CO_2-MDEA-Glycine system is much lower (E_a = 22.95 kj.mol^{-1}) than the one observed for the CO_2-Glycine system (E_a = 67.71 kj.mol^{-1}). This means the reaction proceeds much faster in presence of MDEA. Moreover, it can be further observed that the catalytic effect of the Glycine and MDEA species in the is also significant. Based, on these analysis, Furthermore, it is observed that activation energy for the catalytic effect of MDEA for the formation of carbamate is lower compared to glycine, this also shows the how the presence of base is affecting the overall reaction of the amine system. Based

on these observations, it can be said that observation of Guo et al. [84] on the unique behavior of glycine under basic conditions is true. The AAD% experimental and predicted kinetic data were around 9.3 %. The obtained parity plot has been shown in figure 31.

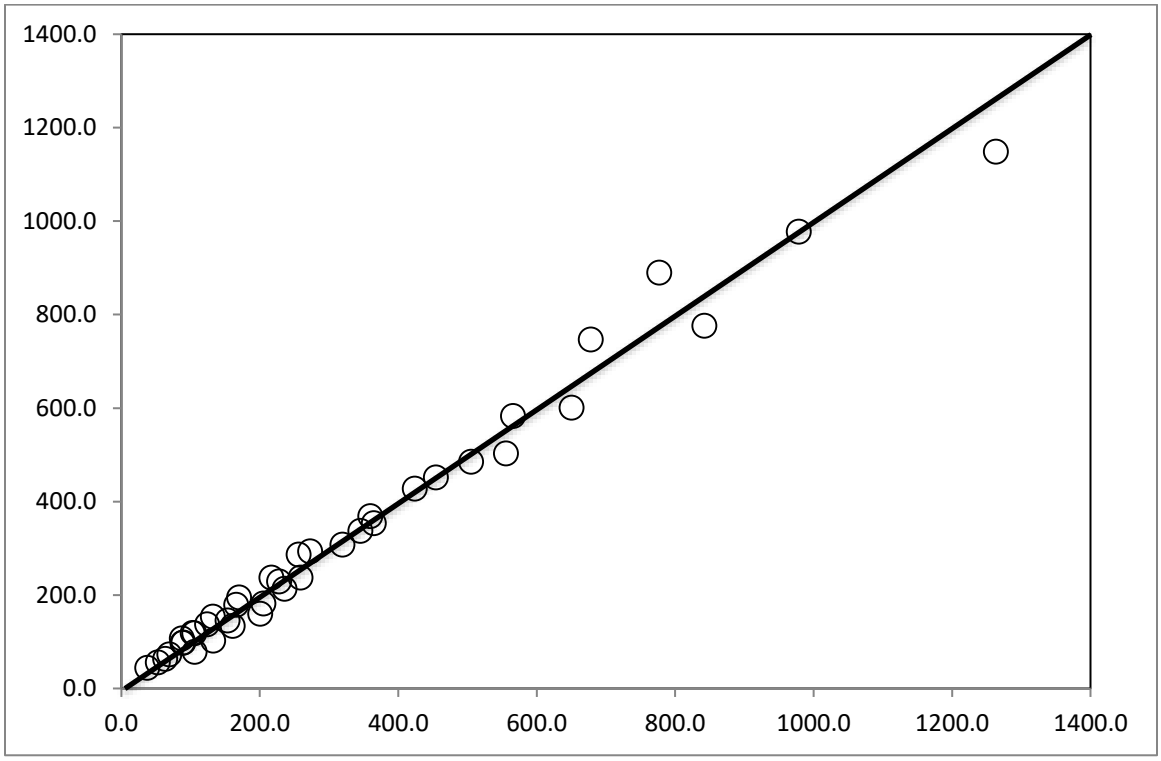

Figure 31: Parity plot of predicted vs experimental rate constants for CO_2MDEA-Glycine reaction obtained via zwitterion mechanism

It is to be noted the termolecular analysis of the CO_2-MDEA-Glycine system did not yield any satisfactory result as was the case for CO_2-Glycine system. Thus, the CO_2-MDEA-Glycine system was only analyzed using the zwitterion mechanism. The table with species

concentration calculations along the predicted reaction rate constant is given in the appendix. (Table D1)

7.5 Reaction of CO_2 with blends of MDEA-L-Arginine

The pseudo first order rate constant (k_{ov}) for the reaction of CO_2 with blends of MDEA-Glycine at different temperatures and concentrations was obtained through the stopped-flow experiments are shown in table 12. The obtained pseudo first order rate constants,' k_{ov}', were plotted against temperature for a one molar total concentration (Figures 32). The overall rate constants (k_{ov}) increased with increasing solution temperature as well as with increased [Arg] proportion in the total mixture. The effect of solution total concentrations under different temperatures and fixed Arg/MDEA ratio of 0.11 on the overall rate constants is shown in Figure 33.

Table 12: *Kinetic Data of CO2-MDEA-L-Arginine reaction*

Concentration, M		Temperature, K			
MDEA	ARG	298	303	308	313
0.975	0.025	99.17	124.65	171.38	213.71
0.950	0.050	177.47	226.15	294.32	357.97
0.900	0.100	312.35	410.33	532.24	625.84
0.475	0.025	82.40	107.15	149.90	188.23
0.450	0.050	152.55	195.64	234.18	310.72
0.400	0.100	320.43	423.84	496.55	632.39
0.225	0.025	60.75	78.32	101.41	130.31
0.200	0.050	125.47	165.36	231.21	302.60
0.175	0.075	214.23	281.52	357.73	451.29

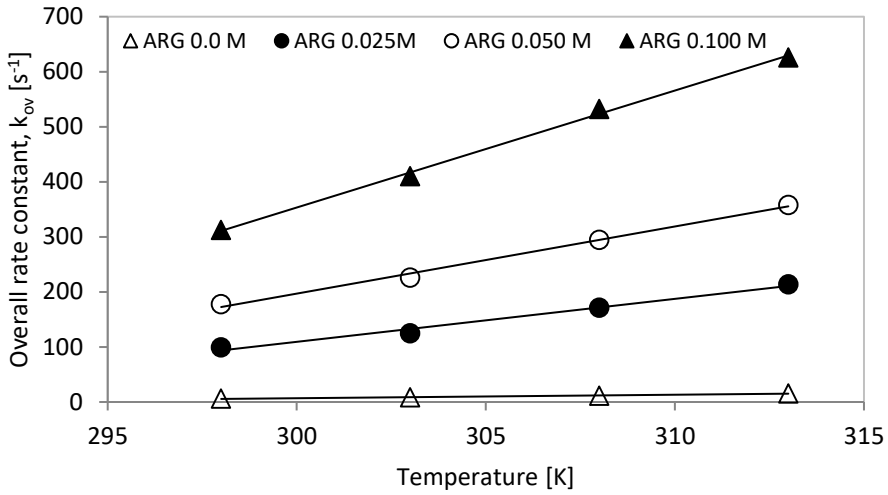

Figure 32: Rate constant,'k_{ov}', versus temperature for total 1 M solution

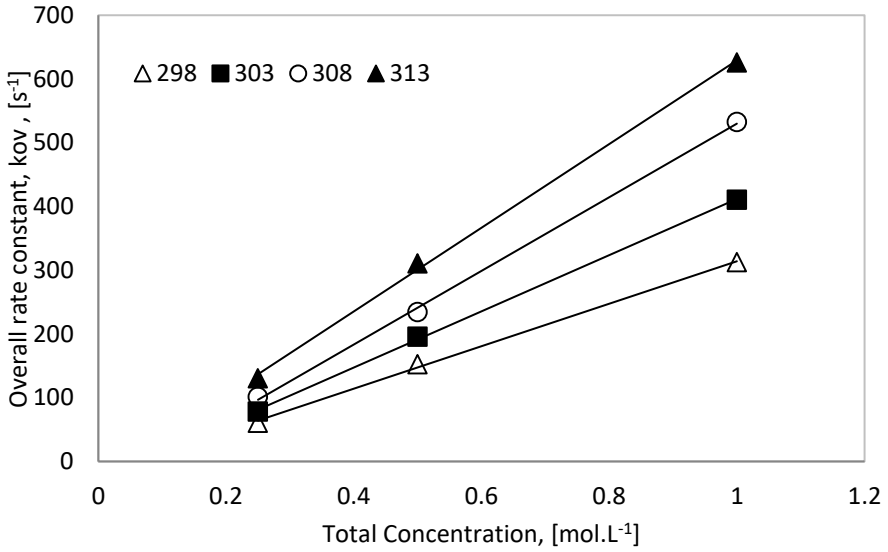

Figure 33:: Overall rate constant, 'k_{ov}', at different total concentrations and fixed Arg/MDEA ratio

Upon applying the power law kinetics to plot overall rate constants against the concentrations of L-Arginine, an average exponent of 0.98 was obtained, which affirms that the pseudo first order regime prevails. Therefore, within the experimental concentration range, the reaction can be analyzed via the zwitterion mechanism [94]. Additionally, the possibility of using the termolecular mechanism to interpret the obtained data was also checked by plotting k_{ov} /[ARG] against [ARG]. The plots show a satisfactory relationship indicating that the termolecular mechanism can be applied to the obtained experimental data. A typical plot regarding the applicability of termolecular mechanism has been shown in figure 34. Hence, obtained experimental data were analyzed using both the zwitterion and termolecular mechanisms.

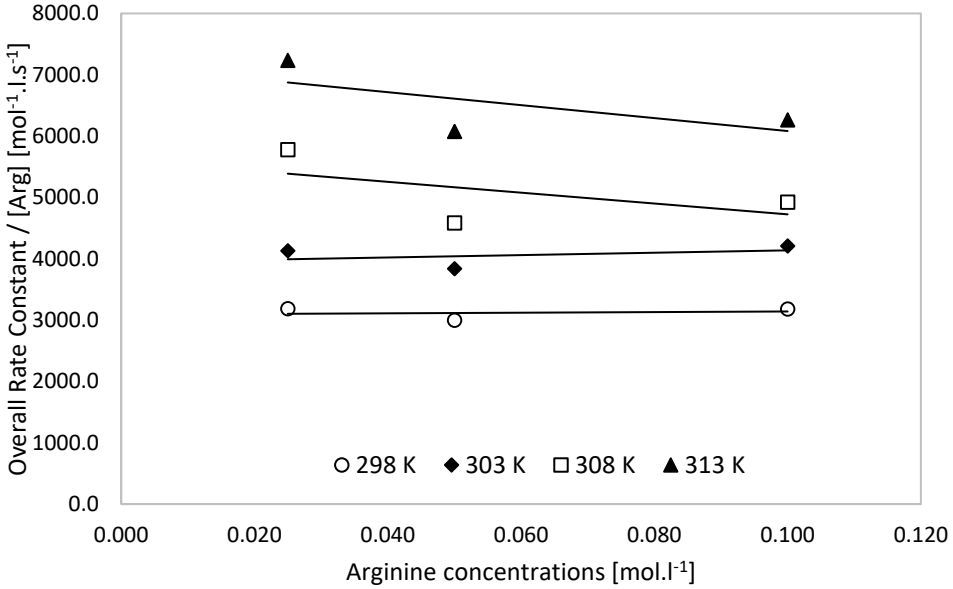

Figure 34:Termolecular Mechanism applicability at 0.5 M total concentration

7.5.1 Zwitterion Mechanism for CO_2-MDEA-L-Arginine system

For the CO_2-MDEA-L-Arginine systems, the approach described in the section 6.4 was used. The previously defined rate expressions of the CO_2-L-Arginine systems were used in the equation 4.49, from which only the rate expression for catalytic effect of the MDEA was determined via non-linear regression using excel solver. The summary of rate expressions for this amine system has been given in the table 13 below;

Table 13: Summary of rate expressions for CO_2-MDEA-L-Arginine systems

Rate	$k_{ov} = k_{MDEA}[MDEA] + k_{OH^-}[OH^-] + \frac{[Arg]}{\frac{1}{k_2} + \frac{1}{k_a[Arg] + k_b[MDEA] + k_w[H_2O]}}$		
	Lnk_0	E_a (kJ.mol^{-1})	Expression
k_{MDEA} ($m^3\,kmol^{-2}\,s^{-1}$)	21.66	49.24	$k_{MDEA} = 2.56x10^9 e^{-\frac{5922.0}{T}}$
k_{OH} ($m^3\,kmol^{-2}\,s^{-1}$)	24.49	554.26	$k_{OH} = 4.33x10^{10} e^{-\frac{66666.0}{T}}$
k_2 ($m^3\,kmol^{-2}\,s^{-1}$)	24.06	37.27	$k_2 = 2.81x10^{10} e^{-\frac{4482.9}{T}}$
k_a ($m^6\,kmol^{-2}\,s^{-1}$)	25.10	38.28	$k_a = 7.96x10^{10} e^{-\frac{4603.8}{T}}$
k_α ($m^6\,kmol^{-2}\,s^{-1}$)	24.83	42.27	$k_\alpha = 6.07x10^{10} e^{-\frac{5083.8}{T}}$
k_w ($m^6\,kmol^{-2}\,s^{-1}$)	18.63	36.29	$k_w = 1.23x10^9 e^{-\frac{4364.7}{T}}$

The predicted overall rate constants obtained using the rate expressions showed good agreement with the experimental rate constant, giving an AAD% of 7.6 %. The parity plot obtained for this system is given below;

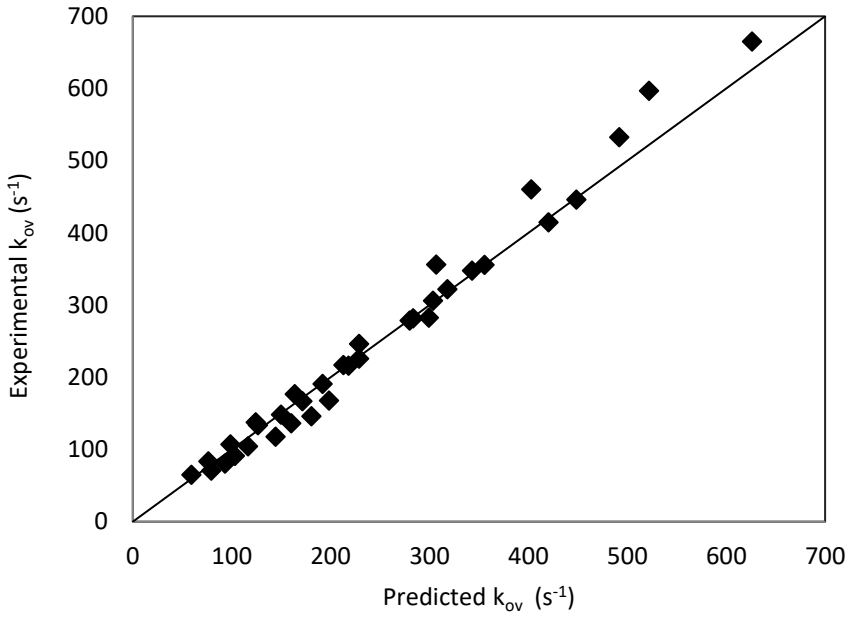

Figure 35: Parity plot of CO2-MDEA-L-Arginine system

The table with species concentration calculations along the predicted reaction rate constant is given in the appendix. (Table E1)

7.5.2 Termolecular Mechanism for CO_2-MDEA-L-Arginine system

Similar approach was taken to determine the to analyze the kinetic data for CO_2-MDEA-L-Arginine using the termolecular mechanism using equation 4.51. The parity plot obtained after the termolecular analysis is given in the figure 36 and rate expression obtained for the catalytic effect of MDEA along with the other terms used are summarized in the table 14.

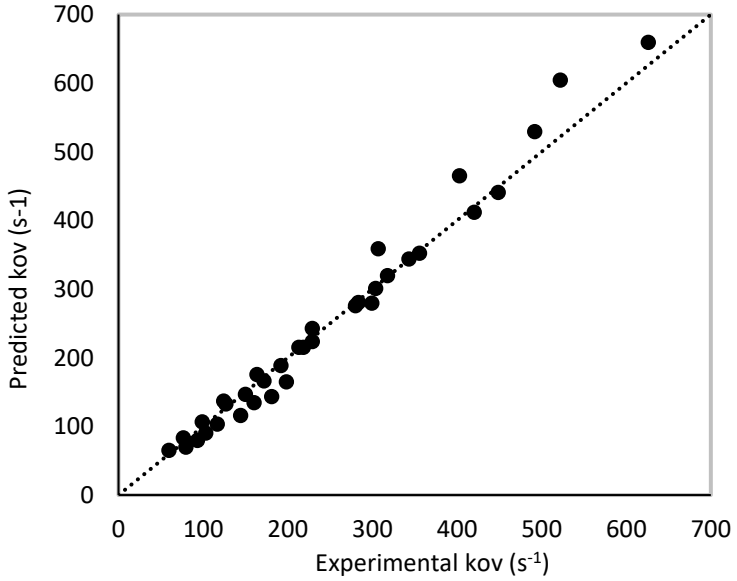

Figure 36: Parity plot for CO_2-MDEA-L-Arginine system obtained via termolecular mechanism

Table 14: Summary of the rate expressions for CO_2-MDEA-L-Arginine systems

Rate	$k_{ov} = k_{MDEA}[MDEA] + k_a[Arg] + k_\alpha[MDEA] + k_w[H_2O]$		
	$\ln k_0$	E_a (kJ.mol^{-1})	Expression
k_{MDEA} ($m^3\,kmol^{-2}\,s^{-1}$)	21.66	49.24	$k_{MDEA} = 2.56x10^9 e^{-\frac{5922.0}{T}}$
k_{OH} ($m^3\,kmol^{-2}\,s^{-1}$)	24.49	554.26	$k_{OH} = 4.33x10^{10} e^{-\frac{66666.0}{T}}$
k_a ($m^6\,kmol^{-2}\,s^{-1}$)	24.77	38.28	$k_a = 5.72x10^{10} e^{-\frac{4769.00}{T}}$
k_α ($m^6\,kmol^{-2}\,s^{-1}$)	23.38	40.65	$k_\alpha = 1.42x10^{10} e^{-\frac{4888.6}{T}}$
k_w ($m^6\,kmol^{-2}\,s^{-1}$)	18.63	36.29	$k_w = 9.41x10^7 e^{-\frac{4365.00}{T}}$

Upon evaluating the obtained rate expression for the 'k_α' term in both mechanisms, it is observed that activation energies in both models are comparable to each other (EaZ = 42.27 kJ.mol^{-1} and EaT = 40.65 kJ.mol^{-1}). Furthermore, it is noticed that regardless of the model used catalytic effect of Arginine (Ea^Z = Ea^T = 38.28 kJ.mol^{-1}) is higher than the catalytic effect of MDEA. Furthermore, AAD% in termolecular mechanism was 8 % which was comparable to that obtained via zwitterion mechanism (7.6%). Based on these observations, it can be concluded that the CO_2-MDEA-Arg reactions can be effectively interpreted using both zwitterion and termolecular mechanisms. The table with species concentration calculations along the predicted reaction rate constant is given in the appendix. (Table E2)

7.6 Comparison with other amine systems.

7.6.1 Comparison with secondary, tertiary and sterically hindered amine

The obtained rate constants data for 1M MDEA-Arg (0.9M MDEA + 0.1M Arg) and 1M MDEA-Gly (0.9M MDEA + 0.1M Gly) were compared with those of DEA [99], MDEA [97] and AMP [74] as shown in Figure 37. It was observed that the rate constants of both MDEA + Gly and MDEA-Arg were much lower than that of secondary amine (DEA) and lower than that of sterically hindered amine (AMP). MDEA+ Gly had higher rate constant than MDEA +Arg. However, the rate constant of MDEA-Arg mixtures were always higher than those of the tertiary amine (MDEA). This elucidates the effect of Amino acids presence in the MDEA-Amino acid blend which can enhance the overall kinetics of the CO2-MDEA reaction and make it comparable to other secondary and hindered amines. Based on the above analysis, the overall rate constants of these amine systems with CO2 were found to be in the following order: DEA > AMP > MDEA-Arg > MDEA-Arg > MDEA.

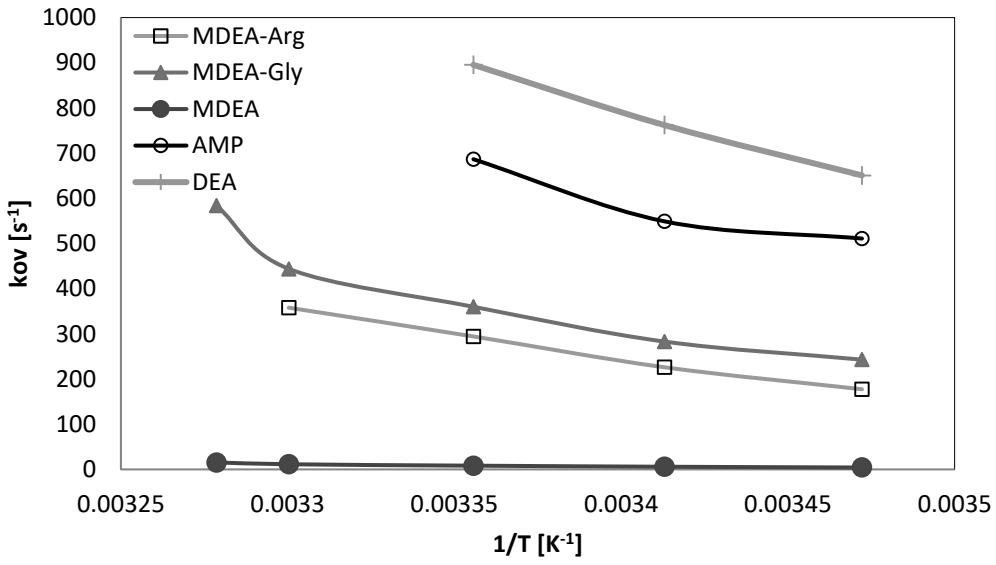

Figure 37: Comparison of the obtained data with MDEA-Arg with other amine systems

7.6.2 Comparison of the promoting effect of Amino acids

The promoting effect of L-Arginine and Glycine was further compared with that of the available data of MDEA-DEA [100] systems at different temperatures and at the same overall concentration (1M) as shown in figure 38. For all three compared systems, the same 0.1M of the promoter was added. It is observed that the addition of 0.1M Arginine in the MDEA-Arg has resulted in higher overall rate constant compared to the addition of the 0.1M DEA. However, the addition of 0.1M Glycine in the MDEA blend has resulted in higher overall rate constant compared to that of 0.1M Arginine. Although the previous study [91] revealed that the kinetics of Arginine alone with CO2 is higher that of the Glycine, Guo et al. [84] observed that the Glycine at higher pH exhibits faster kinetics. Since the presence of MDEA can increase pH of the solution, it triggers the base form of

Glycine to react with the CO2 resulting in a higher overall rate constant in the MDEA-Glycine blend as observed in the work of Benamor et al [97]. Furthermore, activation energy for the reaction of zwitterion intermediate formation of Glycine in the MDEA-Gly is 22.95 kJ.mol^{-1} [97] is also higher than that of L-Arginine (Ea = 37.27 kJ.mol^{-1}) in the MDEA-Arg blend. Therefore, based on this analysis the rate constants of the three blended amine systems with CO2 were found to be in the following order: MDEA-Gly>MDEA-Arg>MDEA-DEA.

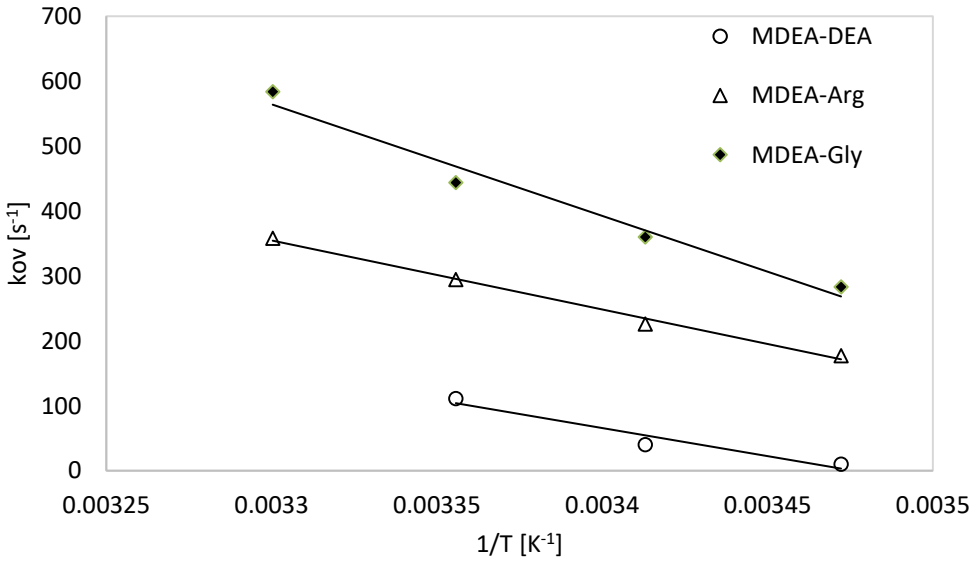

Figure 38: Comparison of the obtained data with MDEA-Arg with other MDEA blends.

Conclusions & Future Work:

Reduction of CO_2 emissions from the industrial power plant is vital to reduce the environmental implications of global warming. Among the several processes available to remove CO_2 from the industrial processes, the amine based post-combustion CO_2 capture process is the most mature one and can be easily retrofitted into existing process plants. However, efficiency of the CO_2 absorption in these processes is highly dependent on the type of the solvent used. Researchers are constantly trying to develop new and efficient solvents that can carb the issues related to the amine-based absorption processes and make it both environmentally and economically feasible. Common solvents like MEA, DEA, MDEA and AMP exhibits positive properties that can serve the purpose of CO_2 but these solvents have several drawbacks relating to operation cost, CO_2 loading, degradation, corrosion, solvent regeneration and energy consumption. Consequently, the use of environmentally friendly amino acids has been proposed in this work.

Amino acids are quite similar in structure to the conventional alkanolamines and there are around 20 amino acids, of which two amino acids, namely; Glycine and L-Arginine have been studied to be used as both as a solvent and a promoter. The kinetics of the CO_2 reaction with aqueous solutions of amino acids Glycine and L- Arginine and their blends were investigated using the stopped-flow apparatus at different concentrations and temperature ranging from 293 to 313 K. the reactions were analyzed using both zwitterion and termolecular mechanism. However, the obtained results

showed that the reaction between Glycine and CO_2 and between seemed to follow only the two-step zwitterion mechanism. While the reaction of Arginine with CO_2 could be explained by both zwitterion and termolecular mechanisms. The overall rate equations for the two reactions and their temperature dependencies were determined and the associated activation energies were evaluated. On evaluating the activation energies of k_2 for two amino acids, we found that the activation energy for CO_2-Arginine reaction was Less than those of CO_2-Glycine reactions. This, indicates that the reaction between Arginine and CO_2 is faster than CO_2-Glycine reactions. The obtained Ea values of CO_2-Glycine under neutral conditions were comparable to the literature.

The rate expressions obtained from the individual CO_2-Glycine and CO_2-L-Arginine reactions were than used to evaluate the kinetic data obtained for CO_2-MDEA-Glycine and CO_2-MDEA-L-Arginine blends. It was found that the rate expressions for CO_2-Glycine systems could not be used for CO_2-MDEA-Glycine as Glycine under basic conditions behaved different than under neutral conditions. A new set of rate expressions that account for the unique behavior of the glycine were than determined and that showed good agreement with the obtained kinetic data for CO_2-MDEA-Glycine systems. With an AAD% of 9.3 %. It was observed that the activation energy of for the formation of intermediate zwitterion, 'k_2'was much lower in the CO_2-MDEA-Glycine systems compared to the CO_2-Glycine systems. Also, the catalytic effect of MDEA was observed to be lower than that of glycine for the formation of carbamate, the kinetics of the reaction of CO_2 with MDEA-L-Arginine in aqueous solutions were then evaluated using the rate expressions obtained from the CO_2-L-Arginine systems. The rate constant to account for

the catalytic effect of MDEA, 'k_{α} 'was correlated well by an Arrhenius equation type. Both of the adopted zwitterion and termolecular model were very successful in accurately representing the experimental data with an AAD of 7.6% and 8.0%, respectively. Analysis of the obtained results analysis on the contribution of Arginine, MDEA and H2O to the catalytic carbamate formation pathway showed that the contribution of amino acid to the overall formation of is more important followed by the contribution of water in both models. While the contribution of MDEA molecules were found to be the least. A comparison of the obtained overall rate constant with other amine systems revealed that both CO_2-MDEA-L-Arginine and CO_2-MDEA-Glycine reactions was faster than MDEA-CO_2 reaction but slower than that of secondary and sterically hindered amine. A further comparison with MDEA-promotor blends showed that the reaction of MDEA-Arginine with CO_2 is slower than MDEA-Glycine but faster than MDEA-DEA.

Based on the kinetic study, it can be concluded that amino acids exhibit the potentials to be used as a solvent or promoter for amine-based CO_2 absorption processes. However, there are still several other aspects of amino acids that require to be studied in future works before it can be truly suggested to be used as solvent for CO_2 capture. It is quintessential to know the solubility of CO_2 into the amino acids and its MDEA blends and studies will be conducted to investigate this property and compare them against the conventional amines. Corrosion studies will also be conducted to investigate the corrosion rate. Future works will also focus on the investigation of heat of absorption of CO_2 in amino acids and formation of degradation products along with their reaction pathways. Finally, process optimization study will be conducted by simulating amino acid-

based CO_2 capture processes using process simulation software like ASPEN Plus, ASPEN HYSYS and Promax to benchmark the amino acid solvents against the current state of the art chemical solvents.

References

[1] K. Schoer, J. Weinzettel, J. Kovanda, J. r. Giegrich, and C. Lauwigi, "Raw material consumption of the European Union–concept, calculation method, and results," *Environmental Science & Technology,* vol. 46, no. 16, pp. 8903-8909, 2012.

[2] B. Petroleum, "BP Statistical Review of World Energy June 2015, 2015," *URL: http://www. bp. com/content/dam/bp/pdf/energy-economics/statistical-review-2015/bp-statistical-review-of-world-energy-2015-full-report. pdf,* 2015.

[3] Z. Chen and G. Chen, "An overview of energy consumption of the globalized world economy," *Energy Policy,* vol. 39, no. 10, pp. 5920-5928, 2011.

[4] B. Zhang, G. Chen, J. Li, and L. Tao, "Methane emissions of energy activities in China 1980–2007," *Renewable and Sustainable Energy Reviews,* vol. 29, pp. 11-21, 2014.

[5] A. Ç. Köne and T. Büke, "Forecasting of CO2 emissions from fuel combustion using trend analysis," *Renewable and Sustainable Energy Reviews,* vol. 14, no. 9, pp. 2906-2915, 2010/12/01/ 2010.

[6] F. Birol, "World energy outlook 2010," *International Energy Agency,* vol. 1, no. 3, 2010.

[7] C. Change, "Synthesis Report (eds Core Writing Team, Pachauri, RK & Meyer, LA)(IPCC, 2015)," 2014.

[8] E. Olale, T. O. Ochuodho, V. Lantz, and J. El Armali, "The environmental Kuznets curve model for greenhouse gas emissions in Canada," *Journal of Cleaner Production,* vol. 184, pp. 859-868, 2018/05/20/ 2018.

[9] T. O. Ochuodho and V. A. Lantz, "Economic impacts of climate change in the forest sector: a comparison of single-region and multiregional CGE modeling frameworks," *Canadian journal of forest research,* vol. 44, no. 5, pp. 449-464, 2014.

[10] J. G. Olivier, J. A. Peters, and G. Janssens-Maenhout, "Trends in global CO2 emissions 2012 report," 2012.

[11] P. Villoria-Sáez, V. W. Y. Tam, M. d. Río Merino, C. Viñas Arrebola, and X. Wang, "Effectiveness of greenhouse-gas Emission Trading Schemes implementation: a review on legislations," *Journal of Cleaner Production,* vol. 127, pp. 49-58, 7/20/ 2016.

[12] A. B. Rao and E. S. Rubin, "A technical, economic, and environmental assessment of amine-based CO2 capture technology for power plant greenhouse gas control," *Environmental science & technology,* vol. 36, no. 20, pp. 4467-4475, 2002.

[13] H. d. Coninck, M. Loos, B. Metz, O. Davidson, and L. Meyer, "IPCC special report on carbon dioxide capture and storage," *Intergovernmental Panel on Climate Change,* 2005.

[14] A. L. Kohl and R. Nielsen, *Gas purification*. Gulf Professional Publishing, 1997.

[15] G. Sartori and D. W. Savage, "Sterically hindered amines for carbon dioxide removal from gases," *Industrial & Engineering Chemistry Fundamentals,* vol. 22, no. 2, pp. 239-249, 1983.

[16] J. Gabrielsen, M. L. Michelsen, E. H. Stenby, and G. M. Kontogeorgis, "Modeling of CO2 absorber using an AMP solution," *AIChE journal,* vol. 52, no. 10, pp. 3443-3451, 2006.

[17] P. S. Kumar, J. A. Hogendoorn, S. J. Timmer, P. H. M. Feron, and G. F. Versteeg, "Equilibrium Solubility of CO2 in Aqueous Potassium Taurate Solutions: Part 2. Experimental VLE Data and Model," *Industrial & engineering chemistry research,* vol. 42, no. 12, pp. 2841-2852, 2003/06/01 2003.

[18] B. Thitakamol, A. Veawab, and A. Aroonwilas, "Environmental impacts of absorption-based CO2 capture unit for post-combustion treatment of flue gas from coal-fired power plant," *International Journal of Greenhouse Gas Control,* vol. 1, no. 3, pp. 318-342, 2007.

[19] G. Couchaux, D. Barth, M. Jacquin, A. Faraj, and J. Grandjean, "Kinetics of carbon dioxide with amines. I. Stopped-flow studies in aqueous solutions. A review," *Oil & Gas Science and Technology–Revue d'IFP Energies nouvelles,* vol. 69, no. 5, pp. 865-884, 2014.

[20] P. D. Vaidya and E. Y. Kenig, "Gas–Liquid reaction kinetics: a review of determination methods," *Chemical Engineering Communications,* vol. 194, no. 12, pp. 1543-1565, 2007.

[21] I. Sreedhar, T. Nahar, A. Venugopal, and B. Srinivas, "Carbon capture by absorption – Path covered and ahead," *Renewable and Sustainable Energy Reviews,* vol. 76, pp. 1080-1107, 2017/09/01/ 2017.

[22] B. Metz, O. R. Davidson, P. R. Bosch, R. Dave, and L. A. Meyer, "Contribution of working group III to the fourth assessment report of the intergovernmental panel on climate change, 2007," ed: Cambridge University Press, Cambridge, UK, 2007.

[23] S. Badr, J. Frutiger, K. Hungerbuehler, and S. Papadokonstantakis, "A framework for the environmental, health and safety hazard assessment for amine-based post combustion CO2 capture," *International Journal of Greenhouse Gas Control,* vol. 56, pp. 202-220, 2017.

[24] G. Krishnan, D. Steele, K. O'Brien, R. Callahan, K. Berchtold, and J. Figueroa, "Simulation of a process to capture CO2 from IGCC syngas using a high temperature PBI membrane," *Energy Procedia,* vol. 1, no. 1, pp. 4079-4088, 2009.

[25] J. D. Figueroa, T. Fout, S. Plasynski, H. McIlvried, and R. D. Srivastava, "Advances in CO2 capture technology—the US Department of Energy's Carbon Sequestration Program," *International journal of greenhouse gas control,* vol. 2, no. 1, pp. 9-20, 2008.

[26] A. Brunetti, F. Scura, G. Barbieri, and E. Drioli, "Membrane technologies for CO2 separation," *Journal of Membrane Science,* vol. 359, no. 1-2, pp. 115-125, 2010.

[27] H. Yang *et al.*, "Progress in carbon dioxide separation and capture: A review," *Journal of environmental sciences,* vol. 20, no. 1, pp. 14-27, 2008.

[28] E. Rubin, L. Meyer, and H. Conincks, "IPCC Special Report on Carbon Capture and Storage," *World Meteorological Organization (WMO)/United Nations Environmental Programme (UNEP) Intergovernmental Panel on Climate Change (IPCC), Intergovernmental Panel on Climate Change (IPCC)(eds.),* 2005.

[29] M. Edali, A. Aboudheir, and R. Idem, "Kinetics of carbon dioxide absorption into mixed aqueous solutions of MDEA and MEA using a laminar jet apparatus and a numerically solved 2D absorption rate/kinetics model," *International Journal of Greenhouse Gas Control,* vol. 3, no. 5, pp. 550-560, 2009.

[30] A. M. Arranz, "Hype among low-carbon technologies: Carbon capture and storage in comparison," *Global Environmental Change,* vol. 41, pp. 124-141, 2016.

[31] G. Rochelle, E. Chen, R. Dugas, B. Oyenakan, and F. Seibert, "Solvent and process enhancements for CO2 absorption/stripping," in *2005 Annual Conference on Capture and Sequestration, Alexandria, VA*, 2006.

[32] K. P. Resnik, J. T. Yeh, and H. W. Pennline, "Aqua ammonia process for simultaneous removal of CO2, SO2 and NOx," *International journal of environmental technology and management,* vol. 4, no. 1-2, pp. 89-104, 2004.

[33] J. T. Yeh, K. P. Resnik, K. Rygle, and H. W. Pennline, "Semi-batch absorption and regeneration studies for CO2 capture by aqueous ammonia," *Fuel Processing Technology,* vol. 86, no. 14-15, pp. 1533-1546, 2005.

[34] O. Pederson, H. Dannstrom, M. Gronvold, D. Stuksrud, and O. Ronning, "Gas treating using membrane gas/liquid contactors," in *Fifth International Conference on Greenhouse Gas Control Technologies, Cairns, Australia*, 2000.

[35] R. Willis, A. Benin, J. Low, R. Bedard, and D. Lesch, "Annual Report Project DE-FG26-04NT42121," *National Energy Technology Laboratory technical report,* 2006.

[36] E. D. Bates, R. D. Mayton, I. Ntai, and J. H. Davis, "CO2 capture by a task-specific ionic liquid," *Journal of the American Chemical Society,* vol. 124, no. 6, pp. 926-927, 2002.

[37] B. E. Gurkan *et al.*, "Equimolar CO2 absorption by anion-functionalized ionic liquids," *Journal of the American Chemical Society,* vol. 132, no. 7, pp. 2116-2117, 2010.

[38] B. F. Goodrich *et al.*, "Experimental measurements of amine-functionalized anion-tethered ionic liquids with carbon dioxide," *Industrial & Engineering Chemistry Research,* vol. 50, no. 1, pp. 111-118, 2010.

[39] X. Li *et al.*, "Absorption of CO 2 by ionic liquid/polyethylene glycol mixture and the thermodynamic parameters," *Green Chemistry,* vol. 10, no. 8, pp. 879-884, 2008.

[40] X. Y. Luo, X. Fan, G. L. Shi, H. R. Li, and C. M. Wang, "Decreasing the viscosity in CO2 capture by amino-functionalized ionic liquids through the formation of intramolecular hydrogen bond," *The Journal of Physical Chemistry B,* vol. 120, no. 10, pp. 2807-2813, 2016.

[41] W. L. Theo, J. S. Lim, H. Hashim, A. A. Mustaffa, and W. S. Ho, "Review of pre-combustion capture and ionic liquid in carbon capture and storage," *Applied energy,* vol. 183, pp. 1633-1663, 2016.

[42] J. Gabrielsen, "CO2 capture from coal fired power plants," *Graduate Schools Yearbook 2005,* p. 61, 2005.

[43] M. E. Majchrowicz, "Amino acid salt solutions for carbon dioxide capture," 2014.

[44] J. Van Holst, P. P. Politiek, J. P. Niederer, and G. F. Versteeg, "CO2 capture from flue gas using amino acid salt solutions," in *proceedings of 8th international conference on greenhouse gas control technologies*, 2006.

[45] P. Singh, J. P. Niederer, and G. F. Versteeg, "Structure and activity relationships for amine based CO2 absorbents—I," *International Journal of Greenhouse Gas Control,* vol. 1, no. 1, pp. 5-10, 2007.

[46] V. Darde, *CO2 Capture Using Aqueous Ammonia: Ph. D. Thesis*. Department of Chemical and Biochemical Engineering, Technical University of Denmark, 2011.

[47] K. A. Hoff, O. Juliussen, O. Falk-Pedersen, and H. F. Svendsen, "Modeling and experimental study of carbon dioxide absorption in aqueous alkanolamine solutions using a membrane contactor," *Industrial & engineering chemistry research,* vol. 43, no. 16, pp. 4908-4921, 2004.

[48] R. J. Hook, "An investigation of some sterically hindered amines as potential carbon dioxide scrubbing compounds," *Industrial & engineering chemistry research,* vol. 36, no. 5, pp. 1779-1790, 1997.

[49] T. Chakravarty, U. Phukan, and R. Weilund, "Reaction of acid gases with mixtures of amines," *Chem. Eng. Prog.;(United States),* vol. 81, no. 4, 1985.

[50] W.-J. Choi *et al.*, "Removal of carbon dioxide by absorption into blended amines: kinetics of absorption into aqueous AMP/HMDA, AMP/MDEA, and AMP/piperazine solutions," *Green Chemistry,* vol. 9, no. 6, pp. 594-598, 2007.

[51] B. M. Lerche, E. H. Stenby, and K. Thomsen, "CO2 capture from flue gas using amino acid salt solutions," *Department of Chemical and Biochemical Engineering. Technical University of Denmark, Denmark,* 2012.

[52] C. Matthews, K. van Holde, and K. Ahern, "Biochemistry, Harlow," ed: Benjamin Cummings, San Francisco, 2000.

[53] J. McMurry, *Fundamentals of organic chemistry*. Thomson Learning, 1998.

[54] G. Hu, K. H. Smith, Y. Wu, S. E. Kentish, and G. W. Stevens, "Screening Amino Acid Salts as Rate Promoters in Potassium Carbonate Solvent for Carbon Dioxide Absorption," *Energy & Fuels,* vol. 31, no. 4, pp. 4280-4286, 2017/04/20 2017.

[55] P. S. Kumar, J. A. Hogendoorn, G. F. Versteeg, and P. H. M. Feron, "Kinetics of the reaction of CO2 with aqueous potassium salt of taurine and glycine," *AIChE Journal,* vol. 49, no. 1, pp. 203-213, 2003.

[56] P. D. Vaidya, P. Konduru, M. Vaidyanathan, and E. Y. Kenig, "Kinetics of Carbon Dioxide Removal by Aqueous Alkaline Amino Acid Salts," *Industrial & engineering chemistry research,* vol. 49, no. 21, pp. 11067-11072, 2010/11/03 2010.

[57] R. J. Littel, M. Bos, and G. J. Knoop, "Dissociation constants of some alkanolamines at 293, 303, 318, and 333 K," *Journal of Chemical & Engineering Data,* vol. 35, no. 3, pp. 276-277, 1990/07/01 1990.

[58] D. E. Penny and T. J. Ritter, "Kinetic study of the reaction between carbon dioxide and primary amines," *Journal of the Chemical Society, Faraday Transactions 1: Physical Chemistry in Condensed Phases,* 10.1039/F19837902103 vol. 79, no. 9, pp. 2103-2109, 1983.

[59] H. Thee, N. J. Nicholas, K. H. Smith, G. da Silva, S. E. Kentish, and G. W. Stevens, "A kinetic study of CO2 capture with potassium carbonate solutions promoted with various amino acids: Glycine, sarcosine and proline," *International Journal of Greenhouse Gas Control,* vol. 20, pp. 212-222, 2014/01/01/ 2014.

[60] A. F. Portugal, F. D. Magalhães, and A. Mendes, "Carbon dioxide absorption kinetics in potassium threonate," *Chemical Engineering Science,* vol. 63, no. 13, pp. 3493-3503, 2008/07/01/ 2008.

[61] S. Paul and K. Thomsen, "Kinetics of absorption of carbon dioxide into aqueous potassium salt of proline," *International Journal of Greenhouse Gas Control,* vol. 8, pp. 169-179, 2012.

[62] M. E. Majchrowicz, S. Kersten, and W. Brilman, "Reactive Absorption of Carbon Dioxide in l-Prolinate Salt Solutions," *Industrial & engineering chemistry research,* vol. 53, no. 28, pp. 11460-11467, 2014/07/16 2014.

[63] A. Sodiq, A. V. Rayer, A. A. Olanrewaju, and M. R. M. Abu Zahra, "Reaction Kinetics of Carbon Dioxide (CO2) Absorption in Sodium Salts of Taurine and Proline Using a Stopped-Flow Technique," *International Journal of Chemical Kinetics,* vol. 46, no. 12, pp. 730-745, 2014.

[64] J.-a. Lim, D. H. Kim, Y. Yoon, S. K. Jeong, K. T. Park, and S. C. Nam, "Absorption of CO2 into Aqueous Potassium Salt Solutions of l-Alanine and l-Proline," *Energy & Fuels,* vol. 26, no. 6, pp. 3910-3918, 2012/06/21 2012.

[65] M. Kim, H.-J. Song, M.-G. Lee, H.-Y. Jo, and J.-W. Park, "Kinetics and Steric Hindrance Effects of Carbon Dioxide Absorption into Aqueous Potassium Alaninate Solutions," *Industrial & engineering chemistry research,* vol. 51, no. 6, pp. 2570-2577, 2012/02/15 2012.

[66] C.-C. Wei, G. Puxty, and P. Feron, "Amino acid salts for CO2 capture at flue gas temperatures," *Chemical Engineering Science,* vol. 107, pp. 218-226, 2014/04/07/ 2014.

[67] S. Shen, Y.-n. Yang, Y. Bian, and Y. Zhao, "Kinetics of CO2 Absorption into Aqueous Basic Amino Acid Salt: Potassium Salt of Lysine Solution," *Environmental Science & Technology,* vol. 50, no. 4, pp. 2054-2063, 2016/02/16 2016.

[68] S. Shen, Y.-n. Yang, Y. Zhao, and Y. Bian, "Reaction kinetics of carbon dioxide absorption into aqueous potassium salt of histidine," *Chemical Engineering Science,* vol. 146, pp. 76-87, 2016.

[69] E. F. da Silva and H. F. Svendsen, "Study of the Carbamate Stability of Amines Using ab Initio Methods and Free-Energy Perturbations," *Industrial & engineering chemistry research,* vol. 45, no. 8, pp. 2497-2504, 2006/04/01 2006.

[70] K.-S. Hwang, D.-W. Park, K.-J. Oh, S.-S. Kim, and S.-W. Park, "Chemical Absorption of Carbon Dioxide into Aqueous Solution of Potassium Threonate," *Separation Science and Technology,* vol. 45, no. 4, pp. 497-507, 2010/02/25 2010.

[71] S. Lee, H.-J. Song, S. Maken, and J.-W. Park, "Kinetics of CO2 Absorption in Aqueous Sodium Glycinate Solutions," *Industrial & engineering chemistry research,* vol. 46, no. 5, pp. 1578-1583, 2007/02/01 2007.

[72] J. v. Holst, G. F. Versteeg, D. W. F. Brilman, and J. A. Hogendoorn, "Kinetic study of with various amino acid salts in aqueous solution," *Chemical Engineering Science,* vol. 64, no. 1, pp. 59-68, 2009.

[73] F. Khalili, A. Henni, and A. L. L. East, "pKa Values of Some Piperazines at (298, 303, 313, and 323) K," *Journal of Chemical & Engineering Data,* vol. 54, no. 10, pp. 2914-2917, 2009/10/08 2009.

[74] S. Xu, Y.-W. Wang, F. D. Otto, and A. E. Mather, "Kinetics of the reaction of carbon dioxide with 2-amino-2-methyl-1-propanol solutions," *Chemical Engineering Science,* vol. 51, no. 6, pp. 841-850, 1996/03/01/ 1996.

[75] G. F. Versteeg and W. P. M. Van Swaaij, "Solubility and diffusivity of acid gases (carbon dioxide, nitrous oxide) in aqueous alkanolamine solutions," *Journal of Chemical & Engineering Data,* vol. 33, no. 1, pp. 29-34, 1988/01/01 1988.

[76] M. Caplow, "Kinetics of carbamate formation and breakdown," *Journal of the American Chemical Society,* vol. 90, no. 24, pp. 6795-6803, 1968/11/01 1968.

[77] P. V. Danckwerts, "The reaction of CO2 with ethanolamines," *Chemical Engineering Science,* Article vol. 34, no. 4, pp. 443-446, 1979.

[78] G. Versteeg and M. Oyevaar, "The reaction between CO2 and diethanolamine at 298 K," *Chem. Eng. Sci,* vol. 44, no. 5, pp. 1264-1268, 1989.

[79] J. E. Crooks and J. P. Donnellan, "Kinetics and mechanism of the reaction between carbon dioxide and amines in aqueous solution," *Journal of the Chemical Society, Perkin Transactions 2,* 10.1039/P29890000331 no. 4, pp. 331-333, 1989.

[80] E. F. da Silva and H. F. Svendsen, "Computational chemistry study of reactions, equilibrium and kinetics of chemical CO2 absorption," *International Journal of Greenhouse Gas Control,* vol. 1, no. 2, pp. 151-157, 2007.

[81] T. L. Donaldson and Y. N. Nguyen, "Carbon dioxide reaction kinetics and transport in aqueous amine membranes," *Industrial & Engineering Chemistry Fundamentals,* vol. 19, no. 3, pp. 260-266, 1980.

[82] E. Jorgensen and C. Faurholt, "REACTIONS BETWEEN CARBON DIOXIDE AND AMINO ALCOHOLS. 2. TRIETHANOLAMINE," *Acta Chemica Scandinavica,* vol. 8, no. 7, pp. 1141-1144, 1954.

[83] J. Benitez-Garcia, G. Ruiz-Ibanez, H. A. Al-Ghawas, and O. C. Sandall, "On the effect of basicity on the kinetics of CO2 absorption in tertiary amines," *Chemical engineering science,* vol. 46, no. 11, pp. 2927-2931, 1991.

[84] D. Guo *et al.*, "Amino Acids as Carbon Capture Solvents: Chemical Kinetics and Mechanism of the Glycine + CO2 Reaction," *Energy & Fuels,* vol. 27, no. 7, pp. 3898-3904, 2013/07/18 2013.

[85] H. Liu *et al.*, "Kinetics of CO2 absorption into a novel 1-diethylamino-2-propanol solvent using stopped-flow technique," *AIChE Journal,* vol. 60, no. 10, pp. 3502-3510, 2014.

[86] J. Li, A. Henni, and P. Tontiwachwuthikul, "Reaction kinetics of CO2 in aqueous ethylenediamine, ethyl ethanolamine, and diethyl monoethanolamine solutions in the temperature range of 298− 313 K, using the stopped-flow technique," *Industrial & engineering chemistry research,* vol. 46, no. 13, pp. 4426-4434, 2007.

[87] S. H. Ali, S. Q. Merchant, and M. A. Fahim, "Kinetic study of reactive absorption of some primary amines with carbon dioxide in ethanol solution," *Separation and purification technology,* vol. 18, no. 3, pp. 163-175, 2000.

[88] A. C. Knipe, D. McLean, and R. L. Tranter, "A fast response conductivity amplifier for chemical kinetics," *Journal of Physics E: Scientific Instruments,* vol. 7, no. 7, p. 586, 1974.

[89] G. Astarita, D. W. Savage, and A. Bisio, *Gas treating with chemical solvents*. John Wiley, 1983.

[90] R. J. Littel, M. Bos, and G. J. Knoop, "Dissociation constants of some alkanolamines at 293, 303, 318, and 333 K," *Journal of Chemical and Engineering Data,* vol. 35, no. 3, pp. 276-277, 1990.

[91] N. Mahmud, A. Benamor, M. S. Nasser, M. J. Al-Marri, H. Qiblawey, and P. Tontiwachwuthikul, "Reaction kinetics of carbon dioxide with aqueous solutions of l-Arginine, Glycine & Sarcosine using the stopped flow technique," *International Journal of Greenhouse Gas Control,* vol. 63, no. Supplement C, pp. 47-58, 2017/08/01/ 2017.

[92] E. S. Hamborg, J. P. M. Niederer, and G. F. Versteeg, "Dissociation Constants and Thermodynamic Properties of Amino Acids Used in CO2 Absorption from (293 to 353) K," *Journal of Chemical & Engineering Data,* vol. 52, no. 6, pp. 2491-2502, 2007/11/01 2007.

[93] T. Edwards, G. Maurer, J. Newman, and J. Prausnitz, "Vapor-liquid equilibria in multicomponent aqueous solutions of volatile weak electrolytes," *AIChE Journal,* vol. 24, no. 6, pp. 966-976, 1978.

[94] E. Alper and W. Bouhamra, "Kinetics and mechanisms of reaction between carbon disulphide and morpholine in aqueous solutions," *Chemical Engineering & Technology,* vol. 17, no. 2, pp. 138-140, 1994.

[95] P. D. Vaidya and E. Y. Kenig, "Termolecular Kinetic Model for CO2-Alkanolamine Reactions: An Overview," *Chemical Engineering & Technology,* vol. 33, no. 10, pp. 1577-1581, 2010.

[96] C. T. Armstrong, P. E. Mason, J. L. R. Anderson, and C. E. Dempsey, "Arginine side chain interactions and the role of arginine as a gating charge carrier in voltage sensitive ion channels," *Scientific Reports,* Article vol. 6, p. 21759, 2016.

[97] A. Benamor, M. J. Al-Marri, M. Khraisheh, M. S. Nasser, and P. Tontiwachwuthikul, "Reaction kinetics of carbon dioxide in aqueous blends of N-methyldiethanolamine and glycine using the stopped flow technique," *Journal of Natural Gas Science and Engineering,* vol. 33, pp. 186-195, 2016.

[98] B. R. W. Pinsent, L. Pearson, and F. J. W. Roughton, "The kinetics of combination of carbon dioxide with hydroxide ions," *Transactions of the Faraday Society,* 10.1039/TF9565201512 vol. 52, no. 0, pp. 1512-1520, 1956.

[99] R. J. Littel, G. F. Versteeg, and W. P. M. Van Swaaij, "Kinetics of CO2 with primary and secondary amines in aqueous solutions—II. Influence of temperature on zwitterion formation and deprotonation rates," *Chemical Engineering Science,* vol. 47, no. 8, pp. 2037-2045, 1992/06/01/ 1992.

[100] A. Benamor and M. J. Al-Marri, "Reactive Absorption of CO2 into Aqueous Mixtures of Methyldiethanolamine and Diethanolamine," *International Journal of Chemical Engineering and Applications,* vol. 5, no. 4, pp. 291-297, 2014.

Appendix

Table A 1: Rate constants for the reaction of CO2 with Glycine based on Zwitterion mechanism

GLY	$OH^{-}\times10^{2}$	$H_2O\times10^{-2}$	$K_{ov\text{-}exp}$	$K_{ov\text{-}pre}$	Error	k_2	k_w
mole/l	mole/l	mole/l	s^{-1}	s^{-1}	%	m^3 /kmole.s	$m^6.kmole^{-2}.s^{-1}$
				T=293K			
0.1000	0.23	0.551	1.42	1.37	3.86	27.56	49.12
0.0875	0.22	0.551	1.10	1.20	8.29		
0.0750	0.20	0.552	1.02	1.02	0.57	AAD%	3.7
0.0625	0.18	0.552	0.88	0.85	2.90		
0.0500	0.17	0.553	0.71	0.68	3.13		
				T=298K			
0.1000	0.24	0.551	2.45	2.24	8.44	45.06	80.83
0.0875	0.23	0.551	1.82	1.96	7.84		
0.0750	0.21	0.552	1.69	1.68	0.53	AAD%	3.7
0.0625	0.19	0.552	1.39	1.40	0.84		
0.0500	0.17	0.553	1.13	1.12	1.07		
				T=303K			
0.1000	0.25	0.551	3.54	3.54	0.09	71.03	127.89
0.0875	0.24	0.551	2.92	3.10	6.18		
0.0750	0.22	0.552	2.72	2.66	2.43	AAD%	3.4
0.0625	0.20	0.552	2.18	2.21	1.78		

0.0500	0.18	0.553	1.89	1.77	6.32		
				T=308K			
0.1000	0.26	0.551	5.23	5.30	1.33	106.27	191.74
0.0875	0.25	0.551	4.42	4.92	4.92		
0.0750	0.23	0.552	4.10	3.98	3.05	AAD%	3.1
0.0625	0.21	0.552	3.49	3.32	5.11		
0.0500	0.19	0.553	2.62	2.65	1.29		
				T=313K			
0.1000	0.27	0.551	7.95	8.24	3.58	166.26	300.45
0.0875	0.25	0.551	7.11	7.21	1.33		
0.0750	0.24	0.552	6.30	6.18	1.82	AAD%	2.0
0.0625	0.21	0.552	5.17	5.15	0.21		
0.0500	0.19	0.553	4.26	4.13	3.16		
				Overall AAD%			3.2

Table B 1: Rate constants for the reaction of CO2 with L-Arginine based on Zwitterion mechanism

ARG	OH $\times 10^{3}$	H_2O $\times 10^{-2}$	k_{ov-exp}	k_{ov-pre}	AAD	k_2	k_β	k_w
mole/l	mole/l	mole/l	s-1	s-1	%	$m^3\ kmole^{-1}.s^{-1}$	$m^6.kmole^{-2}.s^{-1}$	$m^6.kmole^{-2}.s^{-1}$
				T=293K				
0.20	1.42	0.53	522.6	531.8	1.8	6224.76	12002.72	4185.54
0.15	1.22	0.54	374.2	368.7	1.5			
0.10	1.00	0.55	226.5	223.3	1.4		AAD%	1.4
0.05	0.71	0.55	98.0	99.0	1.0			
				T=298K				
0.20	1.57	0.54	680.7	686.6	0.9	8047.41	15113.40	5536.07
0.15	1.36	0.54	482.2	477.1	1.1			
0.10	1.11	0.55	290.1	289.8	0.1		AAD%	0.6
0.05	0.79	0.55	128.7	129.1	0.3			
				T=303K				
0.20	1.73	0.54	920.7	921.4	0.1	11637.26	20780.80	6479.04
0.15	1.50	0.54	634.1	632.8	0.2			
0.10	1.22	0.55	378.0	378.6	0.2		AAD%	0.1
0.05	0.86	0.55	165.0	164.9	0.0			
				T=308K				
0.20	1.89	0.54	1140.2	1139.9	0.0	13324.22	26266.13	8788.60
0.15	1.63	0.54	792.3	788.9	0.4			

0.10	1.33	0.55	473.0	476.6	0.8		AAD%	0.4
0.05	0.94	0.55	211.0	210.4	0.3			
				T=313K				
0.20	2.05	0.54	1450.0	1400.4	3.4	16378.58	31906.06	10922.45
0.15	1.78	0.54	961.9	970.2	0.9			
0.10	1.45	0.55	558.0	586.9	5.2		AAD%	3.1
0.05	1.03	0.55	268.0	259.7	3.1			
				Overall AAD%				1.1

Table C 1: Rate constants for the reaction of CO2 with L-Arginine based on Termolecular mechanism

ARG	OH	H2O	kov-exp	kov-pre	Error	ka	kw
mole.l-1	mole.l-1	mole.l-1	s-1	s-1	%	$m^6.kmole^{-2}.s^{-1}$	$m^6.kmole^{-2}.s^{-1}$
							T=293 K
0.2	0.0014	53.55	522.62	534.02	2.18	4823.74	31.84
0.15	0.0012	54.04	374.18	366.67	2.01		
0.1	0.0010	54.53	226.46	221.88	2.02	AAD%	1.98
0.05	0.0007	55.02	98.00	99.66	1.69		
				T=298 K			
0.2	0.0016	53.55	680.74	689.99	1.36	6098.86	41.64
0.15	0.0014	54.04	482.19	474.80	1.53		
0.1	0.0011	54.53	290.13	288.07	0.71	AAD%	1.11
0.05	0.0008	55.02	128.74	129.81	0.83		
				T=303 K			
0.2	0.0017	53.55	920.68	927.55	0.75	9308.79	51.84
0.15	0.0015	54.04	634.05	629.65	0.70		
0.1	0.0012	54.53	378.00	375.75	0.59	AAD%	0.64
0.05	0.0009	55.02	165.00	165.87	0.53		
				T=308 K			
0.2	0.0019	53.55	1140.21	1147.42	0.63	10708.79	67.14
0.15	0.0016	54.04	792.30	785.17	0.90		

0.1	0.0013	54.53	473.00	473.18	0.04	AAD%	0.45
0.05	0.0009	55.02	211.00	211.46	0.22		
T=313 K							
0.2	0.0020	53.55	1450.00	1415.61	2.37	13327.72	82.40
0.15	0.0018	54.04	961.87	967.79	0.62		
0.1	0.0014	54.53	558.00	582.58	4.40	AAD%	2.60
0.05	0.0010	55.02	268.00	259.98	2.99		
Overall AAD%							1.35

Table D 1: *Rate constants at different temperatures and (MDEA+glycine) concentrations using zwitterion mechanism*

OH	Gly	OH	MDEA	H2O	kapp	kapp-predict
mol/l	mol/l	mol/l	mol/l	mol/l		
4.35E-03	0.50	4.350	1.95	4.27	89.8	97.6
5.00E-03	1.00	4.999	1.90	4.29	236.0	212.7
5.89E-03	2.00	5.895	1.80	4.33	505.4	484.4
3.53E-03	0.50	3.535	0.95	4.92	63.5	63.2
4.17E-03	1.00	4.168	0.90	4.94	153.7	145.1
5.03E-03	2.00	5.031	0.80	4.98	365.1	353.0
2.95E-03	0.50	2.947	0.45	5.25	37.3	43.6
3.56E-03	1.00	3.557	0.40	5.27	87.5	106.6
			0.00			
4.61E-03	0.50	4.606	1.95	4.27	105.7	117.3
5.28E-03	1.00	5.281	1.90	4.29	272.9	292.8
6.21E-03	2.00	6.214	1.80	4.33	650.5	600.6
3.73E-03	0.50	3.735	0.95	4.92	106.0	77.7
4.39E-03	1.00	4.394	0.90	4.94	205.2	181.6
5.29E-03	2.00	5.290	0.80	4.98	454.8	451.0
3.11E-03	0.50	3.107	0.45	5.25	52.6	55.1

3.74E-03	1.00	3.741	0.40	5.27	123.9	137.0
			0.00			
4.87E-03	0.50	4.870	1.95	4.27	132.3	153.0
5.57E-03	1.00	5.572	1.90	4.29	345.7	336.6
6.54E-03	2.00	6.540	1.80	4.33	842.4	775.3
3.94E-03	0.50	3.940	0.95	4.92	132.8	101.9
4.62E-03	1.00	4.624	0.90	4.94	259.2	236.7
5.55E-03	2.00	5.553	0.80	4.98	566.0	582.5
3.27E-03	0.50	3.270	0.45	5.25	69.6	72.5
3.93E-03	1.00	3.927	0.40	5.27	166.0	178.8
			0.00			
5.13E-03	0.50	5.134	1.95	4.27	170.3	194.4
5.86E-03	1.00	5.861	1.90	4.29	423.8	427.0
6.86E-03	2.00	6.862	1.80	4.33	978.9	977.0
4.14E-03	0.50	4.144	0.95	4.92	160.9	133.3
4.85E-03	1.00	4.852	0.90	4.94	319.4	307.6
5.81E-03	2.00	5.812	0.80	4.98	678.5	746.3
3.43E-03	0.50	3.431	0.45	5.25	88.2	97.2
4.11E-03	1.00	4.110	0.40	5.27	216.7	236.5
			0.00			
5.40E-03	0.50	5.396	1.95	4.27	228.1	228.9
6.15E-03	1.00	6.146	1.90	4.29	555.8	502.7
7.18E-03	2.00	7.179	1.80	4.33	1263.3	1148.3

4.35E-03	0.50	4.346	0.95	4.92	200.9	159.7
5.08E-03	1.00	5.076	0.90	4.94	359.6	368.0
6.07E-03	2.00	6.066	0.80	4.98	777.1	889.5
3.59E-03	0.50	3.590	0.45	5.25	103.3	118.1
4.29E-03	1.00	4.289	0.40	5.27	256.0	286.2

Table E 1: *Rate constants at different temperatures and (MDEA+Arg) concentrations using zwitterion mechanism*

ARG	MDEA	OH × 10^3	H2O	k_{ov}	K_{Arg}	$K_{Arg\text{-}pred}$	AAD%
$mol.l^{-1}$	$mol.l^{-1}$	$mol.l^{-1}$	$mol.l^{-1}$	s^{-1}	s^{-1}	s^{-1}	
			298 K				
0.025	0.975	2.07	49.16	99.17	93.30	80.50	
0.050	0.950	2.07	49.14	177.47	171.70	166.90	
0.100	0.900	2.07	49.08	312.35	306.90	356.00	
0.025	0.475	1.46	52.35	82.40	79.50	70.60	7.60
0.050	0.450	1.46	52.32	152.55	149.80	148.10	
0.100	0.400	1.46	52.26	320.43	318.00	321.80	
0.025	0.225	1.03	53.94	60.75	59.40	65.00	
0.050	0.200	1.03	53.91	125.47	124.30	137.50	
0.075	0.175	1.03	53.88	214.23	213.20	216.90	
			303 K				
0.025	0.975	2.21	49.13	124.65	116.50	104.30	
0.050	0.950	2.21	49.11	226.15	218.20	216.20	
0.100	0.900	2.21	49.05	410.33	402.80	460.40	
0.025	0.475	1.56	52.33	107.15	103.20	91.00	6.30
0.050	0.450	1.56	52.31	195.64	191.90	190.80	
0.100	0.400	1.56	52.25	423.84	420.50	414.30	
0.025	0.225	1.10	53.93	78.32	76.40	83.50	
0.050	0.200	1.10	53.90	165.36	163.70	176.50	
0.075	0.175	1.10	53.88	281.52	280.00	278.40	

308 K							
0.025	0.975	2.35	49.11	171.38	160.20	136.10	
0.050	0.950	2.35	49.08	294.32	283.40	281.40	
0.100	0.900	2.35	49.03	532.24	521.90	596.90	
0.025	0.475	1.66	52.32	149.90	144.40	117.60	8.20
0.050	0.450	1.66	52.29	234.18	229.00	246.00	
0.100	0.400	1.66	52.24	496.55	491.90	532.50	
0.025	0.225	1.17	53.92	101.41	98.80	106.90	
0.050	0.200	1.17	53.90	231.21	228.90	225.80	
0.075	0.175	1.17	53.87	357.73	355.70	355.80	
313 K							
0.025	0.975	2.49	49.09	213.71	198.40	167.80	
0.050	0.950	2.49	49.07	357.97	343.10	347.80	
0.100	0.900	2.49	49.02	625.84	611.70	740.80	
0.025	0.475	1.76	52.31	188.23	180.80	145.90	8.40
0.050	0.450	1.76	52.29	310.72	303.70	306.10	
0.100	0.400	1.76	52.24	632.39	626.10	665.10	
0.025	0.225	1.24	53.92	130.31	126.80	133.50	
0.050	0.200	1.24	53.90	302.60	299.50	282.50	
0.075	0.175	1.24	53.87	451.29	448.50	445.90	
AAD%							7.60

Table E 2: *Rate constants at different temperatures and (MDEA+Arg) concentrations using termolecular mechanism*

ARG	MDEA	OH	H_2O	k_{Arg}	$k_{Arg-pred}$	AAD%
$mol.l^{-1}$	$mol.l^{-1}$	$mol.l^{-1}$	$mol.l^{-1}$	s-1	s-1	
			298 K			
0.025	0.975	3.2E-04	49.16	93.3	79.7	
0.050	0.950	4.5E-04	49.14	171.8	166.2	
0.100	0.900	6.2E-04	49.08	306.9	358.9	
0.025	0.475	2.3E-04	52.35	79.5	70.0	7.8
0.050	0.450	3.1E-04	52.32	149.8	146.6	
0.100	0.400	4.1E-04	52.26	318.0	319.9	
0.025	0.225	1.5E-04	53.94	59.4	65.1	
0.050	0.200	2.1E-04	53.91	124.3	136.8	
0.075	0.175	2.4E-04	53.88	213.2	215.2	
			303 K			
0.025	0.975	3.0E-04	49.16	116.5	103.4	
0.050	0.950	4.2E-04	49.14	218.2	215.3	
0.100	0.900	5.8E-04	49.08	402.8	465.2	
0.025	0.475	2.1E-04	52.35	103.2	90.0	6.9
0.050	0.450	2.9E-04	52.32	191.9	188.7	
0.100	0.400	3.8E-04	52.26	420.5	411.9	
0.025	0.225	1.4E-04	53.94	76.4	83.4	
0.050	0.200	1.9E-04	53.91	163.7	175.4	
0.075	0.175	2.2E-04	53.88	280.1	276.0	

			308 K			
0.025	0.98	2.8E-04	49.16	160.2	134.7	
0.050	0.95	3.9E-04	49.14	283.4	280.3	
0.100	0.90	5.4E-04	49.08	521.9	604.6	
0.025	0.48	2.0E-04	52.35	144.5	115.8	8.6
0.050	0.45	2.7E-04	52.32	229.0	242.6	
0.100	0.40	3.6E-04	52.26	492.0	529.2	
0.025	0.23	1.3E-04	53.94	98.8	106.4	
0.050	0.20	1.8E-04	53.91	228.9	223.8	
0.075	0.18	2.1E-04	53.88	355.7	352.2	
			313 K			
0.025	0.98	2.6E-04	49.16	198.5	164.8	
0.050	0.95	3.6E-04	49.14	343.1	343.9	
0.100	0.90	5.0E-04	49.08	611.8	745.2	
0.025	0.48	1.8E-04	52.35	180.8	143.3	8.8
0.050	0.45	2.5E-04	52.32	303.7	301.0	
0.100	0.40	3.3E-04	52.26	626.1	659.5	
0.025	0.23	1.3E-04	53.94	126.8	132.6	
0.050	0.20	1.7E-04	53.91	299.5	279.6	
0.075	0.18	1.9E-04	53.88	448.6	441.0	
			Overall AAD%			8.0